19th International Workshop on Physical Processes in Natural Waters

PPNW2016
Bath (UK)
12-15 July 2016

Proceedings

PPNW 2016

Front cover image: Tiplyashin, A., *Clean water and water bubbles in blue.* Available at http://www.shutterstock.com/pic-78621736/stock-photo-clean-water-and-water-bubbles-in-blue.html?src=zCknP2YnuyDsePsHgnWbkg-1-14. Last accessed 20th June 2016.

PHYSICAL PROCESSES IN NATURAL WATERS: PPNW2016

Proceedings of the 19th International Workshop on Physical Processes in Natural Waters (PPNW2016)

Bath (UK), 12-15 July 2016

Danielle Wain
Lee Bryant
(Editors)

19th International Workshop on
Physical Processes in Natural Waters
PPNW2016
Bath (UK), 12-15 July 2016

Editors: Danielle Wain and Lee Bryant

Department of Architecture and Civil Engineering
University of Bath
Claverton Down Rd
Bath
North East Somerset
BA2 7AY
UK

Bibliographic information:
D. Wain and L. Bryant (Eds.), *Proceedings of the 19th International Workshop on Physical Processes in Natural Waters: PPNW2016, Bath, UK, 12-15 July 2016*

10-digit ISBN: 0-86197-193-0
13-digit ISBN: 978-0-86197-193-0

Table of contents

Preface

The University of Bath (UK) is pleased to host the 19th International Physical Processes in Natural Waters (PPNW) workshop. The PPNW workshops explore the physics of lakes and coastal water bodies. They look at the interactions with the physical and biogeochemical processes that control water quality, ecosystem functions, and the services these systems provide. This year's workshop focused on innovative measurements of turbulence and biogeochemical fluxes in lakes and other stratified waters.

The keynote speakers this year, Professor John Simpson (Bangor University), and Professor Johny Wüest (EPFL/ETH) have produced seminal work in turbulence and other measurements in stratified lakes and oceans. In total, we welcomed 55 scientists and researchers from across the globe to present their work in Bath via oral or poster presentation. In addition to a wide array of talks on the theme of the workshop and beyond, the participants participated in field trips exploring the water aspects of Bath, from our ancient Roman Baths to the River Avon, which runs through the heart of the city. We also hosted a joint event with the launch event for the University of Bath's new Water Innovation and Research Centre.

We would like to thank our sponsors, Rockland Scientific and Unisense, and the University of Bath 50th Anniversary Fund for financial support. We would also like to thank University of Bath students Scott Easter, Zach Wynne, Stefano Simoncelli, Mahan Amani, and Emily Slavin for their assistance in planning and executing the workshop. We would also like to thank Claire Hogg from the Department of Architecture and Civil Engineering and Shan Brandley-Cong from the Water Innovation and Research Centre for helping with the campus events.

Danielle Wain
Lee Bryant
PPNW2016 Co-Chairs

Committees

University of Bath Organising Committee:
Danielle Wain, Department of Architecture and Civil Engineering
Lee Bryant, Department of Architecture and Civil Engineering

International Steering Committee:
Josef Ackerman, University of Guelph, Canada
Hrund Andradóttir, University of Iceland, Iceland
Lars Bengtsson, Lund University, Sweden
Bertram Boehrer, Helmholtz Centre for Environmental Research (UFZ), Germany
Xavier Castamitjana, University of Girona, Spain
Giuseppe Ciraolo, University of Palermo, Italy
Nikolai Filatov, Karelian Research Centre of RAS, Russia
Andrew Folkard, Lancaster University, United Kingdom
Georgiy Kirillin, Institute of Freshwater Ecology, Berlin (IGB), Germany
Charles Lemckert, Griffith University, Australia
Madis-Jaak Lilover, Marine Systems Institute, Estonia
Francisco Rueda, University of Granada, Spain
Geoffrey Schladow, University of California, Davis, United States
Adolf Stips, European Commission, Italy
Arkady Terzhevik, Karelian Research Centre of RAS, Russia
Marco Toffolon, University of Trento, Italy
Lars Umlauf, Leibniz-Institute for Baltic Sea Research (IOW), Germany
Alfred Wüest, Eawag & EPFL, Switzerland
Ram Yerubandi, Canada Centre for Inland Waters, Canada

Keynote lectures

Measurements of turbulent dissipation and lake energy budgets by acoustic Doppler profilers

J. H. Simpson
Bangor University School of Ocean Sciences, Menai Bridge, Anglesey

ABSTRACT

In this presentation, I shall firstly review recent efforts to improve the resolution and coverage of turbulence measurements through the use of acoustic Doppler instruments. In particular, I will concentrate on the results of recent observations of the dissipation of turbulent energy with high frequency ADCPs which demonstrate the power of bottom-mounted and tethered instruments to convincingly determine the turbulence in low energy, environments. I will then show how continuous measurements of dissipation can be combined with parallel measurements with longer range ADCPs and chains of temperature sensors, to determine mixing rates and to estimate the principal components of the energy budget of a lake under wind stress forcing.

20 years of PPNW: Ever-growing interest in the geo-sciences of inland waters

A. Wüest, Eawag and EPFL

ABSTRACT

About twenty years ago, the first clear signs of improving water quality following effects of eutrophication were recognized in the Western Word. I remember well how the future of freshwater aquatic sciences, which focused on biogeochemical cycles, nutrients and oxygen, was considered a dead-end and how lake research in particular was considered a phase-out model. However, the contrary has happened: more sophisticated instrumentation - such as multibeam or satellite imaginary among many others - and new and ongoing questions related to climate change and water resources use have triggered an ever-growing interest in inland aquatic geosciences. In this presentation, I will highlight some of the developments which have supported the advancement of water research to become established as the diverse and dynamic field it is today.

Extended Abstracts

Biogeochemical controls on Manganese and Algae cycling in drinking water reservoir

M. Amani. G.[1]*, D.J. Wain[1] and L.D. Bryant[1]
[1] *Department of Architecture and Civil Engineering, University of Bath, Bath, UK*

**Corresponding author, e-mail m.amani.geshnigani@bath.ac.uk*

KEYWORDS
Water quality; drinking water reservoir; manganese; ResMix system; biogeochemistry.

EXTENDED ABSTRACT

Introduction

Elevated levels of manganese (Mn) and blue-green algae (e.g., cyanobacteria) in drinking water are becoming increasingly problematic issues in the UK and globally. Both Mn and blue-green algae pose a serious threat by potential damage to the nervous system and liver. Additionally, aesthetic problems associated with excess Mn often occur in water-supply infrastructure, e.g., brownish-coloured, metallic-tasting and foul-smelling drinking water. Increased Mn concentrations can also lead to reduced flow in pipes as a result of Mn accumulation. Because of these health and aesthetic problems, Mn and algal toxins are regulated in drinking-water supplies by government agencies. Removal of Mn for meeting the UK drinking water limit (50 µg/L) is feasible but often difficult using conventional water treatment processes because of the complexity of Mn redox kinetics. Algal toxicity is currently regulated based on WHO human exposure limits (low risk: 25k cells/mL). Both Mn and algae removal can be costly due to the need for chemical oxidants (e.g., chlorine) which can also cause taste and odor problems and react with naturally occurring organic matter resulting in formation of carcinogenic disinfectant by-products.

Due to these water quality and treatment issues related to Mn and algae, drinking-water utilities across the UK are using engineered aeration systems in water-supply reservoirs to (1) increase oxygen (O_2) and mixing and subsequently (2) reduce levels of Mn and algae in the influent (i.e., source) water to treatment plants. One of the engineered aeration system is ResMix aeration system which is a surface mixer designed to create circulation within the reservoir, thereby preventing surficial algal blooms and hypolimnetic hypoxia.

Improving the quality of source water ideally minimises the level of treatment required in the plant. Unfortunately, many of the controlling biogeochemical mechanisms involved with aeration effects on water quality are poorly understood, leading to on-going problems with source-water quality.

Materials and methods

A field campaign was ran on local Durleigh Reservoir from 7- 11 Sep 2015, to assess the in-reservoir performance of the new ResMix aeration system from special and temporal perspectives. Durleigh Reservoir is a drinking water reservoir with the surface area of 80 acres, maximum depth of 5.5 m and average depth of 2.7 m, located in the South West UK.

Combined sampling strategy involving YSI castaway CTD and YSI EXO1 water-column profiling paired with water and sediment sampling were performed to assess O_2, algae, and Mn concentrations as a function of distance from the ResMix as well as manganese and total organic carbon in bulk sediment within the reservoir.Water column sampling in 1 meter

increments were done using Von Dorn water sampler for (1) subsequent oxygen concentration measurements via Winkler titration method and (2) total and soluble manganese concentration measurements at the same day via inductively coupled plasma spectroscopy; ICP-MS. Sediment samples were taken using Uwitec sediment corer and sent to the laboratory to determine total manganese and total organic carbon TOC (indicative of precipitated algal biomass) via inductively coupled plasma; ICP and acid digestion.

Results and discussion

CTD profiles were acquired along the fetch showed weak stratification during the first day of the campaign with the temperature difference of 2 degree between the surface and bottom water and for the other days no significant temperature difference was observed, therefore the reservoir was not stratified during the campaign. Water-column profiling O_2, blue-green algae and chlorophyll using EXO1 showed elevated levels of blue-green algae and chlorophyll near the ResMix system, total organic carbon in balk sediment were consistent with this data.

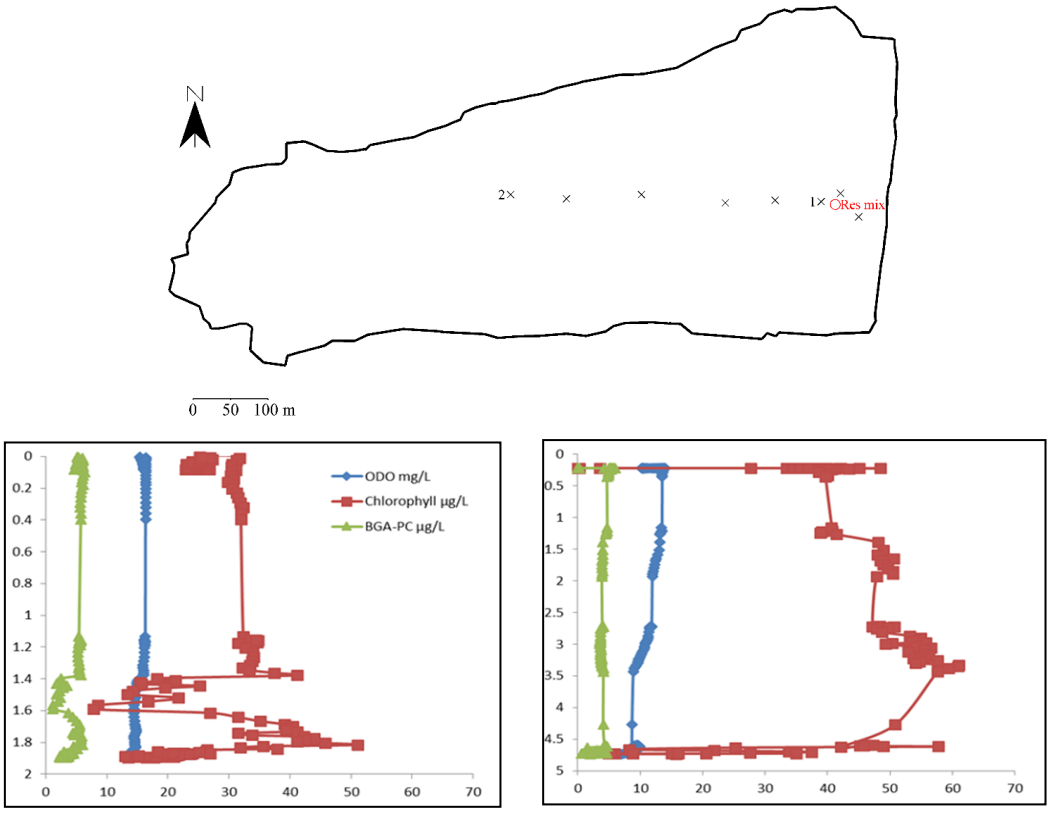

Figure 1. Left: measurements taken at location marked 2 (depth 2 m). Right: measurements taken at location marked 1 (depth 5m).

However oxygen concentration at the bottom of the reservoir at location 1 (10.7 mg/L) was higher than location 2 (8.5 mg/L). Total Mn concentration was also higher at bottom water near ReMmix (117 ug/L) than location 2 about 500 m further than Resmix (82 ug/L). It could be that the ResMix system mixing everything in the water column that despite more oxygen concentration near ResMix, the total Mn concentration is higher. To draw a firm conclusion of the ResMix capacity for suppressing the manganese and algae concentrations throughout the reservoir, a more comprehensive sampling strategy is planned for the upcoming summer 2016.

Non-uniformity of Residence Time in a Brazilian Reservoir

J. W. Y. Bernardo[1]*, T. Bleninger[1]

[1] *Graduate Program on Water Resources and Environmental Engineering, Federal University of Parana, Parana, BR*

**Corresponding author, e-mail juliowernery@gmail.com*

KEYWORDS
Residence time; reservoirs; modelling.

EXTENDED ABSTRACT

Introduction

Increasing computer power made three-dimensional hydrodynamic modeling more accessible. Thus, estimation of spatial distribution of residence times within a reservoir is now possible. Because of that, some researchers (Bárcena et al., 2012; Jouon, Douillet, Ouillon, & Fraunié, 2006) are estimating residence times using two-dimensional or three-dimensional models to obtain a local residence time (one residence time for each sub-region in a domain). In this study, we investigated the spatial representation of the mean residence time in a case study to determine the relevance of the use of spatial distribution of residence times.

Materials and methods

The case study was performed in Vossoroca Reservoir which is located in south of Brazil. The reservoir covers an area of about 3 km² and has a capacity of 36 hm³. The average water depth is about 8 m, maximum depth about 17 m. The catchment area of the reservoir has a size of 151 km² .The immediate surrounding area of the reservoir is used for recreation, whereas the upstream area of the basin is mainly affected by agriculture. The annual rainfall within this area is about 1900 mm, the climate is subtropical and the annual mean discharge is about 4 m³/s.

Mean residence time was estimate using the annual mean outflow discharge and maximum volume. Local residence time was estimated by modeling particles. Delft3D-FLOW was used for the hydrodynamic modeling and Delft3D-PART for the particle tracking. The model was built with a rectangular resolution of 15 m containing 169,200 cells.

The simulation of 150,000 particles, released simultaneously at the three most representative inlets, allowed the calculation of travel time of each particle. The travel time is the time from the inlet to the outlet. The local residence time is the average travel time of particles that crossed the respective cell.

Two simulations were ran in a steady-state scenario with constant temperature (no stratification), at the maximum volume and annual mean discharge. The first simulation does not considered the effect of wind and the second considered a uniform wind in the prevailing direction (East) with average intensity of 1.4 m/s. More details can be found in Bernardo and Bleninger (2015).

Results and discussion

Figure 1 shows that less than ~ 30% of the area is covered by local residence times shorter than mean residence time. Furthermore, the comparison of Figure 1a with 1b shows the inclusion of the wind changed significantly the spatial distribution of residence over the reservoir. In the scenario considering wind most particles leaves quicker than in scenarios without wind. Figure 2 shows the local residence time within the reservoir.

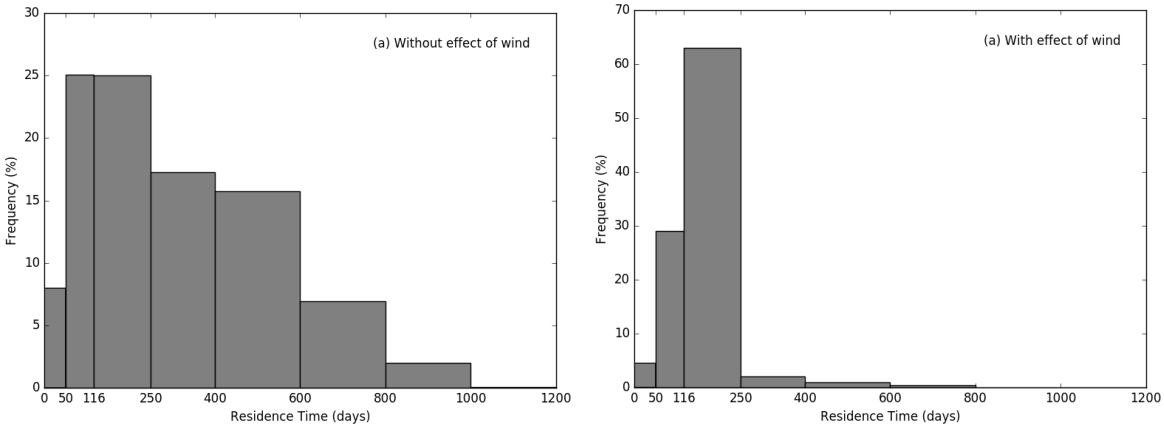

Figure 1. Histograms of the distribution of local residence over the reservoir for the scenario modeled (a) with wind effect and (b) without wind effect.

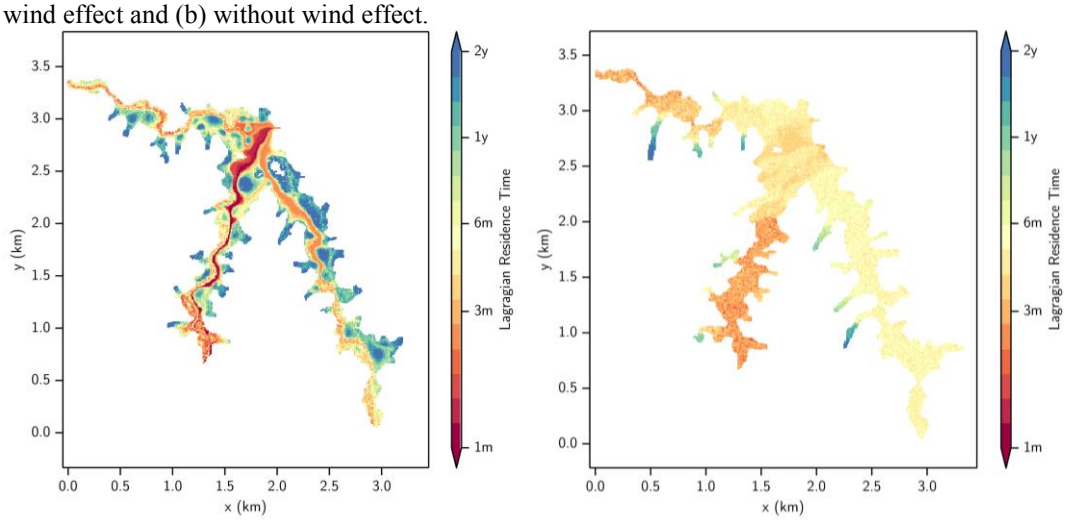

Figure 2. Local residence time within the reservoir for (a) with wind effect and (b) without wind effect.

The results highlights that spatial mean residence time is valid to limited areas and can also be affect by unsteady phenomena. Thus, further studies are encourage to understand if this variability are related with spatial variability of water quality parameters.

REFERENCES

Bárcena, J. F., García, A., Gómez, A. G., Álvarez, C., José, Juanes, A., & Revilla, J. A. (2012). Spatial and temporal flushing time approach in estuaries influenced by river and tide. Estuarine, Coastal and Shelf Science, 112, 40–51.

Jouon, A., Douillet, P., Ouillon, S., & Fraunié, P. (2006). Calculations of hydrodynamic time parameters in a semi-opened coastal zone using 3D hydrodynamic model. Continental Shelf Research, 26, 1395–1415.

Bernardo, J.W.Y.; Bleninger, T.(2015). Interpretation and Applicability of Residence Times in Reservoirs. Proceedings of 36th IHA World Congress. The Hague – Netherlands.

A practical approach to lake water density from electrical conductivity and temperature

S. Moreira[1,2,3,*], M. Schultze[1], and B. Boehrer[1,#]

[1] *UFZ-Helmholtz-Centre for Environmental Research, Department Lake Research, Magdeburg, Germany*

[2] *Laboratoire des Sciences du Climat et de l'Environnement (LSCE), UMR8212, CEA/CNRS-INSU/UVSQ*

[3] *Institute of Hydrobiology. TU-Dresden. Zellescher Weg 40, Dresden, Germany*

**Corresponding author, e-mail santimohr@gmail.com*
 # presenting co-author Bertram.Boehrer@ufz.de

KEYWORDS
Potential density, limnology, stratification, physical chemistry of natural waters.

EXTENDED ABSTRACT

Introduction

Potential density calculations are essential to study stratification, circulation patterns, internal wave formation and other aspects of hydrodynamics in lakes and reservoirs. Currently, the most common procedure is the implementation of CTD profilers and convert measurements of temperature and electrical conductivity into density. In limnic waters, such approaches are of limited accuracy, if they do not consider a lake specific composition of solutes. A new approach is presented to correlate density and electrical conductivity, using only two specific coefficients based on the composition of solutes. First, it is necessary to evaluate the lake-specific coefficients connecting electrical conductivity with density. Once these coefficients have been obtained, density can easily be calculated based on CTD data. The new method has been tested against measured values and the most common equations used in the calculation of density in limnic and ocean conditions. The results show that our new approach reproduces the density contribution of solutes with a relative accuracy of 10% in lake waters from very low to very high concentrations as well as in lakes of very particular water chemistry, which surmounts all commonly implemented density calculations in lakes by far.

Numerical approach

The commonly applied density formula (UNESCO i.e. Fofonoff and Millard 1983 and Chen and Millero, 1986) do not supply a good representation of the density contribution of limnic solutes. Based on ocean conditions especially in water rich in double charged ions pose difficulties. As shown by Moreira et al 2016, deviations usually lie in the range of 25% to 100%, i.e. density differences due to solutes can be double, what is calculated by above mentioned numerical approaches.

We looked for an easy to apply formula for density calculation, which gives a much better representation of the density contribution of solutes by including information on the solute composition. For this purpose we had to collect the relevant coefficients of physical chemistry for density calculation (as in RHOMV by Boehrer et al. 2010) and for electrical conductivity.

A numerical tablet was written to calculate coefficients connecting electrical conductivity (as in PHREEQC algorithm: Parkhust and Appelo, 1999; Atkins and de Paula, 2009)for the given conditions (composition and concentration) for the limnologically interesting temperature range 0 to 30 °C.

This tablet provides an easy surface to key in solute composition. Two coefficients λ_0 and λ_1, which can be inserted in the Moreira et al. (2016) formula:

$$\rho \approx \rho_\lambda(T,\kappa_{25}) = \rho_w(T) + \kappa_{25}[\lambda_0 + \lambda_1 \times (T - 25°C)]$$

A critical assessment of the accuracy of calculated densities for lake waters: Rappbode main dam, Lake Constance, Lake Geneva, Mono Lake, Waldsee mixolimnion and Waldsee monimolimnion, reveals that this simple equation provides an improved calculation of density contribution of solutes at an accuracy of 10% or even better. This surmounts the evaluation according to UNESCO of Chen and Millero by typically a factor of 5 to 10 for limnic waters over the broad range of lake waters we have investigated.

REFERENCES

- Atkins, P., de Paula, A.: Physical Chemistry, 9th ed, Oxford University Press, 2009.
- Boehrer, B., Herzsprung, P., Schultze, M., Millero, F. J.: Calculating density of water in geochemical lake stratification models, Limnol. Oceanogr-Meth., 8, 567 – 574, doi: 10.4319/lom.2010.8.0567, 2010.
- Chen, C.-T.A., Millero, F.J.: Precise thermodynamic properties for natural waters covering only the limnological range, Limnol. Oceanogr., 31, 657 – 662, 1986.
- Fofonoff, N.P., Millard Jr., R.C.: Algorithms for communication of fundamental properties of seawater, UNESCO technical papers in marine science, 44, 1983.
- Moreira S., Schultze M., Rahn K., Boehrer B. (2016) A practical approach to lake water density from electrical conductivity and temperature, HESS, http://www.hydrol-earth-syst-sci-discuss.net/hess-2016-36
- Parkhurst, D.L., Appelo, C.A.J.: Users guide to PHREEQC (version 2). A Computer program for speciation, batch-reaction, one-dimensional transport, and inverse geochemical calculations, Water-Resources Investigation Report 99-4259, U.S. Geological Survey, 1999.

Investigating turbulent flow close to the sediment-water interface in a run of the river reservoir at high spatial resolution

A. Brand[1,2]*, C. Dinkel[1], A. Wüest[1,3], B. Wehrli[1,2], C. Noss[4]

[1] *Eawag, Swiss Federal Institute of Aquatic Science and Technology, Surface Waters - Research and Management, Kastanienbaum, Switzerland*

[2]*Institute of Biogeochemistry and Pollutant Dynamics, ETH Zurich, 8092 Zurich, Switzerland*

[3]*Physics of Aquatic Systems Laboratory—Margaretha Kamprad Chair of Environmental Science and Limnology, ENAC, EPFL, Lausanne, Switzerland*

[4]*Institute for Environmental Sciences, University of Koblenz-Landau, Landau, Germany*

**Corresponding author, e-mail andreas.brand@eawag.ch*

KEYWORDS
Bottom boundary layer; sediment-water interface; turbulence; Vectrino Profiler;

EXTENDED ABSTRACT

Introduction

The flow close to the sediment water interface (SWI) is an important abiotic factor shaping the living conditions in the benthic zone. Bottom shear is the main source of turbulence and mixing in this zone, which in turn governs the exchange of solutes and particles between water column and sediments (Brand et al. 2015; Bryant et al. 2010). Until now, fluid flow in the close vicinity of the SWI was hardly accessible by commercially available measurement devices. A high resolution bistatic profiler (Vectrino Profiler, Nortek), has recently been tested for its applicability to characterize turbulent flow at the SWI by Brand et al. (2016). While the device reliably measures the mean velocity profiles at millimetre resolution, turbulence statistics are only reliable in the very close vicinity (±1mm) of a point with an optimal configuration between emitters and receivers-the so called sweet spot. Out of this spot, flow statistics suffer from noise as well as from signal decorrelation and require complex postprocessing. In the present work, we took advantage of the ability of the Vectrino Profiler to provide reliable flow statistics at one spot simultaneously with the flow velocity gradients at the same location to characterize turbulent mixing at the SWI in a run-of-the-river reservoir.

Materials and methods

Measurements were conducted on the 20th October 2016 in Lake Wohlen, a run-of-the river hydropower reservoir. The water depth at the measurement location was 4.6 m. The Vectrino Profiler was mounted on a lander system (KC Denmark), which allowed precise vertical positioning of the profiler during deployment. 20 minutes bursts were recorded at 32 Hz at several elevations up to ~9 cm above the SWI. The profiles were recorded at 1 mm resolution. In addition, a Nortek Vector ADV recorded data continuously in 10 cm elevation at 32 Hz. All data were despiked (Goring and Nikora 2002) and rotated in natural wind coordinates (Lee et al. 2004) before further processing. Reynolds stresses were calculated at the sweet spot as the negative covariance of the horizontal and vertical velocity fluctuations $-\langle u'w' \rangle$.

Along stream velocity gradients were determined by linear regression from the data in ±3 mm distance from the sweet spot.

Results and discussion

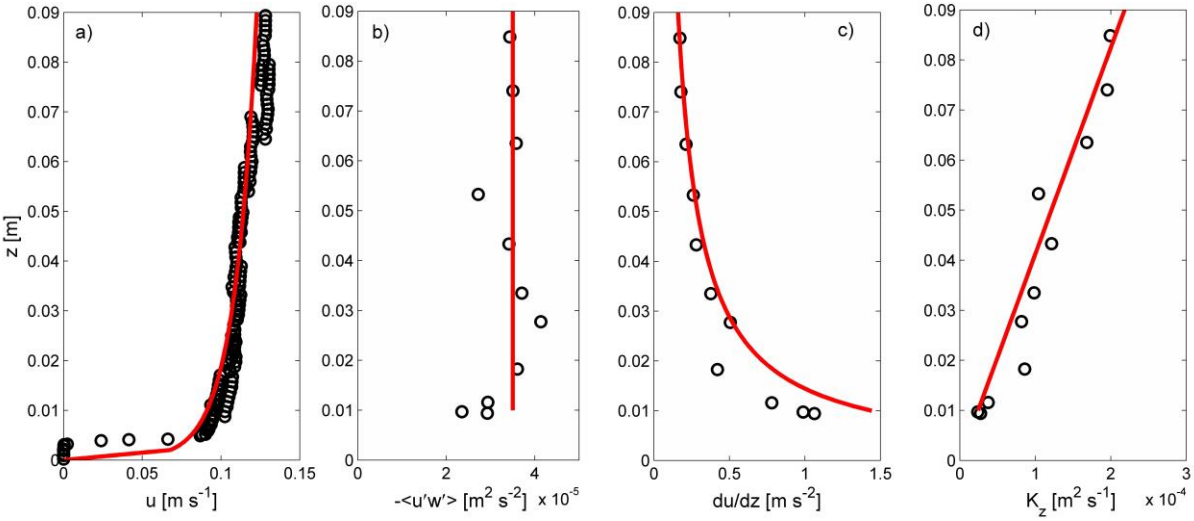

Figure 1. Flow and turbulence parameters above the SWI observed in Lake Wohlen. a) horizontal flow velocity b) Reynolds stress, c) velocity gradient, d) eddy viscosity. Circles denote measurements, the red lines show the values expected assuming a constant stress layer with $u_*=5.9\times10^{-3}$ ms^{-1}.

The along stream flow velocity at 10 cm measured by the ADV was 12.1±0.4 cm s^{-1}, while the shear velocity u_* was 6.2±0.5 mm s^{-1}. This shear velocity was close to the value used for fitting the equations for the constant shear stress layer (u_*=5.9 mm s^{-1}) shown in Figure 1. The average horizontal flow velocity profile is generally well described by the logarithmic law of the wall for smooth flow (see e.g. equations 3-5 in Brand et al. (2016)) (Figure 1a). The deviations of individual profile sections can be explained by the variability of the flow during profile recording (overall recording time was 6 h), while the strong deviation of the velocity values up to 5 mm above the SWI is most likely due to a solid object which causes a disturbance of the acoustic signal in the very close vicinity of the bottom (Koca et al. submitted). There is only a small variation of Reynolds stresses (Figure 1b), suggesting the existence of a nearly constant shear stress layer in the profiling range. Also the measured velocity gradients are in good agreement with the theoretical prediction ($du/dz = u_*/\kappa z$ where κ=0.41 is the von Karman constant and z the distance from the SWI, Figure 1c). The eddy viscosity K_z, which was calculated form the Vectrino data as $K_z = -\langle u'w' \rangle / du/dz$ agrees surprisingly well with the theoretically calculated values (Figure 1d). Our study shows that the Vectrino Profiler opens new possibilities to characterize turbulent boundary layers at high spatial resolution due to its ability to measure mean velocity profiles simultaneously with turbulence statistics.

REFERENCES

Brand, A., C. Noss, C. Dinkel, and M. Holzner, 2016: High resolution measurements of turbulent flow close to the sediment-water interface using a bistatic acoustic profiler. *J. Atmos. Ocean. Technol.*, **in press**, doi:10.1175/jtech-d-15-0152.1.

Brand, A., J. R. Lacy, S. Gladding, R. Holleman, and M. Stacey, 2015: Model-based interpretation of sediment concentration and vertical flux measurements in a shallow estuarine environment. *Limnology and Oceanography*, **60**, 463-481, doi:10.1002/lno.10047.

Bryant, L. D., C. Lorrai, D. F. McGinnis, A. Brand, A. Wuest, and J. C. Little, 2010: Variable sediment oxygen uptake in response to dynamic forcing. *Limnology and Oceanography*, **55**, 950-964, doi:10.4319/lo.2009.55.2.0950.

Goring, D. G., and V. I. Nikora, 2002: Despiking acoustic Doppler velocimeter data. *Journal of Hydraulic Engineering-Asce*, **128**, 117-126, doi:10.1061/(asce)0733-9429(2002)128:1(117).

Koca, K., C. Noss, C. Anlanger, A. Brand, and A. Lorke, submitted: Assessment of the Vectrino Profiler for measuring flow at the sediment-water interface. *Journal of Hydraulic Research*,

Lee, X., W. Massman, and B. Law, 2004: *Handbook of micrometeorology-a guide for surface flux measurement and analysis*. Kluwer, 250 pp.

Primary production enhanced by wind in shallow salty lagoons of altiplano

A. de la Fuente[1]* and J. Vergara[1]

[1] *Departamento de Ingeniería Civil, Universidad de Chile, Santiago, Chile*

**Corresponding author, e-mail aldelafu@ing.uchile.cl*

KEYWORDS
Shallow lagoons, CO2 transport across the air-water interface; primary production

EXTENDED ABSTRACT

Introduction

In the context of an increasing CO2 concentration in the atmosphere, the primary production of aquatic ecosystems is expected to increase as well (Verspagen et al. 2014). This response can be explained by examining the half-saturation constant of CO2 for gross primary production (K_{05}, Jørgensen and Bendoricchio 2001), which enables the computation of the net primary production (P) as a function of the CO2 concentration (C_W):

$$P = P_M \frac{C_W}{C_W + K_{05}} \quad (1)$$

where P_M denotes the rate of primary production in the absence of CO2 limitation. The value of C_W depends on sources and sinks of CO2 in the water and exchanges with the surrounding environment, including diffusion across the air–water interface (AWI) and the water–sediment interface (WSI), and inflows and outflows. Transport across the AWI is written as

$$F_{CO2} = k_a(C_A - C_W) \quad (2)$$

where k_a is the transfer velocities at the AWI, and C_A the saturated concentration of CO2 in the water. $F_{CO2}$is defined positive if CO2 flows from the atmosphere to the lake. Thus, if inflow and outflow contributions are neglected, the steady state is described by $F_{CO2} = P$, showing that primary production can be promoted or limited by diffusive transport across the AWI. An example of the previous dynamics was observed in a time series of CO2 flux exchanged between the atmosphere and the lagoon of Salar del Huasco (20.274ºS, 68.883ºW, 3800 m above sea level, de la Fuente 2014). These measurements show that the lagoon acts as a sink of atmospheric CO2, the flux of CO2 varies between 0 to 10 g CO2 m-2day-1, and this flux of CO2 is strongly modulated by the wind that periodically blows in the afternoons. Salar del Huasco is located in the altiplano of northern Chile. The aim of this article is to analyse these field observations on Salar del Huasco, with an emphasis on characterizing and quantifying the primary production (measured in terms of a flux of CO_2 per surface area of the lagoon) in response to the wind.

Materials and methods

One field campaign was conducted in Salar del Huasco between 31 of October and 2 of November of 2015, with the aims of measuring the time series of the momentum and CO_2 fluxes exchanged between the lagoon and the atmosphere and other parameters (Fig 1). These measurements were conducted with a sonic anemometer with an infrared open-path gas analyser (Irgason, Campbell Scientific). In the conceptual scheme

$F_{CO2} = P$, the limitation of gross primary production by light, nutrients and temperature are included in P_M, which is the rate of primary production in the absence of the CO_2 limitation. As a first approximation, P_M is written as (Jørgensen and Bendoricchio 2001) follows:

$$P_M = \mu_n f(T) f(I); \quad f(T) = \theta^{T-20}; \quad f(I) = 1 - \exp(-I/I_O) \tag{3}$$

where μ_n is the maximum growth rate (g CO_2 day^{-1}) for the standard temperature of 20°C and in the absence of light and CO_2 limitation; and $f(T)$ and $f(I)$ are the limiting functions for water temperature and solar radiation, respectively (Jørgensen and Bendoricchio 2001).

Results and discussion

Accordingly, and provided that a characteristic value of $K_{05} = 50$ μmol/L and $I_O = 90$ W m^{-2} (MacIntyre and Cullen 1995), μ_n was fitted to the observations so as to minimize the least squared error, $\mu_n = 218 \pm 27$ g $CO_2 day^{-1}$ (r^2=0.85). Fig. 2 shows the observed time series of F_{CO2} and the predicted time series. The good match between the observed and predicted F_{CO2} shows that the primary mechanism that explains temporal dynamics observed in F_{CO2} is the limitation by transport across the AWI.

The specific value of the fitted μ_n depends on the values adopted for the other parameters I_o and K_{05}, not as the goodness of the fit (r^2), which does not significantly change as a function of these two parameters. Specifically, the fitted μ_n increases for a larger K_{05} and I_o; however, the fitted μ_n is more sensible to changes in the half saturation constant than to changes in I_o.

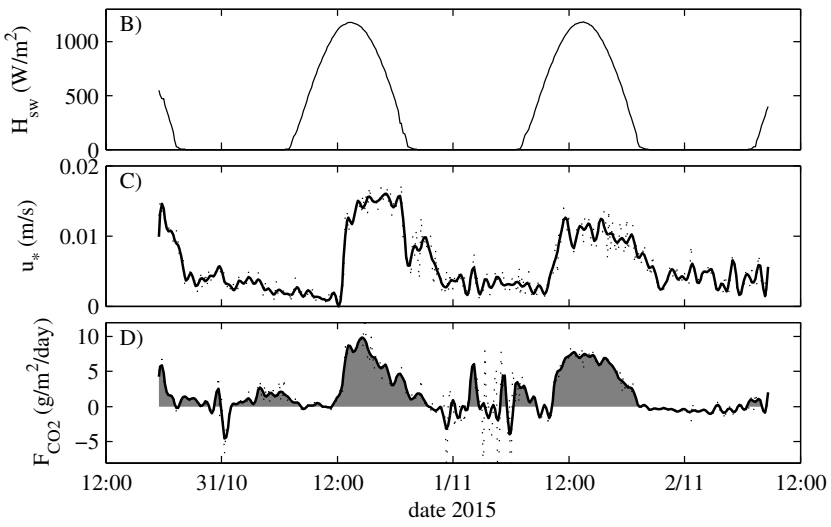

Figure 1: A) Time series of incident shortwave solar radiation. B) Time series of wind shear stress filtered every hour (black line) and direct measurements every 10 min (dotted line). C) Time series of CO2 flux exchanges between the water column and atmosphere. A positive F_{CO2} indicates that CO2 flows from the atmosphere to the lagoon.

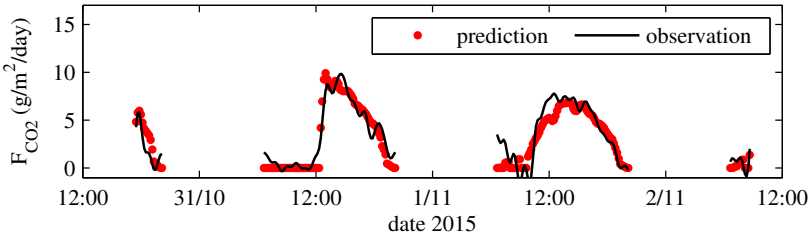

Figure 2. Comparison between the observed (black line) and predicted F_{CO2} using I_o=90 Wm-2, K_{05} = 50 μmol/L, and the fitted μ_n = 218 g CO2day-1.

REFERENCES

de la Fuente, A., 2014. Heat and dissolved oxygen exchanges between the sediment and water column in a shallow salty lagoon. J. Geophys. Res. Biogeosci, 119: 596-613.

Jørgensen, S., and Bendoricchio, G. 2001.Fundamentals of Ecological Modelling.Elsevier Science and Technology.

MacIntyre, H.L. and Cullen, J. J. 1995.Fine-scale vertical resolution of chlorophyll and photosynthetic parameters in shallow-water benthos. Mar. Ecol. Prog. Ser. 122: 227-237.

Verspagen, J.M., Van de Waal, D.B., Finke, J.F., Visser, P.M., Van Donk, E. and Huisman, J., 2014. Rising CO 2 levels will intensify phytoplankton blooms in eutrophic and hypertrophic lakes.

Oxic methane production in mesotrophic Lake Hallwil (Switzerland): evaluating potential sources, sinks and implications

D. Donis[1]*, S. Flury[1], N. Gallina[1], T. Langenegger[1], A. Stöckli[2] and D.F. McGinnis[1]

[1] *Institute F.-A. Forel, University of Geneva, Geneva, Switzerland.*
[2]*Department of Civil Engineering, Transportation and Environment, Canton of Argovia, Aarau, Switzerland.*

**Corresponding author, e-mail daphne.donis@unige.ch*

KEYWORDS
Oxic methane production; mesotrophic lake; methane flux.

EXTENDED ABSTRACT

Introduction

The oversaturation of methane in oxic surface waters (Methane Paradox) has been reported in both lakes (Blees et al., 2015) and oceans (Damm et al., 2010). While the source is still unknown, the surface layer oxic methane production (OMP) appears to positively correlate with primary production (Chlorophyll-a; chl-a), dissolved oxygen, and the thermocline (Grossart et al., 2011; Tang et al., 2014). Lakes where CH_4 is produced in sediments and the anoxic water column via anaerobic methanogenesis typically result in buildup of CH_4 concentrations in the bottom water, where they are isolated from the atmosphere except at lake turnover (Fernandez et al., 2014). In contrast, OMP places a CH_4 source close to the surface, where it can exacerbate CH_4 emissions and significantly contribute to atmospheric emissions (McGinnis et al., 2015).

The most convincing findings supporting OMP in pelagic lake waters are recent experiments with mesocosms. While lateral transport has been shown to be a source of surface CH_4 (Hofmann et al., 2010), at least a fraction of OMP is convincingly shown to occur in situ with mesocosms (Bogard et al., 2014), pointing to a significant component arising from in situ production. The origin of this OMP has been postulated to arrive by various means (Conrad 2009), for example: 1) production and lateral transport from the littoral zone, 2) anoxic micro-niches, 3) byproducts from zooplankton grazing, 4) CH_4 bubble dissolution and 5) algal metabolites, to name a few. Some of these sources are feasible in lakes, but often contradictory when presented with specific evidence.

We discovered a distinct CH_4 peak in the upper oxic layer of Lake Hallwil in 2015. The results obtained from June to October with state-of-the-art physical and biogeochemical measurement approaches allow hypothesizing (and excluding) local source(s) of CH_4 in the surface, oxic layer. These findings represent a step forward in deciphering the "methane paradox" related emissions from lakes, and quantifying the contribution to local and global atmospheric CH_4 emissions.

Study Site

Lake Hallwil (Aargau, Switzerland) is a mesotrophic lake with a surface area of 10.2 km^2, a mean depth of 28.6 m, and a maximum depth of 48 m. Lake Hallwil became eutrophic around the beginning of the 20th century, however the hypolimnetic aeration applied since 1986 has been reported as a successful restoration program (Stökli et al., 2016).

Results and discussion

Methane oversaturation was observed in Lake Hallwil within the upper ~15 m when the lake was stratified. Peak CH_4 values increased from 0.35 µmol L^{-1} (7.5 m depth) in June to 0.84 µmol L^{-1} (8 m depth) in August. An intriguing feature is the presence of a double chl-a maximum, a recent phenomenon in Lake Hallwil that is particularly pronounced during the summer season. Our data consistently show that the CH_4 peak is present at, or very close to, the surface chlorophyll maximum (SCM). While the SCM is associated with chrysophytes, chlorophytes and diatoms, the deep Chlorophyll maximum (DCM) is associated with the filamentous cyanobacteria *Planktothrix rubescens*. The reason the CH_4 peak is associated with SCM (and not DCM) is not understood and needs further investigation.

Water column constituent profiles are shown on Fig. 1 (left), overlying the backscatter time series from the deployed ADCP (acoustic Doppler current profiler; Aug, 2015). The presence of diurnally migrating *Chaoborus flavicans* was previously documented in Lake Hallwil (Lorke et al., 2004), and appear to be present based on ADCP backscatter (Fig 1 left; warm colors indicate high backscatter). As indicated on Fig. 1, the CH_4 concentrations in Lake Hallwil surface layer are significantly correlated with inorganic nitrogen, which can be derived from zooplankton excretions (Oude & Gulati 1988) and peaks where the Chaoborus appear to feed at night (bright green on contour between 5 – 10 m). Overall, the best correlations of the OMP are with water column stability N^2 and NO_3 (R^2 = 0.9; Fig. 1 right). The agreement between the CH_4 peak, temperature and water column stability suggests a physical component behind the observed CH_4 peak.

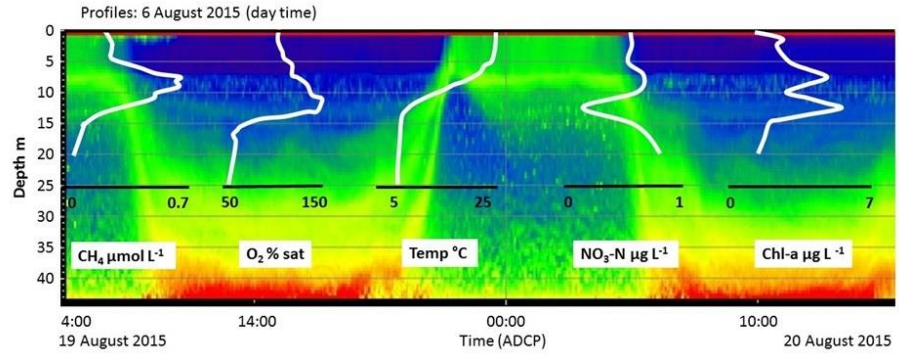

Correlation with CH_4 (0-10 m)	Decreasing R^2
N^2 (w.c. stability)	0.9
NO_3-N	0.9
POC	0.8
chl-a	0.7
PO_4-P	0.6
O_2	0.6
SO_4^{2-}	0.6
DOC	0.4
NH_4-N	0.3

Figure 1. Left) CH_4, O_2 (% sat), Temp, NO_3-N and chl-a depth profiles overlying backscatter ADCP contour plot indicating probable C. flavicans diurnal migration (warm colors = high backscatter). Note that the profiles in white refer to the same sampling day (10:00 a.m. - 3:00 p.m.) while ADCP data span 36 hours. Right) Correlations of various parameters with the CH_4 concentration profiles from 0 – 10 meters.

Sediment porewater $\delta^{13}C$-CH_4 in Lake Hallwil during this period averaged -74‰ and -68‰ in the upper 15 cm at 45 m and 5 m depth stations, respectively. These $\delta^{13}C$-CH_4 are significantly lighter than values we observed in the Lake Hallwil OMP (-58‰), suggesting either different sources or oxidation processes that need to be quantified.

It is plausible that multiple sources act to produce this OMP, and that these may vary from lake-to-lake and may be trophically-dependent. Regardless of the source, the observed OMP sustains an important input to the atmosphere that was estimated as 0.6 ± 0.08 mmol CH_4 m^{-2} d^{-1}. The prevalence of this phenomenon, however, is still unknown, and further research is needed to determine the global existence of this phenomenon in lakes.

REFERENCES

Blees, J., Niemann, H., Erne, M., Zopfi, J., Schubert, C.J. & Lehmann, M.F. (2015), Spatial variations in surface water methane super-saturation and emission in Lake Lugano, southern Switzerland, *Aquat. Sci.*, **77**, 535-545.
Bogard, M.J., del Giorgio, P.A., Boutet, L., Chaves, M.C.G., Prairie, Y.T., Merante, A. *et al.* (2014), Oxic water column methanogenesis as a major component of aquatic CH_4 fluxes, *Nature Communications*, **5**, 5350.
Conrad, R. (2009), The global methane cycle: recent advances in understanding the microbial processes involved, *Environmental Microbiology Reports*, **1**, 285-292.
Damm, E., Helmke, E., Thoms, S., Schauer, U., Noethig, E., Bakker, K. *et al.* (2010), Methane production in aerobic oligotrophic surface water in the central Arctic Ocean. *Biogeosciences*, **7**, 1099-1108.
Fernandez, J.E., Peeters, F. *et al.*. (2014), Importance of the autumn overturn and anoxic conditions in the hypolimnion for the annual methane emissions from a temperate lake, *Environ. Sci. Technol.*, **48**, 7297-304.
Grossart, H.-P., Frindte, K., Dziallas, C., Eckert, W. & Tang, K.W. (2011), Microbial methane production in oxygenated water column of an oligotrophic lake, *Proc. Natl. Acad. Sci. U.S.A.*, **108**, 19657-19661.
Hofmann, H., Federwisch, L. & Peeters, F. (2010), Wave-induced release of methane: Littoral zones as a source of methane in lakes, *Limnol Oceanogr*, **55**, 1990-2000.
Lorke, A., McGinnis, D.F., Spaak, P. & Wuest, A. (2004), Acoustic observations of zooplankton in lakes using a Doppler current profiler, *Freshwat. Biol.*, **49**, 1280-1292.
McGinnis, D.F., Kirillin, G., Tang, K.W., Flury, S., Bodmer, P., *et al.* (2015), Enhancing surface methane fluxes from an oligotrophic lake: exploring the microbubble hypothesis, *Environ. Sci. Technol.*, **49**, 873-880.
Oude, P.J. & Gulati, R.D. (1988), Phosphorus and nitrogen excretion rates of zooplankton from the eutrophic Loosdrecht lakes, *Hydrobiologia*, **169 (3)**, 379-390.
Stöckli, A., D., Sanierung, D., Luzern, K., Vorbild, N., Luzern, K., Aargau, K., et al. (2016), Hallwilersee – nachhaltige Gesundung sicherstellen, **69**, 23−28.
Tang, K.W., McGinnis, D.F., Frindte, K., Bruchert, V. & Grossart, H.-P. (2014). Paradox reconsidered: Methane oversaturation in well-oxygenated lake waters. *Limnol Oceanogr*, **59**, 275-284.

Impact of Natural and Man-Made Factors on the Long-Term Variability of the Caspian Sea Level

G.S. Dyakonov[1,3]*, R.A. Ibrayev[1,2,3]

[1] *P.P.Shirshov Institute of Oceanology of the Russian Academy of Sciences, Moscow, Russian Federation*
[2] *Institute of Numerical Mathematics of the Russian Academy of Sciences, Moscow, Russian Federation*
[3] *Northern Water Problems Institute of Karelian Research Centre Russian Academy of Sciences, Petrozavodsk, Republic of Karelia, Russian Federation*

**Corresponding author, e-mail gleb.gosm@gmail.com*

KEYWORDS
Caspian Sea; climatic variability; level change; water balance; modelling.

EXTENDED ABSTRACT

Introduction

The long-term (climatic) variability of the Caspian Sea level and thermohaline structure observed in the second half of the 20th century is investigated by means of deterministic numerical modeling.

Isolated from the World Ocean the Caspian Sea is highly sensitive to global and regional climate variability. The Caspian Sea level can be regarded as an integral indicator of both regional climate change and circulation of the sea itself. Its water balance is influenced by diverse factors and is composed of three major elements: river discharge, precipitation and evaporation. The first two depend primarily on the external conditions while evaporation is a result of air-sea interaction influenced by both atmospheric parameters and the parameters of the sea such as sea surface temperature (SST), surface area and sea ice distribution. Quantitative estimation of the impact of these factors as well as the estimation of the man-made and climate change impact on the Caspian Sea level is the ultimate goal of our research.

Materials and methods

The tool we use is an eddy-resolving ocean general circulation primitive equation model coupled with models of air-sea interaction and sea ice thermodynamics. The model was developed specifically for the Caspian Sea to account for its peculiar features such as non-trivial water balance, flatness of its shores and wetting and drying of vast shore areas resulting in significant surface area variations. Particular attention is paid to the calculation of water and heat budget components.

Using the model we reconstruct the evolution of the Caspian Sea circulation and level in 1958-2001. The model is forced using the river discharge observational data and the ERA-40 reanalysis dataset which includes both synoptic and climatic variability modes. The atmospheric forcing was partially adjusted to match climatology: the wind speed is increased by 15%, the precipitation intensity is decreased by 34%, and the solar radiation flux is increased by 5%. Non-radiative heat flux components and evaporation are explicitly calculated by the model so the sea surface level and the SST obtained reflect the physical processes occurring in the sea as well as the external climatic variations. Figure 1 compares the observed evolution of the Caspian Sea surface height (SSH) and that reconstructed by the model in two separate runs started from 1958 and 1978. The first run covers almost the entire ERA-40 period, however the climatic regime shift of 1970's is not well reflected by the model and/or the forcing data. The latter model run is more successful, therefore it is used as the basic experiment for the series of sensitivity experiments discussed further.

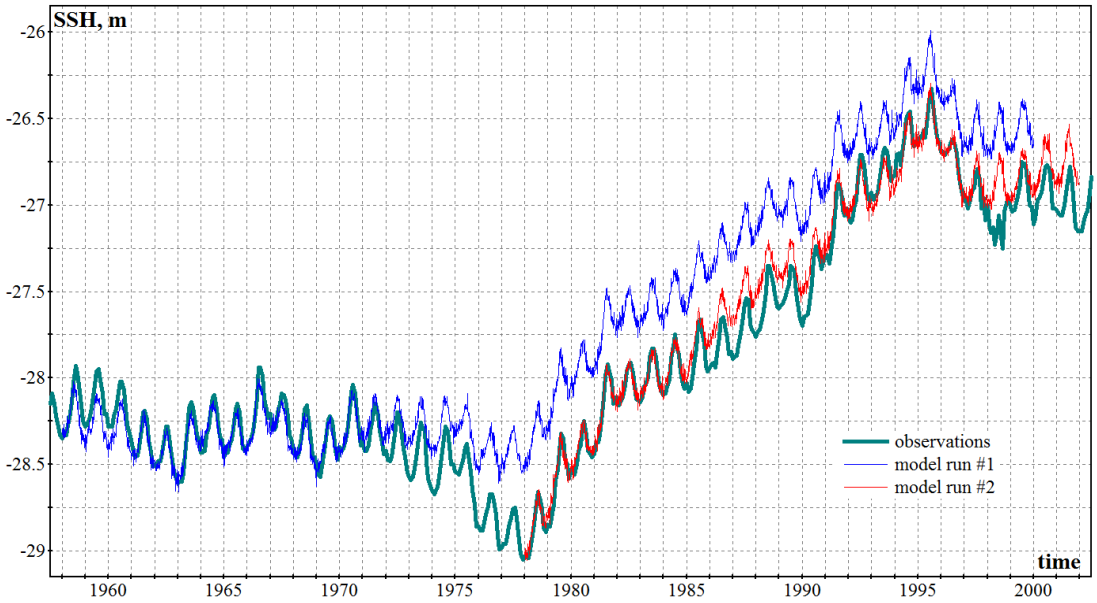

Figure 1. Caspian Sea surface height (SSH) in Baku: observed and obtained in two model runs differing only in the start moment (1958 and 1978) and the initial SSH.

In order to assess the impact of various factors on the water balance of the sea, a series of sensitivity experiments was conducted to study the response of the long-term SSH evolution to variations of atmospheric parameters, surface water and heat fluxes and sea surface area. As a quantitative measure of the sensitivity we use the deviation of the SSH uptrend observed in 1978-1995 from that obtained in the basic experiment (model run #2 on the fig. 1). The rate of the trend is 15.5 cm/year which is close to the observations.

Results and discussion

The results indicate that the water balance of the Caspian Sea is highly sensitive to most of the atmospheric parameters: a systematic 1°C increase of air temperature and a 1°C decrease of dew-point temperature led to a slowdown of the uptrend by the amount of 4.2 cm/year and 3 cm/year respectively. Curiously enough a considerable decrease of wind speed by 13% to match the ERA-40 data rather than climatology had little effect on the SSH: the uptrend rate increased by only 0.5 cm/year. The weakening of evaporation due to the wind speed reduction was not as significant as one could expect, because the corresponding increase of the SST mostly compensated the effect, so the resulting evaporation intensity decreased only slightly. Setting the solar radiation flux according to ERA-40, that is 5% lower than in the basic experiment, strengthened the SSH trend by 4.7 cm/year.

The influence of the Caspian Sea surface area variations on its water balance was also assessed. Disregarding the coastline expansion caused by the raise of the mean sea level, i.e. ‘freezing’ the minimal sea surface area of 1978, resulted in the reduction of the total evaporation flux and an additional SSH increase amounting to 3.6 cm/year. Thus, the negative feedback between the Caspian Sea surface level and its area has a significant damping effect on the variability of both. Additionally, the role of sea ice formation was investigated in the experiment with no account for the influence of the ice cover on the sea water budget: the decrease of the total evaporation flux due to ice cover contributes to the SSH trend about 0.75 cm/year.

Expectedly variations of precipitation and river runoff have strong impact on the Caspian Sea level. Using the ERA-40 precipitation, i.e. adding 50% to the climatology used in the basic experiment, yields additional 8.5 cm/year to the SSH. In turn, specifying the natural rate of the river discharge by addition of 12% of water withdrawn for economic activities in 1970-1980’s boosted the SSH trend by 9.5 cm/year.

Quesnel Lake's response to the catastrophic Mount Polley Mine tailings impoundment failure – 1 year post-spill

K. Graves[1]*, B. Laval[1], A. Hockin[1], S.Vagle [2], S. Petticrew[3] and S. Albers[4]

[1] *Department of Civil Engineering, University of British Columbia, Vancouver, Canada*
[2] *Institute of Ocean Sciences, Department of Fisheries and Oceans Canada, Government of Canada, Sidney, Canada*
[3] *Geography Program, University of Northern British Columbia, Prince George, Canada*
[4] *Quesnel River Research Centre, University of Northern British Columbia, British Columbia, Canada*

*Corresponding author, e-mail kellygraves@civil.ubc.ca

KEYWORDS
Fjord-lakes; environment; field observations; turbidity

EXTENDED ABSTRACT

Introduction

On August 4, 2014, the Mount Polley Mine (MPM) tailings impoundment catastrophically released 25 million cubic meters of tailings, process water, and other unknown materials, flowed down and eroded Hazeltine Creek, and deposited mine waste and Hazeltine Creek bed material into the deep water of the West Basin of Quesnel Lake. This spill drastically altered the physical qualities of Quesnel Lake, a near pristine, salmon bearing lake near the city of Williams Lake, Canada. It is a y-shaped lake with three arms: West, East, and North. The region where the three arms meet is referred to here as the Intersection. The distance from the West Arm to the East Arm spans 81 km. The lake has a mean depth of 157 m, a maximum depth 511 m, and an average residence time of 10.1 years. The West Basin, where the spill occurred, is a portion of the West Arm that is separated from the Main Basin by a sill (maximum depth of 35 m) located at Cariboo Island, and has a maximum depth of 113 m (*Laval et al. 2008*).

Materials and methods

Since the spill, there has been regular monitoring of the West Basin where the spill entered the lake; however, there has been little monitoring of the rest of the lake. In July 2015, one year after the spill, CTD transects were conducted along each arm of the lake to investigate the extent of the turbidity plume from the tailings deposit. Here we report on the time evolution of water properties in the West Basin for 15 months post spill, as well as on lake wide water properties in July 2015, almost one year post spill.

Results and discussion

Immediately after the spill, the turbidity in the deep water (below 35 m) in the West Basin went from a background turbidity of ~ 1 FTU to over 1000 FTU (Petticrew et al, 2015). By November 2014, the turbidity (which increases with depth), decreased to approximately 80 FTU at the bottom. Over the winter of 2014/2015, the West Basin turned over; however, by May 2015, the turbidity increased with depth to a maximum of about 2 FTU. Turbidity continued to decrease throughout the water column until Aug 19 when it started increasing. November 2015, the turbidity in the bottom half of the West Basin ranged from 2-4 FTU.

The West to East Arm turbidity transect of July 2015 (Figure 1a) shows significant regions of elevated turbidity at the Eastern end of the East Arm associated with glacially fed Niagara Creek. This turbidity signal extends downwards along the thalweg to the deepest regions of the East Arm. It also extends westward in the near-surface water suggesting a bifurcation of Niagara water as it flows through Quesnel Lake. To the west of the Intersection there is another near-surface region of elevated turbidity likely associated with the Horsefly River, Quesnel Lake's largest inflow. There is a turbidity signal in the surface water of the West Basin (Figure 1b) near the inflows from Hazeltine Creek). The inflow of the Mitchell River is evident as a near-surface turbidity plume at the north end of the North Arm.

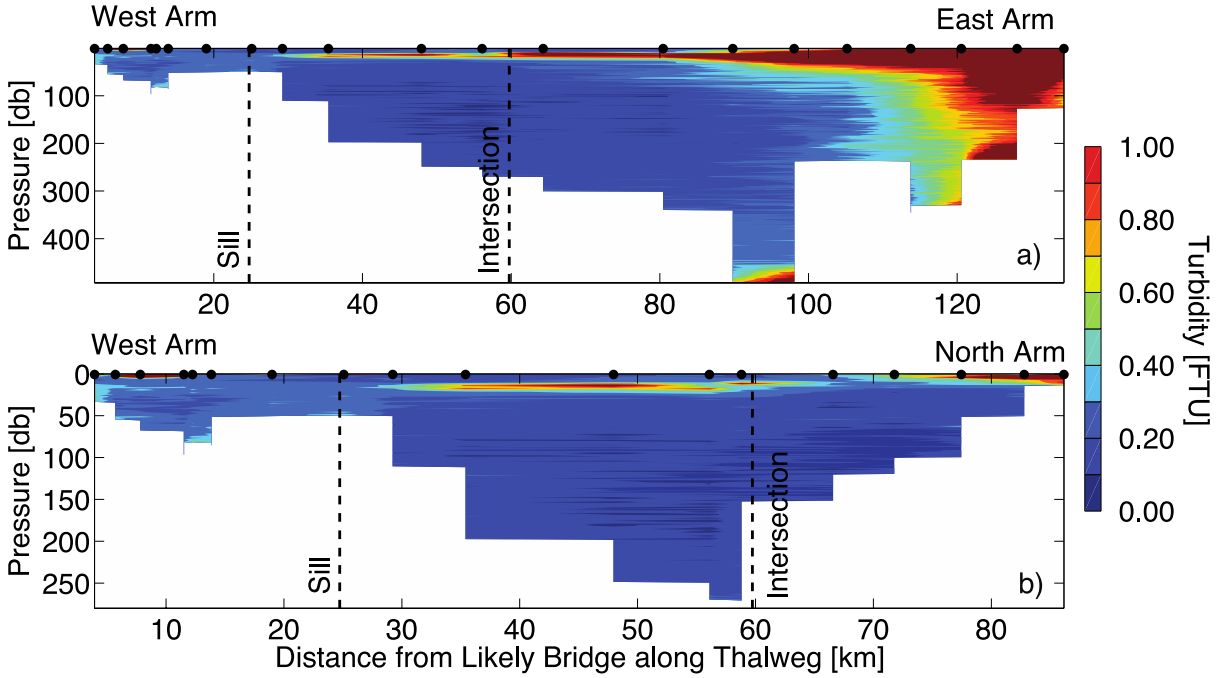

Figure 1 Turbidity transect from a) West to East Arm, and b) West to North Arm. The section from the West Arm to the intersection is the same in Figure 1 a and b.

These July 2015 transects suggest Hazeltine Creek, Horsefly River, Niagara Creek, and Mitchell River are important sources of turbidity into Quesnel Lake. Note the transects occurred near the period of minimum observed turbidity in the West Basin. Because of the various turbidity sources, tracking the turbidity from MPM throughout the lake nearly one year post spill is complicated by the other sources of turbidity and requires determining the origin of each turbidity signal.

REFERENCES

E. Petticrew, S. Albers, S. Baldwin, E. Carmack, S. Déry, N. Gantner, K. Graves, B. Laval, J. Morrison, P. Owens, D. Selbie, and S. Vagle (2015), The impact of a catastrophic mine tailings impoundment spill into one of North America's largest fjord lakes: Quesnel Lake, British Columbia, Canada, Geophys. Res. Lett., 42 (9), 3347-3355, doi: 10.1002/2015GL063345.

B. Laval, J. Morrison, D. Potts, E. Carmack, S. Vagle, C. James, F. McLaughlin, and M. Foreman (2008), Wind-driven summertime upwelling in a fjord-type lake and its impact on downstream river conditions: Quesnel Lake and River, British Columbia, Canada, J. of Great Lakes Res., 34(1), 189-203.

Sediment biogeochemical cycling in Australian subtropical reservoirs

A. Grinham[1]*, B. Gibbes[1], P. Fisher[1], S. Albert[1] and M. Bartkow[2]

[1] *School of Civil Engineering, The University of Queensland, Brisbane, Australia*
[2] *Seqwater, Brisbane, Australia*

**Corresponding author, e-mail a.grinham@uq.edu.au*

KEYWORDS
Sediment; nutrient dynamics; metal cycling; dissolved oxygen; subtopics.

EXTENDED ABSTRACT

Introduction

Benthic biogeochemical cycling plays a pivotal role in chemical loading bottom waters of inland water bodies such as lakes and freshwater reservoirs. Extensive research on these complex and dynamic cycles has been carried out in temperate areas, but fewer studies have addressed subtropical locations. Freshwater reservoirs within the subtropical regional are predicted to experience increasing thermal stratification under current climate projections and benthic biogeochemical processing will likely contribute chemical stratification. There is a need to better understand the vulnerability of freshwater reservoirs to meromixis and consequent reduction in available water supply. A crucial step towards achieving this is to quantify benthic biogeochemical processing rates across multiple systems to inform model development of this region. In this study, long term dissolved oxygen, methane, phosphorous, nitrogen compounds, iron and manganese cycling rates were estimated for sediments and bottom waters of the three freshwater reservoirs; Lake Wivenhoe, Little Nerang Dam and Hinze Dam in South East Queensland, Australia. Catchment land use varies between these reservoirs, where Lake Wivenhoe has 50% agriculture, whilst both Hinze and Little Nerang have over 85% native vegetation coverage and 10-15% agriculture (Burford et al., 2007).

Materials and methods

This study was undertaken using two parallel approaches. Firstly, laboratory sediments incubations from multiple replicates from multiples sites from were performed along dissolved oxygen gradients that mimic the changes that occur in storage bottom waters. Secondly, the processes evaluated in the sediment cores were compared to long term in situ measurements of in reservoir bottom waters. Sediment core collection and long term in situ monitoring were undertaken in the 3 major zones, riverine, transition and lacustrine (Wetzel 2001), to capture the range of sediment quality within each reservoir. Sediment core incubations followed the methodology outlined in Green et al. (2011). In situ monitoring of bottom waters was undertaken at monthly intervals over an annual cycle and followed the methodology of Burford et al. (2007).

Results and discussion

General patterns were observed across the individual core incubations and these changes were closely associated with changes in dissolved oxygen. The initial declines in dissolved oxygen level (aerobic conditions) from saturated levels were accompanied by increasing concentrations of the reduced reactant products, ammonia and dissolved manganese and

reduction in oxidised products nitrate and nitrite (Fig. 1 A). Increased iron and methane concentrations were delayed between 3 to 7 days after core capping under anaerobic conditions (Fig. 1 A). Whilst these patterns were common across sampling sites and reservoirs, distinct differences were observed in the magnitude of sediment flux rates between sites and storages. Peak efflux rates of ammonia, manganese and iron were highest from Lake Wivenhoe compared with Little Nerang and Hinze Dams which were of similar magnitude (Fig. 1 B). Dissolved methane efflux rates were similar between reservoirs (Fig. 1 B). The applicability of the sediment core incubation findings was illustrated by the striking similarities found with changes observed in the in situ monitoring data of bottom waters.

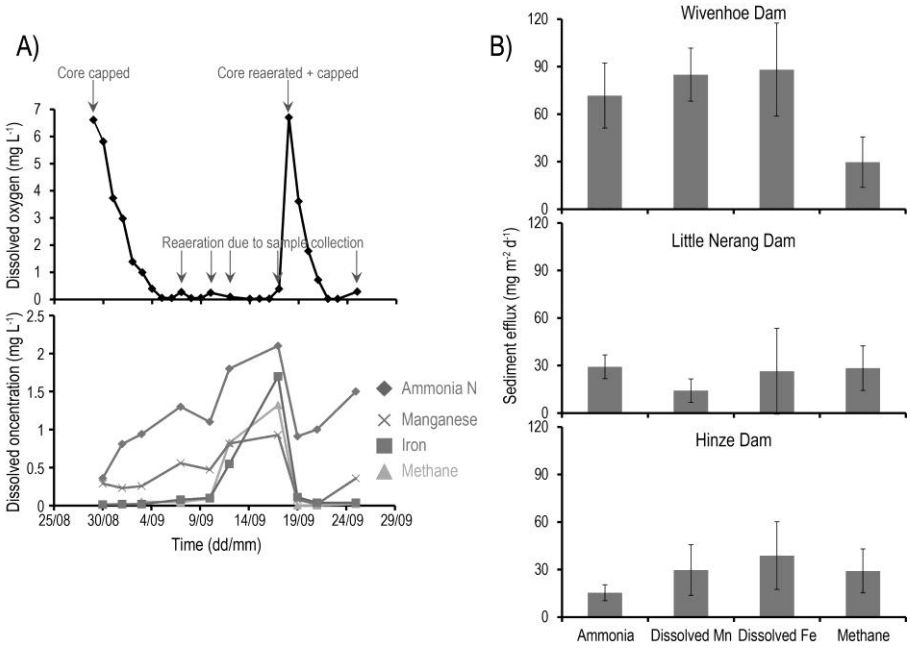

Figure 1. A) Example of the time-series changes in dissolved oxygen, ammonia, manganese, iron and methane concentrations in a single long term core incubation. Please note reaeration on 19/09 was by artificial bubbling and stripped dissolved methane from solution. B) Average peak sediment efflux rates of ammonia, manganese, iron and methane across all sites in the three reservoirs studied.

These findings greatly improve our understanding of benthic biogeochemical processing within reservoirs of the subtropical region and the implications for modelled predictions of reservoir vulnerability to meromixis. Of particular interest were the high sediment efflux rates of iron and manganese suggesting these should be included in reservoir biogeochemical models. This study also highlights the connection between catchment condition and reservoir biogeochemical cycling providing a potential management option to reduce risk of meromixis.

REFERENCES

Burford, M., S. Johnston, A. Cook, T. Packer, B. Taylor, E. Townsley (2007), The relative importance of watershed and reservoir characteristics in promoting algal blooms in subtropical reservoirs, *Wat Res*, **41,** 4204-4114

Green, T., A. Barnes, M. Bartkow, D. Gale, and A. Grinham (2011), Sediment bacteria and archaea community analysis and nutrient fluxes in a sub-tropical polymictic reservoir, *Aquat Microb Ecol*, **65(3)**, 287-302

Wetzel, R. (2001) *Limnology: Lake and River Ecosystems*, 3rd Ed., Academic Press, San Diego, California

Internal-Wave Stokes Drift and Isopycnal Setup Observed in a Sloping Lakebed Boundary Layer

Stephen M. Henderson[1]*, John A. Harrison[1], Bridget R. Deemer[1]

[1] *School of the Environment,*
Washington State University (Vancouver), Vancouver, WA, USA

**Corresponding author, e-mail steve_henderson@wsu.edu*

KEYWORDS
Lakes; mixing; advection; internal waves; boundary layers.

EXTENDED ABSTRACT

Introduction

In stratified lakes, turbulence within internal-wave bottom boundary layers (BBLs) might contribute significantly to basin-wide mixing. Mean advection by sheared BBL velocities is likely vital to persistent BBL mixing (Garrett *et al.* 1993). Mean advection is influenced by internal-wave-induced mass fluxes (Stokes drift), but Stokes drift has been neglected in previous BBL models and observations. We examine the interaction between mixing and mean advection in a sloping lakebed boundary layer, accounting for substantial Stokes drift.

Materials and methods

In Lacamas Lake (2000-m-long, 400-m-wide, 18-m-deep), velocity and temperature fluctuate owing to an upward-propagating internal seiche (period 10-32 hours, Henderson and Deemer 2012). During 2012 and 2015, Acoustic Doppler Profilers (ADPs; HR 2 MHz Nortek Aquadopps) and a vertical string of temperature loggers were deployed on the Thalweg (8-10 m depth), where the lower thermocline intersected the sloping lakebed.

Results and discussion

In the ~1-m-thick BBL (Figure 1), strong and weak stratification were respectively associated with stabilizing ($du/dz<0$) and destabilizing ($du/dz>0$) shear (u=upslope velocity).
Averaged over 48 days, the near-bed Eulerian velocity flowed down-slope (Figure 2, left), and was opposed by up-slope internal-wave Stokes drift (estimated by assuming weakly nonlinear waves propagated without change of form). To examine net transport, while relaxing approximations used to estimate the Stokes drift, the observed temperature range was divided into 0.5 ^{O}C increments, and the depth-integrated, wave-averaged flux of water in each temperature class was calculated. The associated transport velocity for cold, near-bed water was much smaller than the Eulerian mean velocity (Figure 2, right), consistent with near-cancelation by the Stokes drift (adiabatic models predict perfect cancelation, Ou and Mass, 1986). Above the BBL the Stokes drift reverses, consistent with theory.
Mean BBL advection was stabilizing ($du/dz<0$, lower meter of thick grey curve, Figure 2, right), consistent with a theoretical balance between shear-induced generation and mixing-induced destruction of stratification (implied turbulent temperature flux ~10^{-5} ^{O}Cms^{-1}). Wave-averaged stratification was strong (1 ^{O}Cm^{-1}) within 0.2 m of the bed, where turbulence was likely most intense. Furthermore, owing to the downslope Eulerian mean flow, the highest speeds (likely associated with intense turbulence) occurred during downslope flow, when shear enhanced stratification.
The Eulerian mean flow opposing the Stokes drift resembles undertow under surface waves on beaches. Internal wave radiation stresses can also generate a mean thermocline slope, reminiscent of surfzone sea-level setup (Umeyama and Shintani, 2006). Paired upslope and

downslope thermister strings separated by 30 m revealed a mean within-BBL isotherm slope ~$3_5 10^{-3}$ (c.f. above-BBL slope≈0). Resulting lateral BBL-integrated pressure forces were substantial (comparable to wave-averaged bottom drag, given a drag coefficient of 10^{-3}).

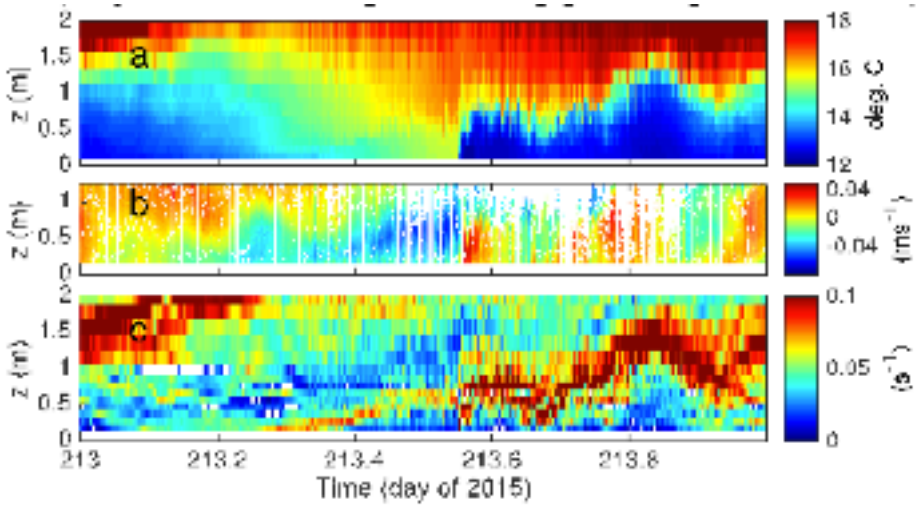

Figure 1. Wave-induced fluctuations in (a) temperature T, (b) upslope velocity u, and (c) buoyancy frequency N. Note arrival of internal bore at t=213.55.

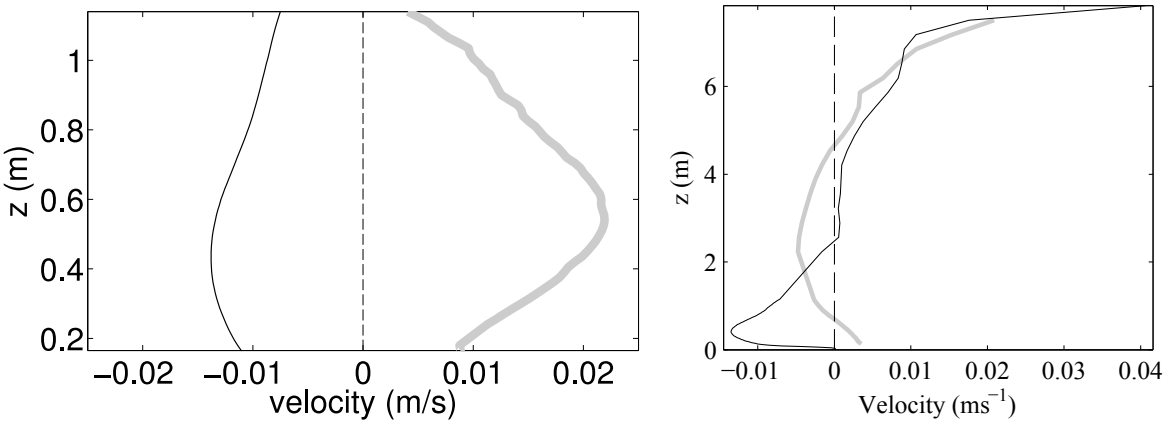

Figure 2. Wave-averaged upslope velocity versus elevation z. Left: Near-bed Eulerian velocity (thin black) and Stokes drift (thick grey). Right: Full-depth profiles of Eulerian (thin black) and Lagrangian (i.e. Eulerian plus Stokes, thick grey, estimated from water fluxes in narrow temperature classes) velocities.

REFERENCES

Garrett, Christopher and MacCready, Parker and Rhines, Peter (1993), Boundary mixing and arrested Ekman layers: rotating stratified flow near a sloping boundary, *Annu. Rev. Fluid Mech.,* **25**, 291-323.

Henderson, Stephen M. and Deemer, Bridget R. (2012), Vertical propagation of lakewide internal waves, *Geophysical Research Letters*, **33**, 1722-1732.

Ou, Hsein Wang and Maas, Leo (1986), Tidal-induced buoyancy flux and mean transverse circulation, *Continental Shelf Research*, **5**, 611-628.

Umeyama, Motohiko and Shintani, Tetsuya (2006), Transformation, Attenuation, Setup, and Undertow of Internal Waves on a Gentle Slope, *J. Waterway, Port, Coastal, Ocean Eng.*, 132, 477-486.

A hydrodynamic approach to sediment distribution verified by hydroacoustic seabed classification in a complex shaped reservoir

S. Hilgert[1]*, J. W. Y. Bernardo[2], N. Bouton[1], T. Bleninger[2] and S. Fuchs[1]

[1] *Institute for Water and River Basin Management, Department of Aquatic Environmental Engineering, Karlsruhe Institute of Technology (KIT), Germany*
[2] *Graduate Program on Water Resources and Environmental* Engineering, Federal University of Paraná, Curitiba - PR, Brazil.

*Corresponding author, e-mail stephan.hilgert@kit.edu

KEYWORDS
Reservoir; hydro-dynamic; hydroacoustic; sedimentation; rouse number; weather scenarios

EXTENDED ABSTRACT

Introduction

Accumulated sediments in reservoirs are known to produce significant amounts of greenhouse gases in dependence to the accumulation rate and specific sediment parameters and boundary conditions such as temperature and age. Especially in developing countries, constructed reservoirs encompass enormous areas, which complicates representative sampling of sediment distribution or gas emission measurements.
In order to facilitate the estimation of sediment distribution and sediment characteristics in a reservoir, it was tested if hydrodynamic simulations could be set in relation to hydroacoustic seabed classification results.
Following the question if the interpolated sediment features apply to hydrodynamic simulation (Delft-3D) results, the Rouse number was selected to investigate deposition and resuspension during different inflow and weather scenarios. They are defined by wind forcing on the water surface and the discharge through the reservoir. Both aspects are represented by average and extreme situations. The aim of the study was to investigate, to which extend local and spatial sediment characteristics could be described by hydrodynamic modelling. Relevant parameters were granulometric distribution, sediment magnitude and organic content.

Materials and methods

Capivari reservoir is located 40 km northeast of Curitiba in the state of Paraná, Brazil at a latitude of about 2°S. The surface covers an area of 13.1 km^2 at an altitude of 788 masl. Its average depth is around 13.6 m while the deepest parts reach 45 m. By conducting hydro-acoustic surveys using a 38/200 kHz single beam echo sounder, basic morphometric and sediment information was obtained. Additionally, seabed classification was conducted, including extensive ground truthing (18 cores), which allowed for the spatial interpolation of the found results. The hydrodynamic model was created with the Delft3D suite of Deltares, which allowed as well for the execution of the simulations. Further treatment of the results involved Matlab and ArcGIS. Three discharge situations were considered to reflect the most frequent situations in the reservoir with a normal discharge and two flood events as the average of the yearly and decennial maxima of daily mean discharge. These values were derived from the operational records for the years from 1971 to 2013.

The simulation of the flow in the lake is performed under the influence of three wind speeds, all coming from NE. The chosen wind speeds represent a calm day, a light breeze and a gale. All together nine weather scenarios were run and the rouse number modeled for the reservoir. The Rouse number (P) was estimated by modeled eddy viscosity and settling velocity estimated by Stoke's equation for particles with d90=63µm. More details can be found in Bouton (2016).

Results and discussion

Strong winds cause an overall resuspension, while high inflow volumes (floods) lead to a differentiation of P-patterns over the lake. Simulated hydrodynamic conditions could be verified through the granulometric analysis at the coring positions (Figure 1). Where lower Rouse numbers reflected coarser material. However, results showed that short-term hydrodynamic simulation alone was not able to reproduce spatial sediment distribution. The morphometry could be identified to have a major influence on the sediment parameters, but seems to be complicated to be reproduced by the hydrodynamic simulations. The differing nature of the two sets of variables, the Rouse number on the one side and the sediment layer thickness on the other side, gave ground to the choice to evaluate the area that could be assigned to a data point. Extremely shallow parts and parts close to the shoreline were excluded, as well as those parts above steeper slopes of the lakebed and the sidearms. Among this restrained dataset, two classes were defined. One corresponds to the thickest 10 % quantile and the other to the thinnest 10% quantile. In absolute terms both classes brought together, 0.15 km^2 and 0.2 km^2, respectively. The total area assigned to the data points in each of these two classes was subdivided relative to the Rouse number and hence to the tendency to suspension and sedimentation conditions. According to Julien (2010) and the particle size considered the relevant Rouse number threshold is 1.25 above which sedimentation prevails and beneath which turbulence overcomes gravity and prevents particles from sinking to the lakebed. This led to two tables of partial areas where for each environmental situation, the total area was split in four and associated with one of the Rouse number classes. The comparison of relative sizes of these partial areas showed that contrary to the hypothesis, the areas of thicker sediment layers had a greater share under suspensive conditions and the areas of less sediment accumulation had larger parts under sedimentation conditions. This indicates contrary to the results of the analysis of the sampling site related observation, that a correlation of the Rouse number and the sediment layer thickness cannot be established under these simplified model choices. Future research may focus on the relation between Rouse number results and hydro-acoustic lakebed classification.

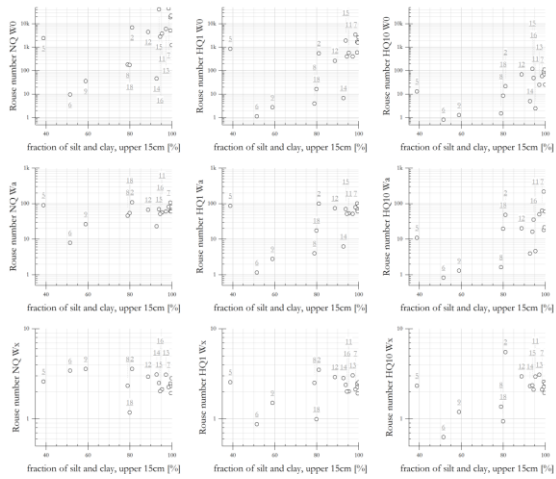

Figure 1. *Rouse number during different weather scenarios (NQ to HQ10 for floods and W_0 to Wx for no wind to extreme winds) versus fraction of silt and clay in the upper 15 cm of the sediment at the sample sites*.

REFERENCES

Julien, P. Y. (2010) Erosion and sedimentation, 2nd ed. Cambridge University Press, Cambridge, New York.

Nicolas Bouton (2016). A hydrodynamic approach to sedimentation and resuspension patterns in a morphologically complex reservoir (Master's thesis. Karlsruhe Institute of Technology, Karlsruhe, Germany).

Salt/fresh-water exchange in a small river delta with highly-modified inflows

B.R. Hodges[1]*, Z. Li[1]

[1] *Department of Civil, Architectural, and Environmental Engineering, University of Texas at Austin, USA*

**Corresponding author, e-mail hodges@utexas.edu*

KEYWORDS
Restoration; estuary; marsh; hydrodynamic model; high-resolution; wind effects; hypersalinity.

EXTENDED ABSTRACT

Introduction

The physics of salt/fresh-water exchange in river deltas is inextricably linked to the hydrological regime of inflows and flooding, which have been highly modified throughout the developed and developing world. Understanding how modifications of the hydrologic regime effect the upstream extent of salinity and duration/extent of brackish zones is critical to managing flows and maintaining ecosystem function. In this study, we look at the Nueces River delta, which is small (5 x 12 km) system of tidal creeks and marshes along Gulf of Mexico coast in Texas (USA). The delta's historic flooding pattern has been almost entirely eliminated by dams that isolate the majority of the 43,000 km^2 of watershed. As a consequence, the marshes have seen increasing water salinities and salt pans have developed in poorly-flushed areas. As part of restoration efforts, the City of Corpus Christi has installed a system of pumps and piping to provide controlled freshwater inflows. The key questions for the city are (1) how should the pumping system be operated to maximize the effect of the available fresh water? and (2) can physical modification of the bayous and creeks be used to improve the flushing effectiveness? To address these questions, we have developed a hydrodynamic model to evaluate the interplay between tide, wind, and inflows that affects flushing through the tidal creeks. Herein, we present some of the model results and discuss both the successes and limitations in representing the complex physics in the marsh/creek exchange zone for salt and fresh water

Materials and methods

The model applied to the Nueces delta is the Fine Resolution Environmental Hydrodynamics (Frehd) model, which is a research code written in Matlab. Frehd is solves the three-dimensional semi-implicit Navier-Stokes equations on a rectilinear mesh in a conservative finite different/volume formulation with fully 2nd-order discretization. The model uses numerical techniques similar to TRIM and ELCOM, which have been developed over the past 25 years (Hodges, 2014). For the Nueces delta we use Frehd's options for two-dimensional (2D) hydrostatic solution with conservative transport. The model bathymetry is developed from a 1 x 1 m lidar data set[1], which would require 45 million grid cells and 50 million time steps per year for direct simulation (slower than real time on a desktop workstation). By coarsening the grid to 30 x 30 m (Hodges, 2015) we obtain 160,000 grid cells and 500,000 time steps per year, which can run about 15 times faster than real time on a desktop

[1] Developed and validated by J. Gibeaut, Texas A&M University – Corpus Christi.

workstation with 2x2.66 Ghz 6-core Intel Xeon processors. With 16 Gb of RAM, four simulations were run at the same time on a single machine so that a wide range of scenarios to be efficiently simulated.

Results and discussion

Of critical importance is providing flooding with brackish water (less than 25 ppt) of at least 1 cm depth for 1/4 of a tidal cycle (6.2 hours), which is shown in Figure 1 for the existing system. Among the range of scenarios examined, we looked at how adding new channels could improve the inundation (Figure 2).

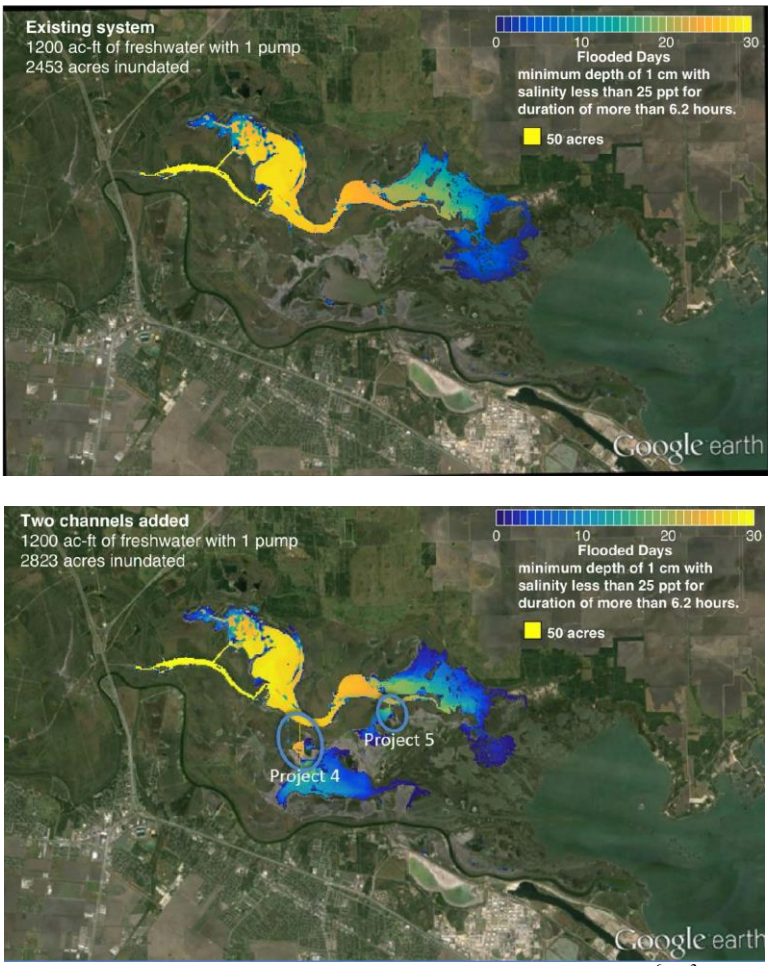

Figure 1. Baseline 60-day simulation (upper panel) with 1200 acre-feet (1.5×10^6 m^3) of freshwater pumped for 2453 acres of inundation (9.9 km^2). Proposed channel modifications (lower panel) for same conditions acre-feet provides 2823 acres of inundation (11.4 km^2).

The state-of-the-art for modelling of marsh systems needs improvement in several areas. Of principal importance are (1) transfer of wind shear to the water in depths less than 20 cm, (2) representation of small-scale creeks and channels at practical (coarse) modelling scales, and (3) the pore/surface water interchange that affects salinity storage and fluxes.

REFERENCES

Hodges, B.R., (2014). A new approach to the local time stepping problem for scalar transport, *Ocean Modelling*, **77**,1-19.

Hodges, B.R. (2015). Representing hydrodynamically important blocking features in coastal or riverine lidar topography, *Nat. Hazards Earth Syst. Sci.*, **15**, 1011–1023.

Scaling of benthic fluxes in permeable sediments

M. Holtappels[1,2,3*], A. Neumann[4], S. Ahmerkamp[1], H. Marchant[1], C. Winter[2]

[1]*Max Planck Institute for Marine Microbiology, Bremen, Germany*
[2]*Marum, Center for Marine Environmental Sciences, Bremen, Germany*
[3]*Alfred Wegener Institute, Helmholtz Center for Polar and Marine Research, Bremerhaven, Germany*
[4]*Helmholtz Center Geesthacht, Center for Materials and Coastal Research, Geesthacht, Germany*

**Corresponding author, e-mail moritz.holtappels@awi.de*

KEYWORDS
Permeable sediments; Porewater flow; Denitrification; Mineralization; Modelling

EXTENDED ABSTRACT

Introduction

Permeable sediments allow porewater advection and thus a flux of organic matter and electron acceptors which is orders of magnitude higher compared to diffusive flux. This fast transport sustains a diverse microbial community that lives attached to sand grains and has a large capacity to mineralize organic matter using mostly O_2 and NO_3^- as oxidants.

Despite their wide-spread occurrence, the role of permeable sediments in regional and global elemental cycling is poorly constrained, most likely because the dynamic forcing of porewater flow complicates the investigation of benthic-pelagic exchange processes. Porewater flow is driven by pressure gradients induced by the current flow across small scale topographies such as ripples or biogenic mounds. Thus, porewater flow depends on current velocity, bedform topography, and permeability. Consequently, the porewater flow controls the O_2 flux across the sediment-water interface, which further depends on O_2 bottom water concentrations and sedimentary O_2 consumption rates. Detailed investigations on how each of the independent variables affects the flux are rare, and generalizations from case studies to biogeochemical models are missing, which makes it difficult to elucidate the role of permeable sediments in global C and N-cycling.

Materials and methods

We developed a mathematical model, which allows an order of magnitude scaling of benthic fluxes for permeable sediments. The model is based on the analytical model of porewater advection of Elliot and Brooks (1997) which has been extended for the use reactive solutes and combined with empirical relations to reduce the number of necessary variables. Data from field studies are used to validate the model. In two field studies, the penetration depth of O_2 (North Sea) and NO_3- (N-W African shelf) was measured along with the volumetric consumption rate of the respective oxidant in the sediment (O_2, NO_3^-). The flux was determined by integrating the volumetric consumption rates over the penetration depth. In addition, a multitude of parameters (current velocity, seabed topography, sediment grain size as a proxy for permeability, bottom

water concentrations of O_2 and NO_3^-) were measured and fed into the model. Finally, the results of model and measurements were compared.

Results and discussion

The model: The flux of a reactive solute is estimated as a function of grain size (d_n), current velocity (U), bottom water concentration (C), kinematic viscosity (ν) and the volumetric reaction rate (R):

$$J = b\, d_n\, U \sqrt{\frac{RC}{\nu}} \qquad (1)$$

where b is a constant of approx. 3.4 x 10^{-3}. Interestingly, the flux scales linearly with grain size and velocity, but only with the square root of reaction rate and concentration. In diffusion limited muddy sediments, the flux can be estimated as $J = \sqrt{2\, D\, C\, R}$ and scales with the square root of the molecular diffusion coefficient (D). In comparison, the variables responsible for the porewater flow in (1), i.e. grain size (d_n) and current velocity (U), have a much greater effect on the flux, also because their magnitude can vary by two orders of magnitude in natural environments.

Field studies: Fluxes of O_2 and NO_3^- were moderately (North Sea) and significantly (N-W Africa) elevated compared to respective fluxes from diffusion limited muddy sediments. The NO_3^- flux on the N-W African shelf increased significantly with sediment grain size and permeability, indicating the important role of advective porewater transport.

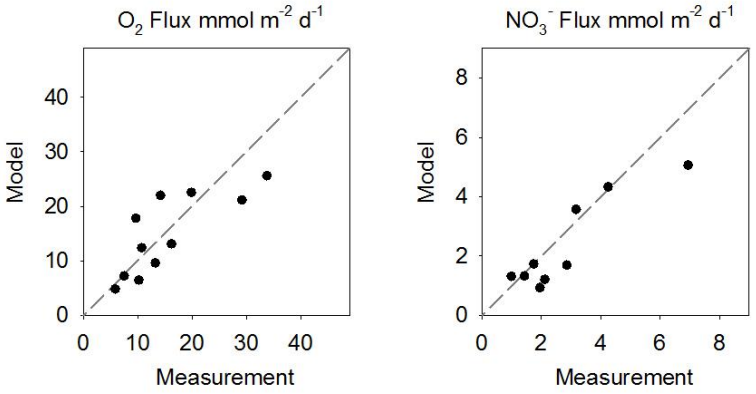

Figure 1. Comparison of measured and modelled fluxes from field sites in the North Sea (left) and N-W African shelf (right).

Using the measured boundary condition at the field sites, the fluxes were also calculated from equation 1. Modelled and measured fluxes agreed well (Figure 1) suggesting that the rather simple model captures a large part of the natural variability. The advantage of the model is that many of the input variables are either easy to measure or available from data depositories, which reduces the effort to estimate and extrapolate fluxes to regional scales.

REFERENCES

Elliott, A. H., and N. H. Brooks (1997), Transfer of nonsorbing solutes to a streambed with bedforms: Theory, Water Resour. Res., 33(1), 123-136, doi:10.1029/96WR02784.

Wind Wave Processes in Base Mine Lake

D. Hurley[1]*, G. Lawrence[1], E. Tedford[1]

[1] *Department of Civil Engineering,*
University of British Columbia, Vancouver, CA

**Corresponding author, e-mail dlhurley@ncsu.edu*

KEYWORDS
Wind waves, pit lakes, surfactant oil layer.

EXTENDED ABSTRACT

Introduction

Base Mine Lake (7.9 km^2), a small artificial lake in the Canadian oil sands, contains large quantities of fluid fine tailings (FFT) and oil sands process affected water (OSPW). One feature that is of specific interest is the release of hydrocarbons from the FFT and OSPW to the lakes surface. Once on the surface the hydrocarbons form an oil slick and can modulate the wind wave field (Behroozi et al., 2007). Since wind waves are the driving force behind many physical processes, their modification has direct implications on the remediation of BML. In this research the wind driven surface waves are examined numerically and the effect of oil on wind wave formation, growth, and whitecapping are studied in the laboratory and field.

Materials and methods

Numerical modelling of the wind waves in BML was carried out in SWAN using insitu measurements of the hourly average wind speed and direction (collected 1km NE of BML) along with 2m resolution bathymetry. The simulations were performed for a 2 week period in October 2014 on a nested curvilinear grid with a coarse and fine resolution of 50m and 5m respectively. Model output was validated to pressure data collected by an RBR DUO pressure sensor sampling at 6Hz and located 10m from shore along the northeast embankment. A GoPro Hero3+ camera was setup to capture an image of a 4m^2 patch of water every 30 minutes in the center of BML. These images were used to characterize the percentage of whitecapping with wind speed and inform the whitecapping dissipation parameter in SWAN.

A laboratory investigation into the effect of oil on waves was carried out in two parts. The first experiment used a 4mm diameter drop of water from a syringe mounted above the center of a cylindrical tank to generate a “ripple” wave field and observe the wave damping in the presence of oil. In the second experiment wind waves were generated in a small rectangular channel and their formation and growth on an oil surface was observed. In both experiments the water was dyed with rhodamine and wave statistics were measured using a high resolution Canon EOS 5Dsr aimed at a laser light sheet bisecting the center of each tank.

Results and discussion

The first laboratory experiment showed that oil has no effect on the damping of the observed gravity-capillary waves ($\lambda \sim 3cm$). Although previous works have shown an increase in the damping of pure capillary waves ($\lambda < 1cm$) (Behroozi et al., 2007), our generated waves are restored primarily by gravity. In the second experiment the oil was observed to eliminate the wave field almost completely (Fig. 1). It has been suggested that this effect is due in part

to the dampening of the high frequency waves, which leads to a shift in the wavenumber of maximum growth (Creamer and Wright, 1992), and to an increase in the critical wind speed (Kawai, 1979).

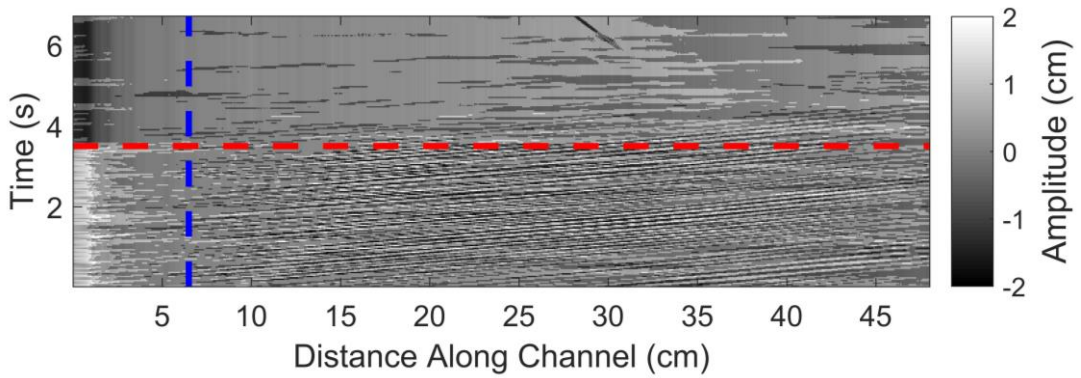

Figure 1. Wave amplitude before and after addition of oil layer (--). The presence of waves downwind after the addition of oil is because time is needed for the oil to cover the tank. The wind is not fully developed on the tank for the first few centimetres (--).

The model output shows good agreement with BML observed significant wave height (H_s) during storm events (RMSE~5cm). However, there is a general overprediction of H_s throughout the record, and especially during calm periods. In addition to the model not accounting for varying surface tension effects it is also likely that offsite wind speeds are not realistic of wind conditions near the pressure sensor. This is readily seen when the wind is out of the North and would therefore be significantly reduced by an embankment within a few meters of the shore.

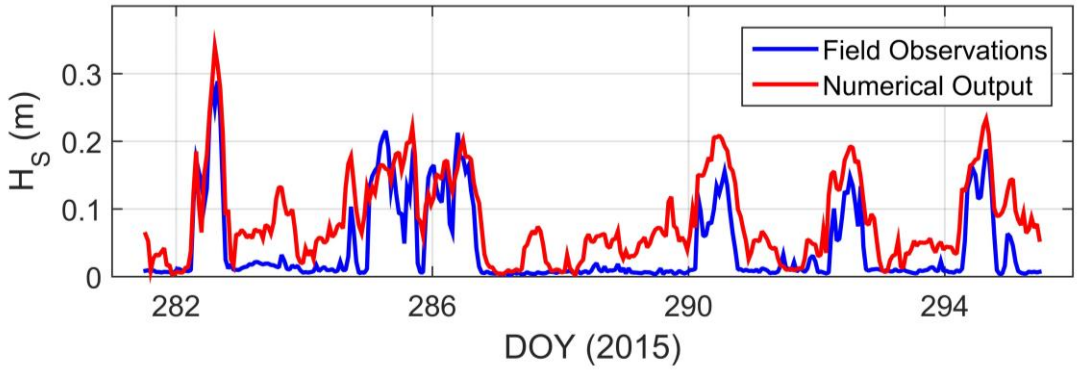

Figure 2. Numerical output and field observations of significant wave height (H_s) during a two week period in October 2014 on BML. Storm events coincide with winds out of the west.

References

Behroozi, P., et al. (2007), The calming effect of oil on water, *Am. J. Phys.*, **75(5)**, 407-414, doi: 10.1119/1.2710482

Creamer, D., J. Wright (1992), Surface films and wind wave growth, *J. Geophys. Res.,* **97**, 5221-5229.

Kawai, S. (1979), Discussion on the critical wind speed for wind-wave generation on the basis of shear flow instability theory, *J. Oceanographical Society of Japan.*, **35**, 179-186.

A process-based model for simulation of lake oxygen and dissolved inorganic carbon

P. Kiuru[1,2]*, A. Ojala[3], I. Mammarella[4], J. Heiskanen[4], T. Vesala[4] and T. Huttula[1]

[1] *Freshwater Centre, Finnish Environment Institute, Jyväskylä, Finland*
[2] *Department of Physics, University of Jyväskylä, Jyväskylä, Finland*
[3] *Department of Environmental Sciences, University of Helsinki, Lahti, Finland*
[4] *Department of Physics, University of Helsinki, Helsinki, Finland*

**Corresponding author, e-mail petri.kiuru@ymparisto.fi*

KEYWORDS
Lakes; gas exchange; carbon dioxide; modelling; biogeochemistry.

EXTENDED ABSTRACT

Introduction

Freshwater lakes are important in carbon cycling especially in the boreal zone, ventilating carbon originally fixed by the terrestrial system. The effect of climate change on lacustrine ecosystems is greatest in the high latitude regions. Higher air temperature shortens the length of the ice season and accelerates biological processes, and increased precipitation may result in elevated terrestrial carbon loading. However, the number of mechanistic models simulating the carbon cycle in boreal lakes is low. Advances in long-term high-frequency measurement of surface water concentration and air-water flux of carbon dioxide (CO_2) (Mammarella et al., 2015) form the basis for model development and enable reliable model validation. We present a 1D process-based model for simulating the vertical distribution and the air-water exchange of dissolved oxygen (DO) and dissolved inorganic carbon (DIC) in boreal lakes.

Materials and methods

Our model is an extension of a lake model MyLake (Saloranta and Andersen, 2007), which simulates lake thermodynamics and phosphorus-phytoplankton dynamics. Our model includes DO production by photosynthesis and surface aeration as well as DO consumption by autotrophic respiration and degradation of autochthonous and allochthonous organic carbon both in the water column and in the sediment. The model uses a previously developed module for microbial and photochemical degradation of dissolved organic carbon (DOC) in the water column (Holmberg et al., 2014). The production of CO_2 is coupled to the consumption of DO.

Lake Kuivajärvi is a humic lake in Southern Finland (61°50′ N, 24°17′ E) with a mean depth of 6.4 m (maximum 13.2 m) and an area of 0.64 km^2. We set up a model application for the lake for the years 2013-2014. We used measurements from the nearby SMEAR II station in Hyytiälä or from the measurement raft on the lake as the meteorological forcing data. In the model setup and calibration, we have made use of the comprehensive measurement data available on carbon inflow and the concentration of DOC in the lake as well as the continuous high-frequency measurements of water column concentrations of CO_2 and temperature.

Results and discussion

The model was calibrated for temperature, DO, and CO_2 for the year 2013. The simulated temperature was well in accordance with the measurements (surface temperature RMSE =

1.08 °C) (Figure 1A). The position of the thermocline, which is an important factor in the dynamics of dissolved substances, was also reasonably captured by the model. First model results for the seasonal dynamics of DO and CO_2 were relatively satisfactory as well (Figure 1B and 1C). The role of physical processes in dissolved gas dynamics is pronounced in this boreal dimictic lake. The short mixing period that was due to late ice melt in spring 2013 was not correctly captured by the model because of the 24 hour temporal resolution. The model tends to produce under-ice turnover before ice melt because of increased radiative heating of surface water and consequential convective mixing. The radiative heat flux through ice is governed by thermal and optical properties of snow and ice, which may vary greatly during late winter and are hence difficult to parametrize.

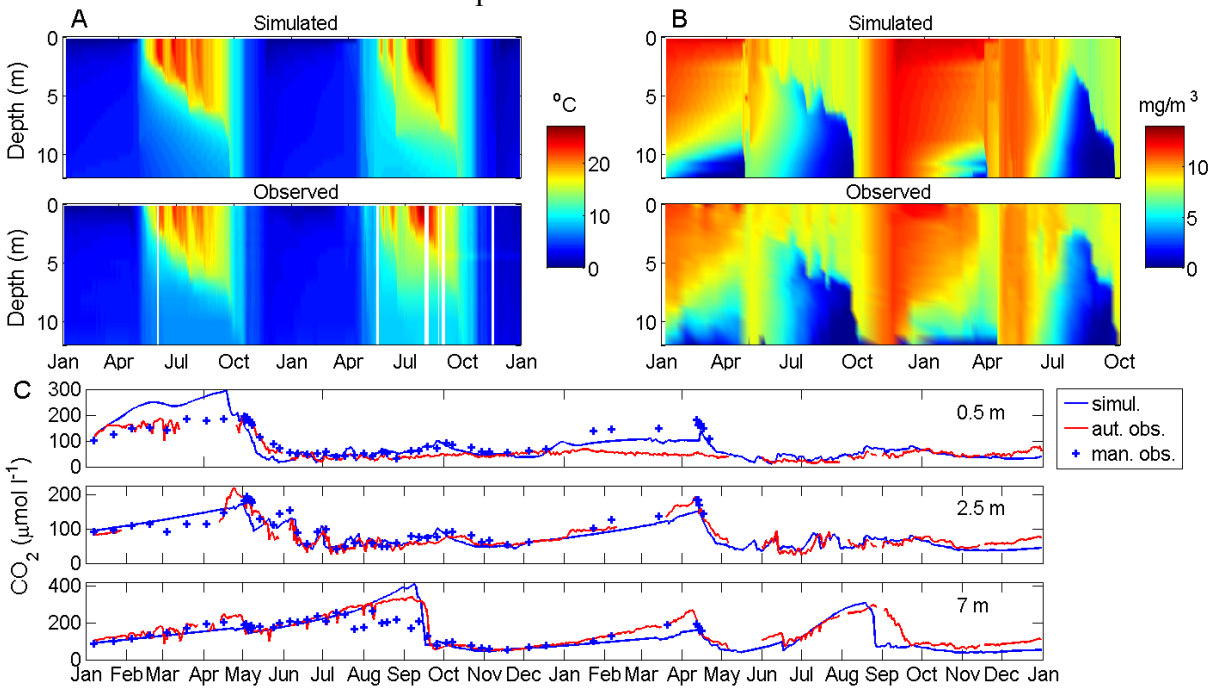

Figure 1. Comparison between simulated and observed profiles of water temperature (A) and dissolved oxygen (B) as well as simulated and both automatically and manually measured CO_2 concentrations at the depths of 0.5, 2.5, and 7 m (C) in Lake Kuivajärvi in 2013–2014.

Our model is intended to serve as a starting point for more detailed modelling of evasion of greenhouse gases and thus enables the further development of a process-based modelling tool for studying the effect of higher atmospheric temperatures and increased carbon loading on the dynamics of greenhouse gases in boreal lakes.

REFERENCES

Holmberg, M., M.N. Futter, , N. Kotamäki, S Fronzek, M. Forsius, P. Kiuru, N. Pirttioja, K. Rasmus, M. Starr, and J. Vuorenmaa (2014), Effects of changing climate on the hydrology of a boreal catchment and lake DOC – probabilistic assessment of a dynamic model chain, *Boreal Env. Res.* **19 (A),** 66-82

Mammarella, I., A. Nordbo, Ü. Rannik, S. Haapanala, J. Levula, H. Laakso, A. Ojala, O. Peltola, J. Heiskanen, J. Pumpanen, and T. Vesala (2015), Carbon dioxide and energy fluxes over a small boreal lake in Southern Finland, *J. Geophys. Res. Biogeosci.*, **120 (7)**, 1296-1314, doi: 10.1002/2014JG002873

Saloranta, T.M., and T. Andersen (2007), MyLake – A multi-year lake simulation model code suitable for uncertainty and sensitivity analysis simulations, *Ecol. Model.*, **207 (1)**, 45-60

Baroclinic response to wind in a multi-arm multi-basin lake

Y. Imam[1,2], B. Laval[2*], R. Pieters[2], and G. Lawrence[3]

[1] *Irrigation and Hydraulics Department, Faculty of Engineering, Cairo University, Giza, Egypt, 12613.*
[2] *Department of Civil Engineering, University of British Columbia. Vancouver, British Columbia, Canada, V6T 1Z4.*
[3] *Department of Earth, Ocea nand Atmospheric Sciences, University of British Columbia. Vancouver, British Columbia, Canada, V6T 1Z4.*

**Corresponding author, e-mail blaval@civil.ubc.ca*

KEYWORDS
Lakes; modelling; internal waves; modal analysis.

EXTENDED ABSTRACT

Introduction

Wind acting on the surface of stratified lakes energizes basin-scale baroclinic wave modes, also known as internal seiches (Hutter et al., 2011). Excitation, amplification, and decay of baroclinic modes are influenced by lake bathymetry, the spatial and temporal characteristics of the wind forcing, density stratification, and dissipative processes (Lemmin et al, 2005; Shimizu et al. 2007). Identification of modes that dominate the baroclinic response to wind is important to understanding water movement and mixing in lakes. The conventional method for identifying dominant modes in lakes applies spectral or time-frequency analysis to the baroclinic response at few locations within lakes (e.g. Lemmin et al., 2005). A more recent method is modal decomposition of the spatial structure of in-lake temperature and velocity fields (Shimizu et al., 2007; Valerio et al., 2012; Rozas et al. 2013; Guyennon et al, 2014). This spatial decomposition is done at regular time intervals over the period of observed or simulated response to wind. By assuming that wind-induced deflections of the metalimnion are a linear superposition of baroclinic modes and that mixing is negligible, modal decomposition gives the magnitude and damping time-scale of the baroclinic modes (Shimizu et al., 2007).

Here we examine the internal wave response to wind forcing in Nechako Reservoir located in central British Columbia, Canada (Figure 1). Completion of Kenney Dam in 1952 flooded several lakes and river reaches to form this long (~200 km), narrow (~2 km) reservoir with multiple basins and arms. There is currently no outlet at Kenney Dam, and a cold-water release facility has been proposed to regulate summertime river temperature downstream in the Nechako River with the intention of improving spawning salmon returns downstream of the dam. This study was motivated by the need to predict the availability of cold water at the proposed release facility. Our focus is on the two basins nearest Kenney Dam, Natalkuz and Knewstubb Lakes, and the flooded river section joining them; collectively referred to here as Natalkuz-Knewstubb Lake. Natalkuz-Knewstubb Lake is a water body 75 km long with an average width of 2 km, and two basins and six arms. The wind was found to be relatively uniform along the length of the basin.

Methods

Three-layer modal decomposition of data from a validated three-dimensional hydrodynamic numerical model (ELCOM) is used to identify the dominant baroclinic modes.

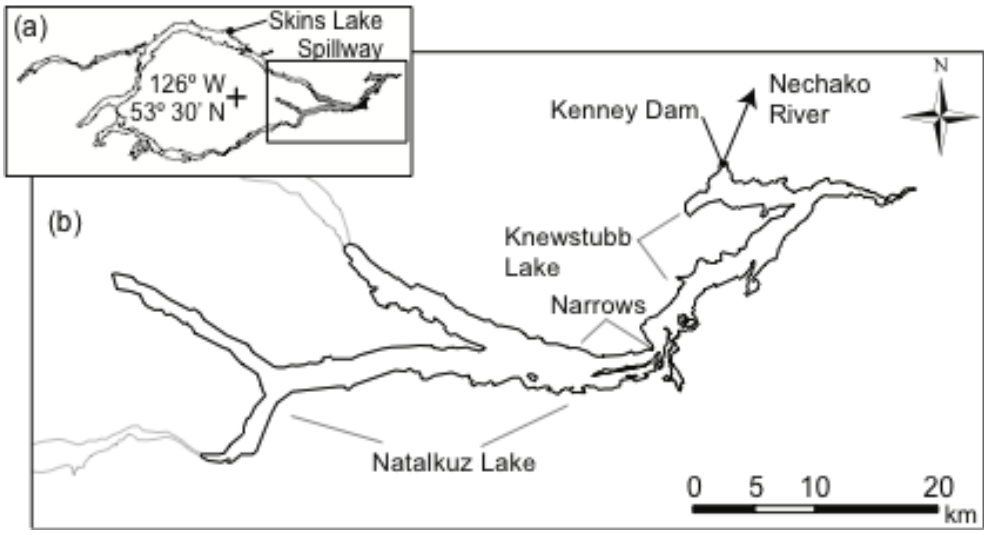

Figure 1. (a) Map of Nechako Reservoir. (b) Map of the eastern part of Nechako Reservoir showing Knewstubb and Natalkuz Lakes, shaded in (a). Reservoir shoreline corresponds to the high water mark, at 853.4 m above mean sea level. The solid triangles indicate the location of the thermistor moorings and floating weather stations deployed in 1994. Locations of CTD profiles, also conducted in 1994, are indicated by numbered circles. (c) Polar histogram of wind direction at station SK for June to September, 2005 to 2010. The histogram is for wind speeds exceeding 2 m s^{-1}.

Results and discussion

As observed in many lakes and reservoirs of simpler geometry, the most energetic mode in Natalkuz-Knewstubb Lake is the first-vertical first-horizontal mode (V1H1) along the length of the whole basin. However, changes in thalweg orientation with respect to local wind direction (particularily in Knewstubb Arm), as well as the geometric constriction between basins (at the Narrows) results in the excitation of higher vertical and horizontal modes by effectively acting to partition the lake into smaller sub-regions, each with their own oscillations superimposed on the lake-wide V1H1. The first horizontal mode of each sub-region is observed as higher horizontal modes in Natalkuz-Knewstubb Lake. Second vertical mode oscillations in sub-regions are associated with metalimnetic compression at the downwind end of a sub-region with commensurate metalimnetic expansion at the upwind end. These changes in metalimnetic thickness lead to metalimnetic intrusions following the relaxation of wind forcing. The findings of this study contribute to characterizing the baroclinic response of lakes with complex bathymetry.

REFERENCES

Guyennon, N., G. Valerio, F. Salerno, M. Pilotti, G. Tartari, and D. Copetti. (2014), Internal wave weather heterogeneity in a deep multi-basin subalpine lake… *Adv. Wat. Res*. **71**: 149–161. doi:10. 1016/j.advwatres.2014.06.013.

Hutter, K., Y. Wang, and I. P. Chubarenko. (2011), Physics of Lakes: Vol 2. Springer. pp 646.

Lemmin, U., C. H. Mortimer, and E. Baüerle. (2005), Internal seiche dynamics in Lake Geneva. *Limnol. Oceanogr*. **50**: 207–216.

Shimizu, K., J. Imberger, and M. Kumagai. (2007), Horizontal structure and excitation of primary motions in a strongly stratified lake. *Limnol. Oceanogr.* **52**: 2641-2655.

Rozas, C., A. de la Fuente, H. Ulloa, P. Davies, and Y. Niño. (2013), Quantifying the effect of wind on internal wave resonance in Lake Villarrica, Chile. *Env. Fluid Mech.* **14**: 1–23.

Valerio, G., M. Pilotti, C. Luisa Marti, and J. Imberger. (2012), The structure of basin-scale internal waves in a stratified lake… *Limnol. Oceanogr.* **57**: 772–786.

Towards Relaxed Eddy Accumulation Measurements of Fluxes at the Sediment-Water Interface in Aquatic Ecosystems

B. J. Lemaire[1]*, C. Noss[2], A. Lorke[2]

[1] *LEESU, AgroParisTech, ENPC, UPEC, Université Paris-Est, 77455, Marne-la-Vallée, France*
[2] *Institute for Environmental Sciences, University of Koblenz-Landau, 76829, Landau, Germany*

*Corresponding author, e-mail bruno.lemaire@agroparistech.fr

KEYWORDS
Shallow water; nutrient; micropollutant; sediment release; internal load.

EXTENDED ABSTRACT

Introduction

Nutrients and micropollutants from bottom sediment are major drivers and pressures in aquatic ecosystems, especially in shallow lakes where they can be brought back to the water column by frequent wind mixing. Vertical fluxes of nutrients are expected to exhibit a strong hourly variability, as was observed by eddy covariance for their proxy, the dissolved oxygen flux (Murniati et al., 2015). However, this dynamics cannot be resolved with available techniques, like laboratory sediment incubation, vertical concentration gradient measurements and mass balance in benthic chambers or in the water body. Nor are the fast-response sensors required for eddy covariance (EC) available for nutrients and micropollutants. At the land-atmosphere interface, relaxed eddy accumulation (REA) removes this requirement and has been used for 25 years to measure turbulent fluxes of various trace gases and particles (Foken, 2008). Air moving upwards and downwards is sampled separately at a frequency of around 10 Hz and the samples accumulated over 30-min segments. The eddy flux F is proportional to the difference between the concentrations $\overline{C_{\uparrow}}$ and $\overline{C_{\downarrow}}$ in updraft and downdraft samples:

$$F = b\sigma_w\left(\overline{C_{\uparrow}} - \overline{C_{\downarrow}}\right) \quad (1)$$

where σ_w is the standard deviation of vertical current velocity and b an empirical coefficient. The concentrations are measured *in situ* with slow-response sensors or in the laboratory. REA looks promising in shallow aquatic ecosystems and could provide the dynamics of all kinds of scalar fluxes, including dissolved and particulate nutrients and micropollutants. In a first attempt, we assessed the feasibility of conditional sampling and flux computation through a re-analysis of eddy-covariance measurements.

Materials and methods

We simulated REA fluxes with eddy-covariance measurements of velocity, temperature and dissolved oxygen at the sediment-water interface of a riverine lake in Germany. The 30-400 min time series were measured at 8 Hz with an acoustic Doppler velocimeter, a micro-thermistor and oxygen micro-electrodes, during 19 deployments over a year, 15 cm above the sediment and at depths 3.3-7.7 m (Murniati et al., 2015). We computed EC fluxes with a classical processing: double axis rotation on 30-min segments, high-pass filtering of turbulent fluctuations and correction of the delay due to sensor separation by maximising fluxes (*e.g.*,

Lorke et al., 2013). Conditioning sampling with such a processing does not look feasible, thus we limited velocity processing to a double axis rotation for each whole deployment and velocity filtering for REA simulations. The *b* coefficient is of particular importance and was extracted from Eq. 1 by equating on each segment EC and REA fluxes for momentum, heat and oxygen fluxes.

Results and discussion

It was necessary to subtract an advective term linking velocity and concentration averages from the REA flux, since vertical velocities can be biased in the rough processing. In the atmosphere, *b* coefficients vary with stability due to convective effects (Ammann and Meixner, 2002). Here we found them independent from dimensionless height $z\,u^*/\nu$, where u^* is friction velocity and ν water kinematic viscosity. Their average value was about double the theoretically value of 0.627 for a Gaussian distribution of turbulent fluctuations, *i.e.* 1.42 ± 0.25 ($n = 104$) for the coefficient for momentum fluxes. With this average value, REA fluxes matched EC fluxes for heat and oxygen, with a mean absolute error divided by mean EC fluxes of around 50 % (Fig. 1). The improvement by segment rotation and delay correction, probably impossible to achieve *in situ*, is minor, by 5 %.

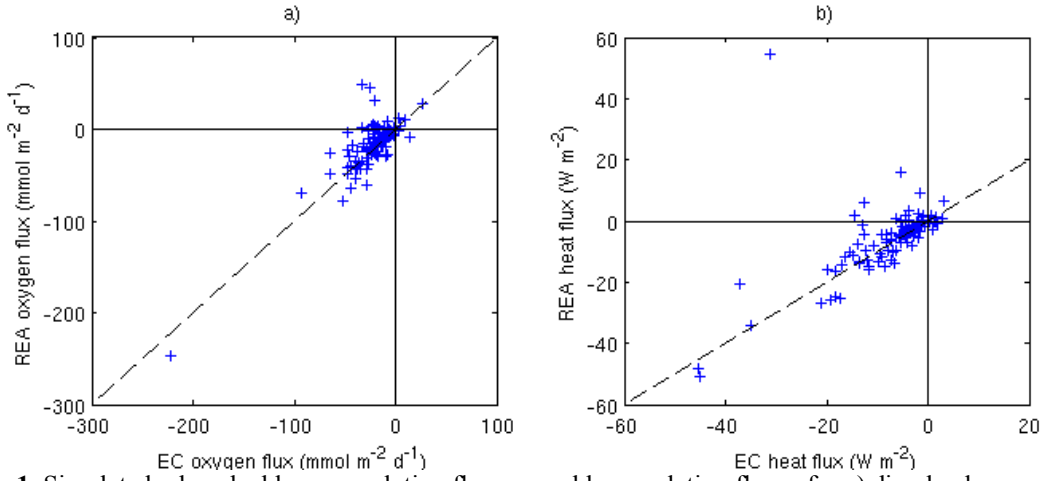

Figure 1. Simulated relaxed eddy accumulation fluxes vs eddy correlation fluxes for a) dissolved oxygen, b) heat. REA fluxes were computed with a constant value of 1.42.

This shows that REA should be feasible in aquatic environments, provided that velocity is high-pass filtered and coordinate axes aligned with the bottom before sampling. Other technical challenges remain: fast separate sampling, sample preservation and, most of all, sufficient analytical precision. For phosphates of instance, colorimetry accuracy must be improved by a factor 1000 compared to common practice to resolve the expected fluxes.

REFERENCES

Ammann, C., and F. X. Meixner (2002), Stability dependence of the relaxed eddy accumulation coefficient for various scalar quantities, *Journal of Geophysical Research-Atmospheres*, **107(D7-8)**.

Foken, T. (2008), Micrometeorology, Springer, Berlin, Germany.

Lorke, A., D. F. McGinnis, and A. Maeck (2013), Eddy-correlation measurements of benthic fluxes under complex flow conditions: Effects of coordinate transformations and averaging time scales, *Limnology and Oceanography: Methods*, **11**, 425-437.

Murniati, E., S. Geissler, and A. Lorke (2015), Short-term and seasonal variability of oxygen fluxes at the sediment–water interface in a riverine lake, *Aquatic Sciences*, **77(2)**, 183-196.

Estuarine Circulation versus Reverse Estuarine Circulation in the Gulf of Finland

M.-J. Lilover* and J. Elken

Marine Systems Institute at Tallinn University of Technology, Estonia

**Corresponding author, e-mail madis-jaak.lilover@msi.ttu.ee*

KEYWORDS
Gulf of Finland; ADCP measurements; estuarine circulation; reverse estuarine circulation.

EXTENDED ABSTRACT

Introduction

In case of estuarine circulation (EC) driven by density differences along an elongated estuary an outflow in the upper layer and inflow in the bottom layer takes place and in case of reverse estuarine circulation (REC) the flow directions in both layers are reversed. The current reversals in the deep layer are responsible for the appearance and disappearance of the saline water wedge in the bottom layer at the entrance area of the Gulf of Finland (GoF). The latter, in turn, is correlated with hypoxic and oxygenated conditions in the bottom layer. The REC gradually weakens the vertical density stratification and the consecutive mixing of the entire water column can take place similar to the wintertime thermal convection. Some earlier observations (Elken *et al*., 2003; Liblik *et al*., 2013) reported estuarine circulation reversals with the duration of a couple of weeks both for the summer and winter seasons. The aim of this study was to determine the statistics of the described phenomena and to characterize its background forcing.

Materials and methods

Five bottom-mounted current profilers (ADCP, 300 kHz, Teledyne RD Instruments) time series (RW21, R25, P9, P22 and RE20) were performed along the thalweg of the gulf at 4 different location (Figure 1). At stations RW21 and RE20 the measurements were performed at winter/spring 2012 and at R25 at winter/spring 2014. Stations P9 and P22 had the same location in the central part of the study area but different observation periods, summers of 2010 and 2012, respectively.

Results and discussion

There are four different flow regimes corresponding to the sign combinations of zonal current speed near the surface and near the bottom: estuarine circulation (EC, $u_s < 0$, $u_b > 0$), reverse estuarine circulation (REC, $u_s > 0$, $u_b < 0$), unidirectional inflow (UIN, $u_s > 0$, $u_b > 0$) and unidirectional outflow (UOUT, $u_s < 0$, $u_b < 0$). Results of analysis presented in Table 1 show that during the summer observation period in 2012 when the mean zonal wind stress was 0.028 N m^{-2}, the prevailing flow type at P22 was bidirectional flow (71% of time) where EC took place in 27% and REC in 44% of time, UIN and UOUT took place in 14% and 15% of time respectively. During another summer of 2010 when mean zonal wind stress was lower (0.011 N m^{-2}), observations at P9 revealed also dominating bidirectional flows, but EC prevailed over REC (43% vs 17%). For winter/spring periods the unidirectional and two-

directional flows were roughly in balance. As a winter mean EC took place in about 17% and REC in about 30% of time.

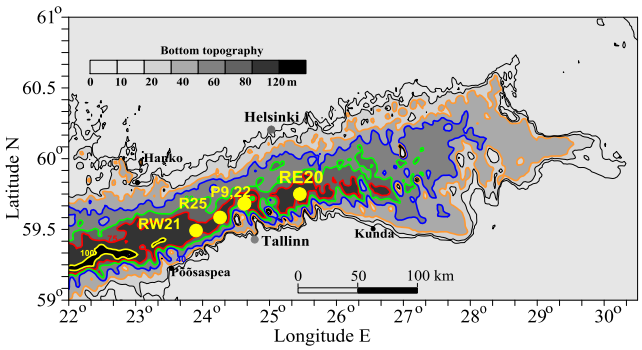

Figure 1. Map of the Gulf of Finland with bathymetry. The locations of the bottom-mounted ADCP measurements along the thalweg are indicated by yellow dots (4 locations, 5 measurements series).

We have found observational evidence that deep along-basin current velocities depend on the wind velocity with correlations above 0.7: maximum deep inflows occur in winter during north-easterly winds and in summer during easterly winds, and outflows during the winds from reverse direction. This relation is in agreement with the results of calculations of along the channel axis wind forced flows, using the analytical model by Winant (2004). For the estuarine flow reversal in real conditions, W or SW wind speed must be stronger from some critical value. Rough guidance to the critical value of wind speed may obtained by analysis of Wedderburn number.

Table 1
Frequency (%) of vertical structures of flow: bidirectional estuarine (EC) and reversed estuarine (REC) flow, unidirectional inflow (UIN) and outflow (UOUT).

Station	EC (%)	REC (%)	UIN (%)	UOUT (%)
Winter (RW21)	14	28	**45**	13
Winter (R25)	21	31	24	24
Winter mean	*17*	*30*	*34*	*19*
Summer (P22)	26	**44**	15	15
Summer (P9)	**43**	17	15	25
Summer mean	*34*	*31*	*15*	*20*
Mean	26	30	25	19

Acknowledgements
The study was partly supported by institutional research funding IUT 19-6 of the Estonian Ministry of Education and Research, and partly by the Estonian Science Foundation grants 9278 and 9382. We are grateful to the crew and the scientific team of R/V Salme for assistance in the deployment of the ADCP, to Irina Suhhova for the assistance in ADCP data processing as well as to Jaan Laanemets and Urmas Lips for providing ADCP current measurements data.

REFERENCES
Elken, J., Raudsepp, U. and Lips, U., 2003. On the estuarine transport reversal in deep layers of the Gulf of Finland. *Journal of Sea Research*, *49*(4), pp.267-274.

Liblik, T., Laanemets, J., Raudsepp, U., Elken, J. and Suhhova, I., 2013. Estuarine circulation reversals and related rapid changes in winter near-bottom oxygen conditions in the Gulf of Finland, Baltic Sea. Ocean Science, 9(5), pp.917-930.

Winant, C.D., 2004. Three-dimensional wind-driven flow in an elongated, rotating basin. Journal of Physical Oceanography, 34(2), pp.462-476.

Predicting hypolimnetic oxygenation and epilimnetic mixing in a shallow eutrophic reservoir using a coupled three-dimensional hydrodynamic model

S. Chen [1], C. Lei [1], C.C. Carey [2], J.C. Little [3]*

[1] *School of Civil Engineering, The University of Sydney, Sydney, NSW 2006, Australia*
[2] *Department of Biological Sciences, Derring Hall, Virginia Tech, Blacksburg, VA 24061, USA*
[3] *Department of Civil and Environmental Engineering, Durham Hall, Virginia Tech, Blacksburg, VA 24061, USA*

**Corresponding author, e-mail:jcl@vt.edu*

KEYWORDS
Bubble plume; water jet; mixing; modelling; water quality.

EXTENDED ABSTRACT

Introduction

Water quality problems, including algal blooms and hypoxia, threaten the sustainability of aquatic ecosystems and the reliability of drinking water supply reservoirs. Various mixing and oxygenation systems are deployed to control these problems. Bubble-plume and side-stream supersaturation hypolimnetic oxygenation systems have been shown to successfully add oxygen to the hypolimnion of stratified lakes and reservoirs, with bubble-plume systems more successful in deeper water and side-stream supersaturation systems only recently shown to be successful in shallower water. A three-dimensional hydrodynamic model, Si3D, has been used to analyze these systems. A recently developed water-jet model is coupled with Si3D to simulate the side-stream supersaturation system, while a previously validated, coupled bubble-plume model is used to simulate an epilimnetic mixing system. In a case study, the two coupled-models are used to quantify the effect of mixing on thermal structure, providing simple relationships that can be used for design and operation.

Materials and methods

A bubble-plume epilimnetic mixer (EM) as well as a side-stream supersaturation (SSS) hypolimnetic oxygenation system are deployed in Falling Creek Reservoir (FCR), which is a drinking-water reservoir managed by the Western Virginia Water Authority, Virginia, USA. FCR is a shallow reservoir (maximum depth of 9.3 m and average depth of 4 m) that experiences hypoxia and occasional algal blooms during stratified periods [*Gerling et al.*, 2014]. The SSS is designed to add oxygen to the hypolimnion without causing destratification while the EM system is designed to simultaneously mix and deepen the thermocline and redistribute algal species vertically, thereby limiting light and nutrient availability for the growth of algae [*Visser et al.*, 2015]. The effect of mixing on the water temperature in FCR is investigated using the coupled Si3D model, in conjunction with the *in-situ* experiments during a summer period when the SSS and EM systems were operating sequentially.

Results and discussion

The numerical results obtained from the coupled Si3D model are compared with the experimental observations. The coupled water-jet and bubble-plume models in Si3D are used to simulate mixing induced by the SSS and EM systems. The comparison of the numerical and field temperature contours in Figure 1 shows that the model predicts the development of the thermal structure and the extent of the mixing correctly.

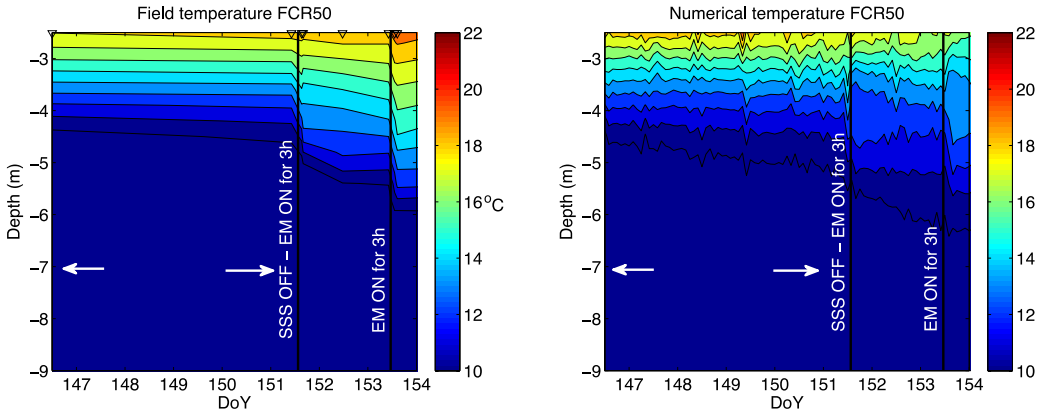

Figure 1. Time series of the field and numerical temperature contours at FCR50 during the sequential operation of the SSS and EM systems.

A case study is carried out using the Si3D. The study shows the extent to which the SSS and EM systems affect the thermal structure of the reservoir. For the SSS system, the relationship between the steepness (k) of the thermocline depth over time (fitted by a linear function) and the operational flow rate of the SSS system is characterized by a simple exponential function as:

$$k = -0.24e^{-0.004Q_{sss}} \quad (1)$$

where Q_{sss} represents the flow rate of the SSS system within the operational range in FCR. As for the EM system, the thermocline depth can be characterized by a double exponential function in terms of the duration of operation and the flow rate:

$$h = (h_0 - 0.63{Q_{EM}}^{0.21})e^{0.04d} + 0.63{Q_{EM}}^{0.21}e^{-1.72{Q_{EM}}^{0.24}d} \quad (2)$$

where h_0 is the initial depth of thermocline on top of the hypolimnion measured from the water surface, d is the duration of operation in days, and Q_{EM} represents the EM flow rate within the operational range in FCR.

These correlations represent an attempt to reveal mixing mechanisms induced by the SSS and EM systems and can be used when planning the future operation of the systems in FCR.

References

Gerling, A. B., R. G. Browne, P. A. Gantzer, M. H. Mobley, J. C. Little, and C. C. Carey (2014), First report of the successful operation of a side stream supersaturation hypolimnetic oxygenation system in a eutrophic, shallow reservoir, Water Research, 67(0), 129-143.

Visser, P., B. Ibelings, M. Bormans, and J. Huisman (2015), Artificial mixing to control cyanobacterial blooms: a review, Aquat Ecol, 1-19.

The role of sediment structure in gas bubble storage and release

L. Liu*, J. Wilkinson, K. Koca, C. Buchmann and A. Lorke

Institute for Environmental Sciences,
University of Koblenz-Landau, 76829 Landau, Germany

**Corresponding author, e-mail liu@uni-landau.de*

KEYWORDS
Sediment properties; methane; bubble formation; ebullition.

EXTENDED ABSTRACT

Introduction

Ebullition is an important pathway for the emission of biogenic methane from inland waters. However, methane fluxes associated with ebullition are intermittent and often characterized by "hot moments", which makes the accurate quantification and upscaling of methane fluxes from inland waters difficult [Bastviken et al., 2011]. Ebullition is often triggered by atmospheric/hydrostatic pressure changes. Although generally linear relationships between ebullition and the magnitude of pressure drop were observed in field data, uncertainties have also frequently been found [Maeck et al., 2014], which were linked to sediment characteristics and gas storage [Varadharajan and Hemond, 2012]. To improve our mechanistic understanding of methane bubble formation, storage and release in aquatic sediments, we conducted extended laboratory incubation experiments to study methane bubble formation and release dynamics in different sediments with different grain size distributions.

Materials and methods

Homogenized clayey, silty and sandy sediments (initially quasi-uniform through the depth of the columns, sediment thickness 30 cm) were incubated anaerobically in chambers (diameter 18.5 cm, height 49 cm) for three weeks. Total daily gas production (P_{tot}) was measured using a gas bag; daily gas entrapment in the sediments (S_{tot}) was measured by water level change; daily ebullition volume (E_b) was calculated as the difference between P_{tot} and S_{tot}; sediment water interface (SWI) level was measured daily to calculate the volume of free gas trapped by sediment expansion (S_{exp}). Total volumetric gas content (θ_{tot}) and the fraction of gas trapped by sediment expansion (θ_{exp}) were calculated from S_{tot} and S_{exp} (by dividing by the sediment volume). After the three-week incubation, hydrostatic head changes were applied to these sediments. The development of volumetric gas content in the sediments and the volume of ebullition triggered by hydrostatic head change were measured.

Results and discussion

Our results show that the methane bubble dynamics in sediments can be divided into three stages: Stage I – formation of micro bubbles, displacing mobile water in sediment pores with negligible ebullition; Stage II – formation of large bubbles, displacing surrounding sediment particles with concurrently increasing ebullition; Stage III – formation of conduits, with relatively steady ebullition (Fig. 1). The maximum depth-averaged gas content at steady state varied from 19% in clayey to 12% in silty and 13% in sandy sediment.
The gas storage mode and capacity depended highly on the grain size distribution of the sediment: in fine-grained sediment, free gas was mainly stored by sediment expansion, whereas in coarser sediments capillary invasion of the sediment matrix dominated gas storage.

A gas-enriched upper layer developed in each sediment column, with a thickness depending on sediment type (Fig. 2). The volume of individual ebullition episodes was found to be linearly correlated to hydrostatic head drop and its magnitude decreased from clayey to sandy to silty sediment (Fig. 3). The gas stored in the surface gassy layer was an important source of gas released by ebullition, but the ebullition potential was determined by the total amount of free gas in the sediment column.

The combination of these findings with sediment transport and deposition models could help resolve spatial heterogeneities in methane ebullition at large scales in inland waters.

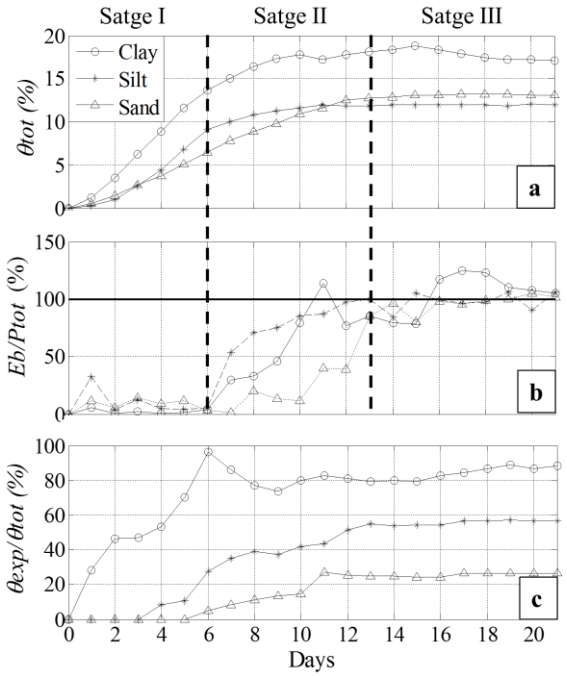

Fig. 1 a. Total gas content (θ_{tot}) in the sediments; b. Ratio of daily ebullition to total daily gas production (E_b/P_{tot}); c. Ratio of the gas content due to sediment expansion (θ_{exp}) and θ_{tot}. The two dashed lines separate the three stages of gas content development.

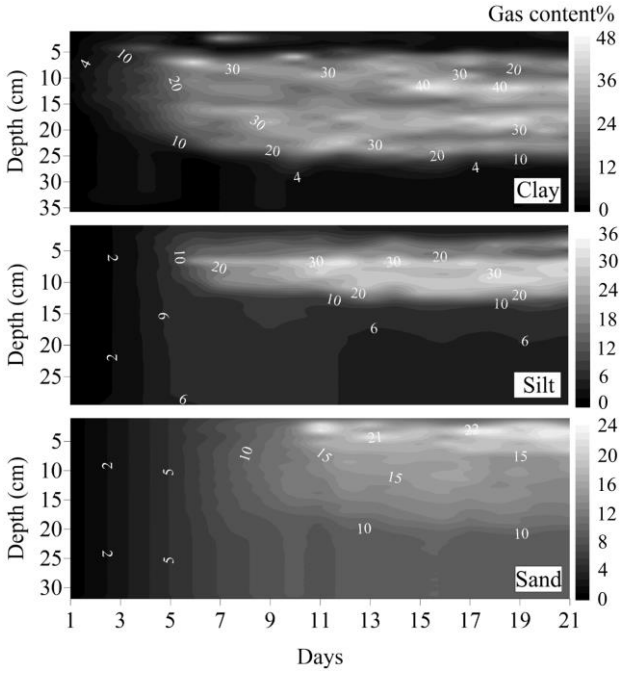

Fig. 2 Spatial and temporal dynamics of the volumetric gas content in three sediment columns.

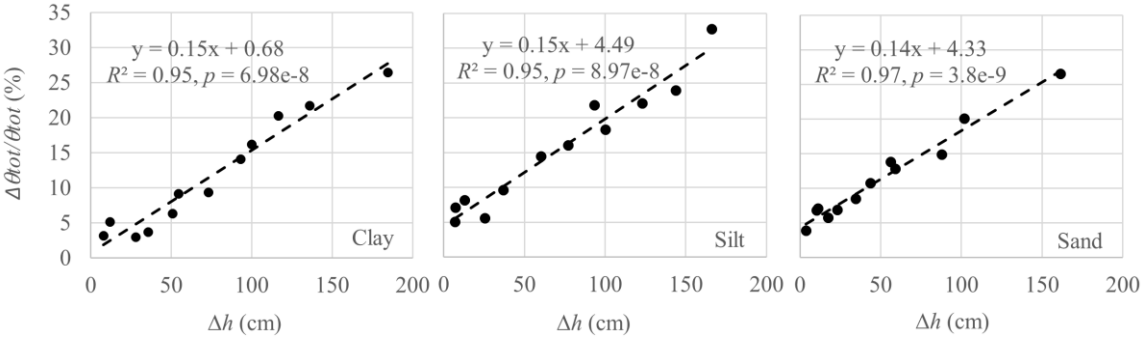

Fig. 3 Changes in gas content due to ebullition ($\Delta\theta_{tot}/\theta_{tot}$) in relation to reduction in hydrostatic head (Δh).

REFERENCES

Bastviken, D., L. J. Tranvik, J. A. Downing, et al. (2011), Freshwater methane emissions offset the continental carbon sink, *Science*, **331(6013)**, 50-50.

Maeck, A., H. Hofmann, and A. Lorke (2014), Pumping methane out of aquatic sediments: ebullition forcing mechanisms in an impounded river, *Biogeosciences*, **11(11)**, 2925-2938.

Varadharajan, C., and H. F. Hemond (2012), Time-series analysis of high-resolution ebullition fluxes from a stratified, freshwater lake, *J. Geophys. Res.*, **117**, G02004, doi:10.1029/2011JG001866.

Daily variation of CO2 fluxes in two Brazilian sub-tropical reservoirs

M. Mannich[1]*, C. V. S. Fernandes[2], J. W. Y. Bernardo[3] and T. B. Bleninger[1]

[1] *Department of Environmental Engineering, Federal University of Paraná, Curitiba, Brazil*
[2] *Graduate Program on Water Resources and Environmental Engineering, Federal University of Paraná, Curitiba, Brazil*

**Corresponding author, e-mail mannich@ufpr.br*

KEYWORDS
Reservoirs; CO_2 fluxes; greenhouse gas emissions; floating chamber; temporal variability.

EXTENDED ABSTRACT

Introduction

Carbon emissions from reservoirs, mainly carbon dioxide (CO_2) and methane (CH_4), are considered in research since the pioneering paper of Rudd et al. (1993). The challenges of measuring greenhouse gas (GHG) emissions are mainly related to their temporal and spatial variability (Teodoru et al., 2012). Usually more attention is given to seasonal changes than to diurnal variability. However the amplitude of daily fluxes may be as large as those occurring on larger timescales (Teodoru et al., 2015; Nimick et al., 2011; Xiao et al., 2013). For example, CO_2 fluxes across the air-water interface may be affected by photosynthesis, respiration, gas solubility dependence on temperature, wind shear and mixing processes. Furthermore, most of the flux measurements using floating chambers were done during the day, thus do not represent nocturnal processes.

Materials and methods

The CO_2 flux behaviour over a whole day was observed at two sub-tropical reservoir in South Brazil, namely Capivari and Vossoroca Reservoirs. The reservoir consolidation of both systems 1970 and 1949, respectively, make them very interesting for research purposes. The CO_2 flux at the air-water interface was measured with a floating chamber with a cross section area of 0,194 m^2, volume of 25,95 L, which corresponds to an area/volume ratio of 7,48 m^{-1} and a wall extension below the water level of 5 cm. The gas was pumped in a closed loop and concentration measured by a CARBOCAP® GMP343 sensor from Vaisala. A small fan promoted homogeneity in the chamber head space. Measurements were done up to 6 times over the day to capture daily temporal variability.

Results and discussion

Fluxes varied in the range of −800 to 600 $mgCO_2m^{-2}d^{-1}$. In winter the data showed an unexpected behaviour compared to expected photosynthesis and respiration processes where the reservoir showed CO_2 absorption during night time and emission to the atmosphere during the day. In summer fluxes were neutral or indicate absorption. Between 00h00 and 12h00 the fluxes are mostly neutral and from 12h00 to 00h00 there is absorption. This indicates that data interpretation only by biological processes can not explain all natural observations. There is a component related to thermal stratification in the reservoir and mixing processes induced by

meteorological forcing acting at the water surface. For example, vertical profiles showed a temperature variation of about 1°C in the upper layer (2 m deep). Additionally, daily variations of dissolved inorganic carbon and pH were observed, which changes the CO_2 concentration in water.

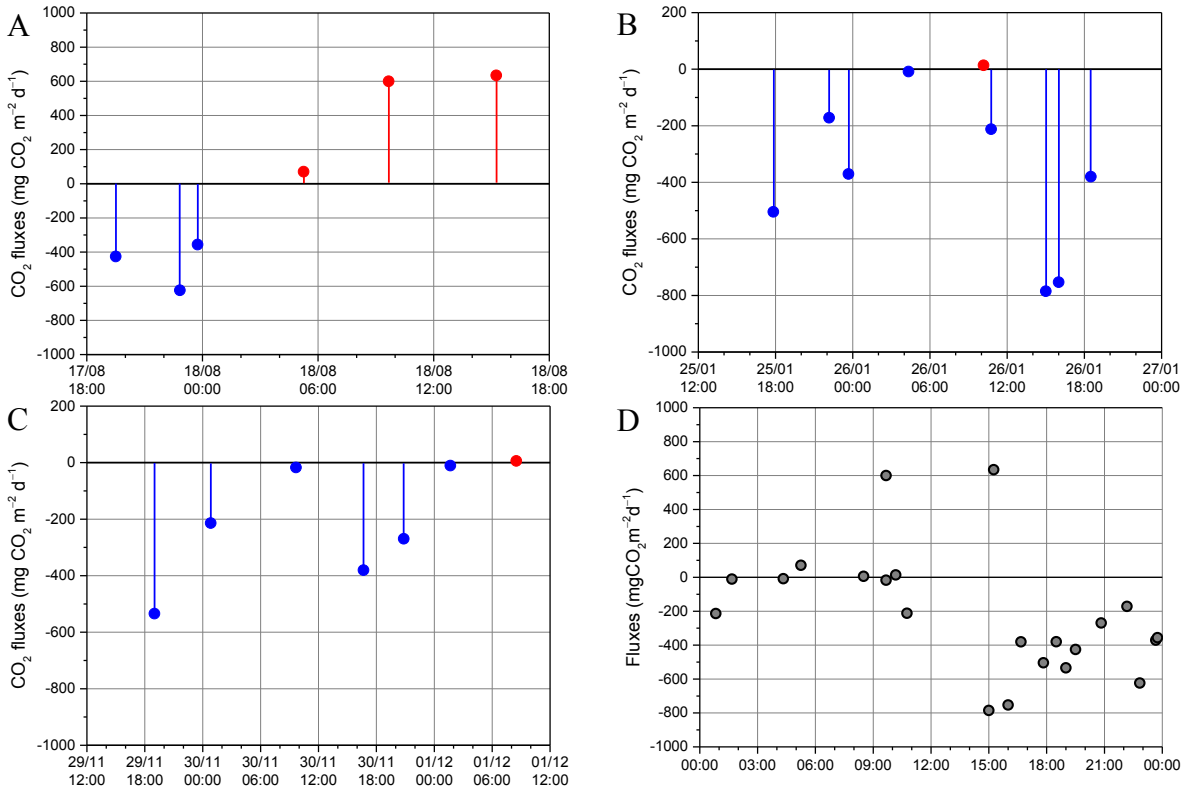

Figure 1. Temporal CO_2 fluxes in different seasons and reservoirs. **A** Vossoroca Reservoir in august 2012. **B** Vossoroca Reservoir in January 2013. **C** Capivari Reservoir in November 2012. **D** All measurements together.

REFERENCES

Teodoru, C. R., Nyoni, F. C., Borges, A. V., Darchambeau, F., Nyambe, I., and Bouillon, S. (2015) Dynamics of greenhouse gases (CO_2, CH_4, N_2O) along the Zambezi River and major tributaries, and their importance in the riverine carbon budget, *Biogeosciences*, **12**, 2431-2453, doi:10.5194/bg-12-2431-2015.

Nimick, D. A., Gammons, C. H., Parker, S. R. (2011) Diel biogeochemical processes and their effect on the aqueous chemistry of streams: A review. *Chemical Geology*, **283**, 3-17.

Xiao, S., Liu, D., Wang, Y., Yang, Z., Chen, W. (2013) Temporal variation of methane flux from Xiangxi Bay of the Three Gorges Reservoir. *Sci. Rep.* **3**, 2500; doi:10.1038/srep02500.

Characterization of lacustrine groundwater discharge and resulting lake-internal upwelling by thermal infrared imaging and fibre-optic distributed temperature sensing: a mesocosm experiment

A.I. Marruedo Arricibita[1]*, J. Lewandowski[1], S. Krause[2] and D.M. Hannah[2]

[1] *Department of Ecohydrology, Leibniz-Institute of Freshwater Ecology and Inland Fisheries, Berlin, Germany*
[2] *School of Geography, Earth and Environmental Sciences, University of Birmingham, Birmingham, UK*
**corresponding author, email: marruedo@igb-berlin.de*

KEYWORDS
Lacustrine groundwater discharge (LGD); Lake, Fibre-Optic Distributed Temperature Sensing (FO-DTS); Thermal Infrared (TIR); Temperature.

EXTENDED ABSTRACT

Introduction

Detecting lacustrine groundwater discharge (LGD) still remains a challenge. The buoyancy of groundwater during winter and early spring can be used for identification of groundwater up-welling related hotspots on surface water by TIR imaging (TIR). TIR has been successfully used to image and screen relatively large surface areas of coastal zones, lakes, reservoirs and large rivers for groundwater contributions (Hare et al. 2015). Still, quantitative interpretations of groundwater fluxes are hampered by the lack of understanding how the groundwater upwelling signal propagates from the sediment-water interface through the water column to the water-air interface and what perturbations and signal losses occur along this pathway.

Materials and methods

In the present study, groundwater discharge to a surface water body was simulated in a mesocosm experiment. Under winter conditions water of 14 °C to 16 °C was discharged at the bottom of a 10x2.8 m mesocosm where surface water varied from 4 °C to 7.4 °C. Four layers (20, 40, 60 and 80 cm above the sediment) of the 81 cm deep mesocosm were equipped with fibre-optic distributed temperature sensing (FO-DTS) for tracing thermal patterns in the water body of the mesocosm and TIR imaging was deployed to monitor temperature pattern at the water surface in order (1) to analyze the propagation of the temperature signals through the water column to the water surface by FO-DTS (2) to characterize the spatial distribution of groundwater upwelling at the pond surface by FO-DTS and TIR and (3) to compare the impact of advective heat inputs and non-advective heat losses on temperature signals at the pond surface. Different LGD rates were simulated in order to establish the minimum rate of groundwater upwelling that can be reliably detected at the water surface by TIR imaging.

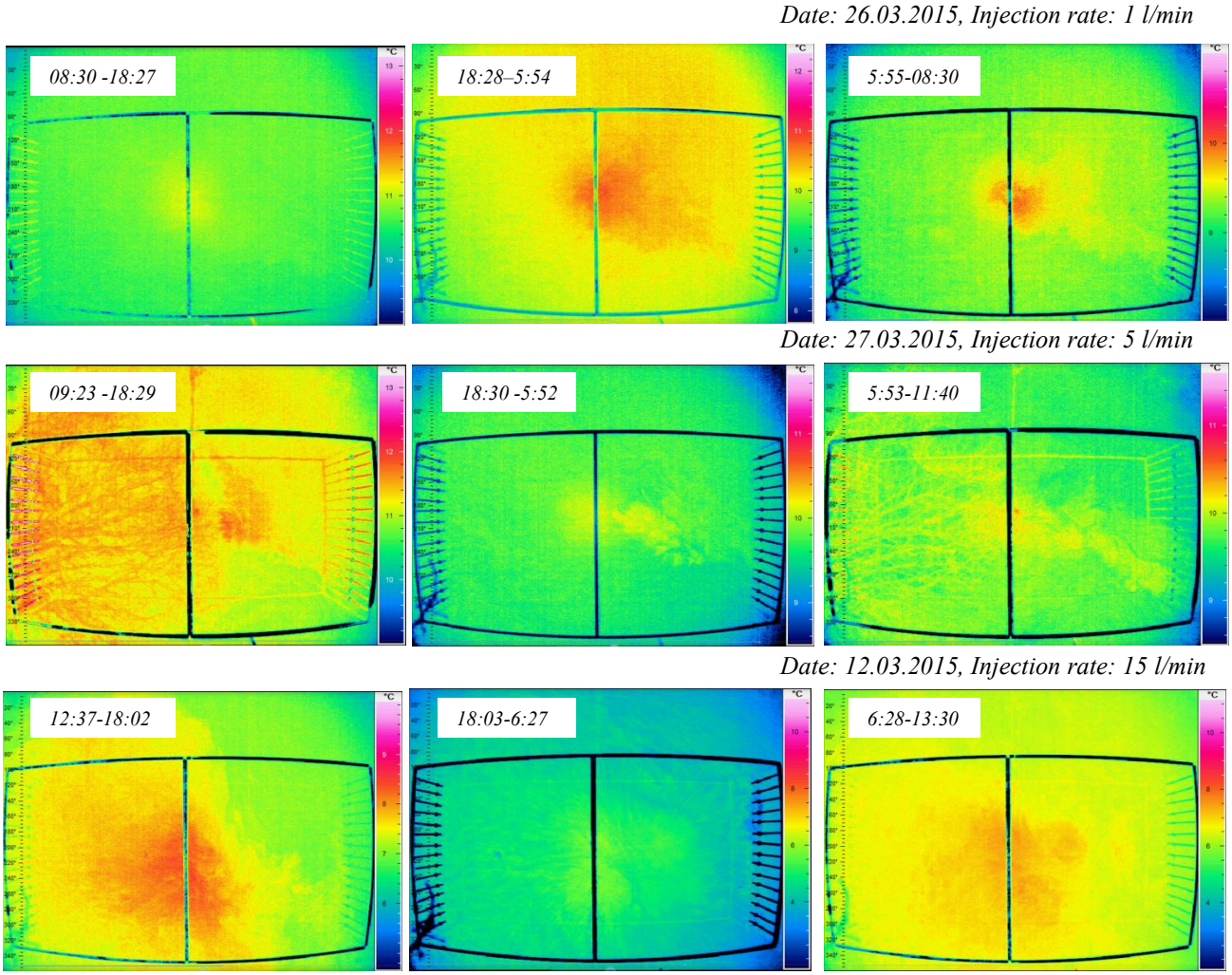

Figure 1. TIR images of the water surface of the mesocosm. The camera was placed above the mesocosm and directed downwards. The horizontal and vertical lines originate from a metal frame used to fix the fibres of the DTS system. The outlet of the warm water used for simulating LGD was placed in the center of the frame at the bottom of the lake. The upwelling in the water body is well visible in most images as warmer water patches in the center of the images. Some TIR images show reflections of a tree partly shading the mesocosm. During the measurements the weather was cloudy. Note that the temperature scales differ between images. Each image contains date and time stamps as well as discharge rates.

Results and discussion

Our experiments revealed that the signal of simulated groundwater discharge travelled from the pond bottom through the water column and was visible at the mesocosm surface. The signal was best visible under cloudy conditions and at night. Higher discharge rates resulted in a stronger signal but even the lowest discharge rate that was technically realizable with our setup resulted in a signal that could be observed at the water surface.

The experiments allow us to evaluate scale dependencies and the adequacy of both methods, FO-DTS and TIR: Temporal and spatial patterns of the upwelling water on the water surface observed by TIR are highly variable. TIR images are vulnerable to environmental factors such as adjacent vegetation, wind, and weather conditions. DTS is more consistent in spatial and temporal patterns observed during the 24 hours lasting experiments but it doesn't show small changes in time and space as the TIR images do. An optimum combination of patterns observed with both methods requires a combination of scales covered by DTS and TIR.

REFERENCES

Danielle K. Hare, Martin A. Briggs, Donald O. Rosenberry, David F. Boutt, John W. Lane, A comparison of thermal infrared to fiber-optic distributed temperature sensing for evaluation of groundwater discharge to surface water, Journal of Hydrology, Volume 530, November 2015, Pages 153-166, ISSN 0022-1694, http://dx.doi.org/10.1016/j.jhydrol.2015.09.059.
(http://www.sciencedirect.com/science/article/pii/S0022169415007428)

Use of autonomous profilers in a hydroelectric reservoir

R. Pieters[1,2]*, and G. Lawrence[2]

[1] *Earth, Ocean and Atmospheric Sciences, University of British Columbia, Vancouver, Canada*
[2] *Civil Engineering, University of British Columbia, Vancouver, Canada*

**Corresponding author, e-mail rpieters@eos.ubc.ca*

KEYWORDS
autonomous profiler; hydroelectric reservoir; interflow; internal waves; aquatic productivity.

EXTENDED ABSTRACT

Introduction

Hydroelectric reservoirs provide a reliable and highly flexible source of renewable energy. In the past, reservoirs have been operated to maximize the production of electricity. However, the operation of reservoirs has come under increasing constraint to account for environmental and social values such as fisheries. Our long-term goal is to understand how change in reservoir operation affects the aquatic productivity within the reservoir. Our short-term goal is to characterize the physical processes that contribute to aquatic productivity. Here we focus on the degree to which nutrients in the inflow spend time in the photic zone (Pieters and Lawrence 2012). We describe the novel use of Teledyne Webb profilers (a type of Argo float) adapted to collect temperature, conductivity and turbidity data in a reservoir, and some preliminary insights from the data collected.

The profilers were deployed in Revelstoke Reservoir, British Columbia, Canada. Revelstoke Reservoir is long (130 km), and narrow (~1 km), with an area of 115 km^2, and a maximum depth of 120 m. Inflow enters the top of Revelstoke Reservoir from the upstream Kinbasket Reservoir (570 m^3/s), and from local tributaries (230 m^3/s). Revelstoke Reservoir is operated run-of-the-river, where the water level is maintained within 1.5 m of normal full pool. Revelstoke Dam has a current capacity of 2,840 MW, the second largest in British Columbia. With a mean annual outflow of 800 m^3/s, the reservoir generates 7,800 GWh.

Materials and methods

The Teledyne Webb APEX APF9I profiler was attached with sliders to a low-friction line held tight between an anchor (70 kg) at the bottom and a float (35 kg) just below the surface. The profiler began at the bottom of the line, and after a prescribed interval, increased its buoyancy, rose along the line, and collected data from both a SBE 41cp CTD (Conductivity, Temperature and Depth sensors) and from a Seapoint turbidity sensor. Data were stored internally. After reaching the top of the line, the profiler decreased its buoyancy and descended to the bottom of the line to wait for the next cycle. The profilers successfully collected CTD profiles every 5 hours over 1 month, and daily over a year.

Results and discussion

From early June to mid-July, the upstream Kinbasket Reservoir provided little inflow, while local tributaries provided high inflow of low salinity snowmelt (Figure 1a). This low salinity input gave rise to a fresh surface layer that deepened over time as shown for Revelstoke forebay in Figure 1c. The upper part of this fresh layer stratified thermally, giving rise to a shallow epilimnion (Figure 1b).

After mid-July, outflow of colder and more saline water from Kinbasket Reservoir increased (Figure 1a). Monthly CTD surveys (not shown), indicate this inflow moved as an interflow at ~30 m depth from the upstream end of the reservoir to the outlet at the dam (29 m). If this interflow passed through the reservoir without entering the photic zone, nutrients from this inflow would short-circuit through Revelstoke Reservoir without contributing to aquatic productivity. The interflow can be seen in the profiler data from Revelstoke forebay as a layer of higher salinity water from ~15 m to 45 m depth that begins in late August and continues through September (Figure 1c). The profiler data indicate there are significant internal motions with a period of a week to ten days. From late-August to mid-October, these motions brought water from the interflow into the photic zone for significant periods of time.

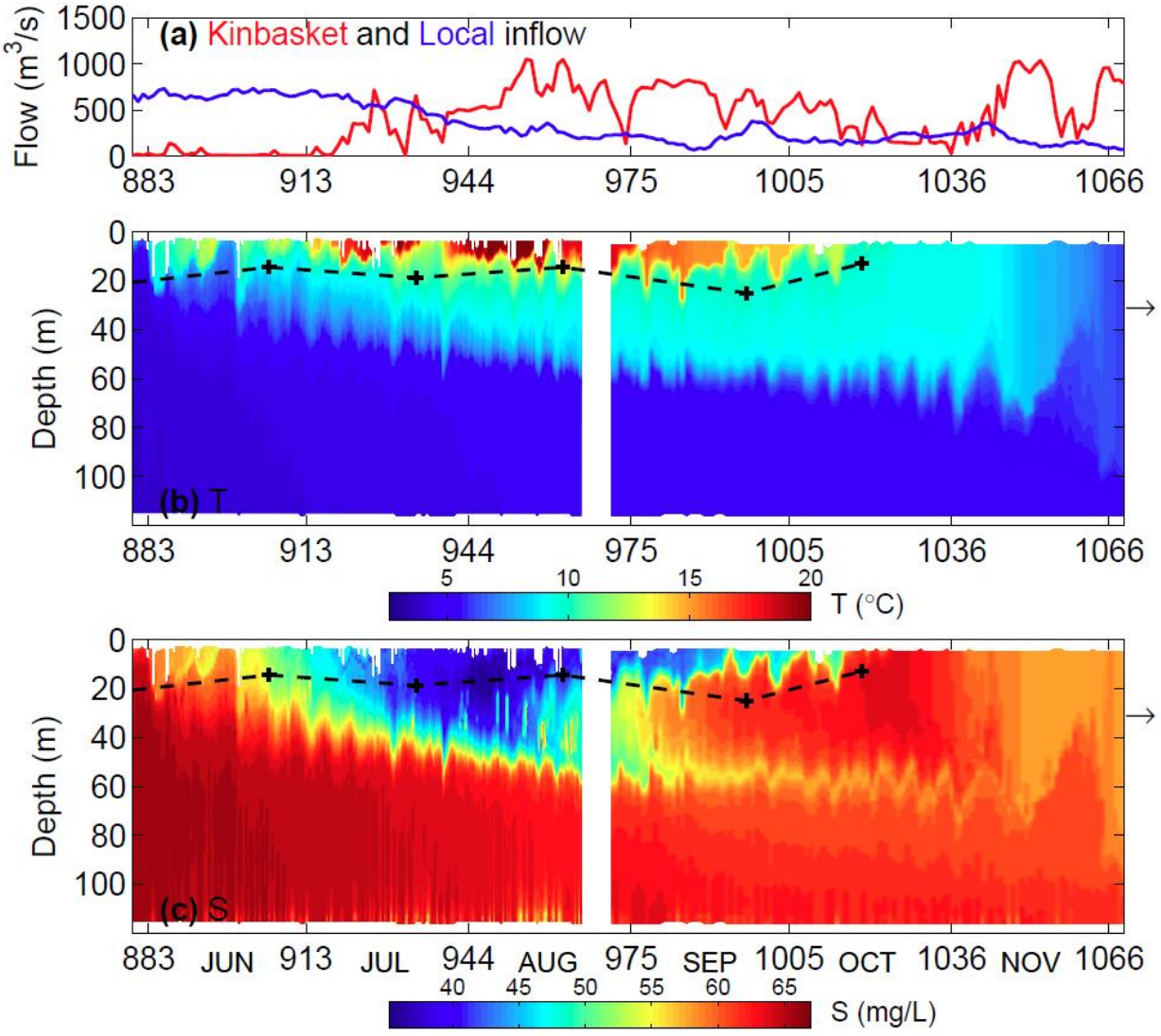

Figure 1. (a) Inflow to Revelstoke Reservoir from upstream Kinbasket Reservoir and from local tributaries. The (b) temperature and (c) salinity in the Revelstoke Reservoir forebay, June to November 2014. Time is in days of 2012. The black dash line marks the estimated depth of the photic zone. The arrow marks the depth of the outlet. White sections of missing near-surface data occurred when the profiler failed to ascend all the way.

REFERENCES

Pieters, R. and G.A. Lawrence (2011), Plunging inflow and the summer photic zone in reservoirs, *Water Quality Res. J. of Canada*, **47.3-4,** 268-275, doi: 10.2166/wqrjc.2012.143

Reconstruction of the 3D distribution of physical parameters in the northern part of Lake Iseo

M. Pilotti[1]*, G. Valerio[1] , L. Gregorini[1] and S. Simoncelli[2]

[1]*Department DICATAM, Università degli Studi di Brescia, Brescia, Italy*
[2] *Department of Architecture & Civil Engineering, University of Bath, Bath, UK*

**Corresponding author, e-mail marco.pilotti@unibs.it*

KEYWORDS
Lakes; alpine area; eutrophication; internal waves.

EXTENDED ABSTRACT

Introduction

In this contribution we present some results of a very detailed experimental campaign accomplished in the northern part of Lake Iseo to monitor the distribution of dissolved oxygen in the layer between the surface and the depth of 60 m. The research was aimed to a better understanding of the evolution of the oxygen demand over a period of two years. This 256 m deep lake, has undergone a process of progressively de-oxygenation: in 1967 it was oligotrophic with almost complete oxygen saturation at the bottom; the current situation is characterised by hypoxia below 140 m and total anoxia below 200 m. Although several countermeasures to limit the nutrient input to the lake have been introduced, the phosphate concentration is not decreasing and it is of interest to understand the current rate of oxygen demand within the metalimnic waters. This purpose goes in hand with a better comprehension of the hydrodynamics of this lake (e.g., Valerio et al., 2012, Pilotti et al., 2014b, Pilotti et al., 2014a), such as the comprehension of the space distribution of pollutants entering from the two tributary rivers in the northern part of the lake.

To this purpose, after an extensive experimental campaign, a 3D space interpolation was used to reconstruct the volumetric distribution of the investigated variables. Actually, the visualization of measured water constituents of interest through two-dimensional horizontal and vertical contoured sections inevitably implies a loss of spatial information with respect to the complexity of the prototypal 3D processes that would rather require a volumetric representations like the one that can be obtained by the use of 3D raster-based models, known as VOLEX (VOLume pixEL) structures. In turn, this requires spatial interpolation as a prerequisite for estimating variables at unsampled points as a weighted average of measured data.

To this purpose, a Weighed Inverse Distance (IWD) algorithm was set up and used. Lake Iseo proved to be a rather challenging environment for this task due to the strong anisotropy caused by thermal stratification between epilimnic waters and deeper layers. To reconstruct a 3D continuous surface of the measured parameters a vertical distortion of the coordinate was needed, with a procedure that can be of interest also for other large thermally stratified lakes. Moreover, the obtained results confirmed the effect of the Coriolis force on the deflection of the water of the tributaries and the following role on the oxygen distribution, as well as the role of the internal waves, which cause displacements of the isopicnotic surfaces making the interpretation of the results more complex. To this purpose the experimental data have been compared with the results obtained with a dynamic model of the lake.

Materials and methods

On 29 and 30 September 2014 an extensive experimental campaign was carried out in the northern part of Lake Iseo, Italy. During this field experiment, 179 vertical profiles of temperature, conductivity, dissolved oxygen, chlorophyll A and turbidity were measured between 0 and 60 m of depth, with an average horizontal distance of about 350 m. In the experimental period, the two main inflows conveyed 40-80 m^3/s in the lake, with a likely intrusion depth around 20 m. A similar campaign had been accomplished in the period 2-6 July 2012.
The wide measured data set was used to test the capability of several interpolations methods in representing the spatial distribution of the variables. Although EPA recognizes that in some cases kriging could be a more accurate option, Inverse Distance Weighting method (IDW) was finally selected because of its efficiency and ease of implementation within MATLAB environment. On the other hand, one of the fundamental assumption of kriging is that mean and variance of the data are invariant with translation, i.e. stationarity of the investigated parameters. Although detrending approach can be used, so that the requirement is imposed on the residuals, the strong vertical variation of the mean values of these parameters hinders the fulfilment of the hypothesis of stationarity in the overall data set.
The successful 3D interpolation through IDW was accomplished with optimal exponent of 3 for temperature, 2 for turbidity and 1 for the other variables.

Results and discussion

A first result of this research is that an effective and necessary way for the use of IDW for the reconstruction of the 3D pattern of physical variables in a stratified lake goes through a pre-processing of measured data, that relaxes the original anisotropy by a suitably devised vertical expansion. To this purpose the use of the Brunt–Väisälä frequency was tested, in order to reduce the uncertainty associated with the methodology. The volumetric representation of the data show that the persistent role of Coriolis force manifests itself also in a different average distribution of the oxygen in the western side of this lake. Moreover, the effect of Earth's rotation clearly emerges from the systematic temperature differences in east-west transects.
A detailed monitoring campaign must be followed by a detailed modelling of the lake hydrodynamics that helps in the interpretation of the measurements. Without this type of support, the analysis of the data would evidence spatial and temporal heterogeneities that, in reality, are an effect of the highly transient field of internal waves.

The comparison between the measured data and the results of the model prove that a correct reproduction of the internal waves at a local scale demands a very detailed reconstruction of the wind flow field. However, even a state of the art simulation of the distributed pattern of wind on the lake surface, can't reproduce some fine structures that emerge from the experimental campaign.

REFERENCES

Pilotti, M., Valerio, G., Gregorini, L., Milanesi L. and Hogg C. (2014a), Study of tributary inflows in Lake Iseo with a rotating physical model, *J. Limnol*., **73(1),** doi: 10.4081/jlimnol.2014.772.

Pilotti, M., Simoncelli, S., Valerio, G. (2014b), A simple approach to the evaluation of the actual water renewal time of natural stratified lakes, *Water Resources Research*, **50(4)**, 2830–2849, doi:10.1002/2013WR014471.

Valerio, G., M. Pilotti, C.L. Marti, C.L. and J. Imberger (2012), The structure of basin scale internal waves in a stratified lake in response to lake bathymetry and wind spatial and temporal distribution: Lake Iseo, Italy, *Limnol. Oceanogr.*, **57(3)**, 772-786.

Sensitivity analysis of a 1D reservoir heat transport model regarding meteorological measurements

B. A. Polli[1]*, T. Bleninger[1]

[1] *Graduate Program on Water Resources and Environmental Engineering, Federal University of Paraná, Curitiba, Brazil*

**Corresponding author, e-mail brunapolli@gmail.com*

KEYWORDS
Lake; meteorological monitoring; heat fluxes; modelling; one-dimensional heat transport.

EXTENDED ABSTRACT

Introduction

Lakes and reservoirs usually show a seasonal behaviour related to their physical structure, due to meteorological and hydrological influence. The main heat transfer occurs at the air-water interface due to solar radiation (absorbed over the water column), long wave radiation, sensible and latent heat. These energy fluxes can develop thermal stratification, due to temperature differences between the water layers, i.e., water density, and the lack of sufficient energy to prevent the stratification – solar heating dominates mixing due to wind and flow.

Mixing in reservoirs occurs due to the mixing energy from inflowing waters and the energy transfer at the air-water interface, mainly through wind shear or other meteorological conditions. This work compares interface heat fluxes due to two distinct locations of meteorological measurements and analyzes the impacts of these differences in a one-dimensional heat transport model and temperature gradients.

Materials and methods

Meteorological data from Capivari Lake (Paraná State, Brazil) measured at the margin of the reservoir and over a floating platform was analyzed regarding the importance of parameter variability for the estimation of heat fluxes in reservoirs and their impact on temperature modelling. The observed variability was than studied for a similar reservoir closeby (50 km distance), where a floating platform measuring temperature profiles was installed, however with only one meteorological station.

Sensitivity analysis of meteorological data was performed in Vossoroca Lake (Paraná State, Brazil). Vossoroca has a maximum and mean depth of 17 and 8 m (area of 3.3 km^2), respectively, and is monitored since 2012: meteorological data (measured at the margin) was measured with 2 min time step and water temperature was measured with seven temperature sensors at the deepest region of the reservoir. Vossoroca is a monomitic reservoir. Vossoroca Lake model showed good agreement with measurements and high temporal resolutions. The one-dimensional model MTCR-1 (Polli and Bleninger, 2015) solves the one-dimensional heat transport equation with high spatial and temporal resolutions.

Results and discussion

Table 1 shows mean values of meteorological measurements in Capivari Lake. Energy fluxes vary significantly due the different location of the sensors in Capivari Lake, although being close by each other (1 km distance). The energy fluxes were calculated with Heat Flux Analyzer (Woolway et al., 2015). The main differences in heat fluxes occurred in sensible and latent heat: in the former, sensible heat with data from the onshore weather station was −10.03±8.06 Wm^{-2}, while over the floating platform, −16.51±15.96 Wm^{-2}. The latent heat was −38.81±20.37 Wm^{-2} (onshore station) and −73.15±50.46 Wm^{-2} (floating platform station). Net heat flux estimated was −126.16±86.60 Wm^{-2} and −89.76±50.05 Wm^{-2}, for the floating platform and onshore weather stations, respectively. Figure 1 shows the net heat flux (Q_{tot}) for

Capivari Lake. Sensitivity analysis of meteorological measurements was performed based on mean absolute difference between data from Capivari Lake.

Mean values	Wind speed	Air temperature	Relative Humidity	Solar radiation
Onshore station	0.72 m/s	20.57 °C	86.09%	202.14 W/m^2
Floating platform	2.33 m/s	21.22 °C	84.70%	206.64 W/m^2

Table 1. Mean values of meteorological measurements in Capivari Lake

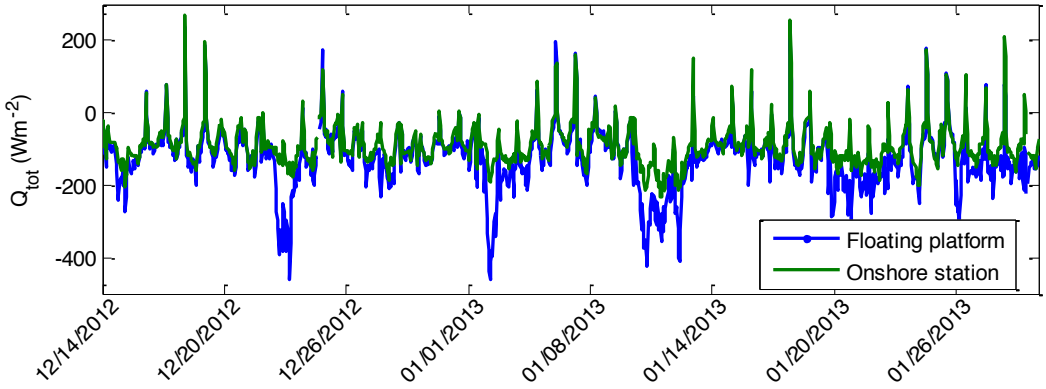

Figure 1. Air-water net heat flux in Capivari Lake

The one-dimensional heat transport model (MTCR-1) was implemented in Vossoroca Lake and calibrated based on meteorological data measured at the margin of the reservoir (Polli and Bleninger, 2015). Temperature profiles measured in Vossoroca Lake show temperature gradients (surface and bottom) between June/2012 and February/2013 being higher than 7°C and gradients higher than 2°C occuring during 216 days. Figure 2 shows Vossoroca modelling results with data from onshore station and from differences estimated in Capivari Lake. Gradients (between surface and bottom) higher than 2ºC in Figure 2.a occurred in 158 days (from 271 days of simulation), while in Figure 2.b (mainly increasing wind speed) these differences occurred in 13 days. One dimensional modeling is essential for reservoir management. Usually closeby meteorological data is used to simulate temperature profiles and periods of stratification. The present article showed, that such modeling is significantly depending on the location of the meteorological station. Differences of surface temperatures can be up to 3.7 °C, compared to simulations based on terrestrial weather stations.

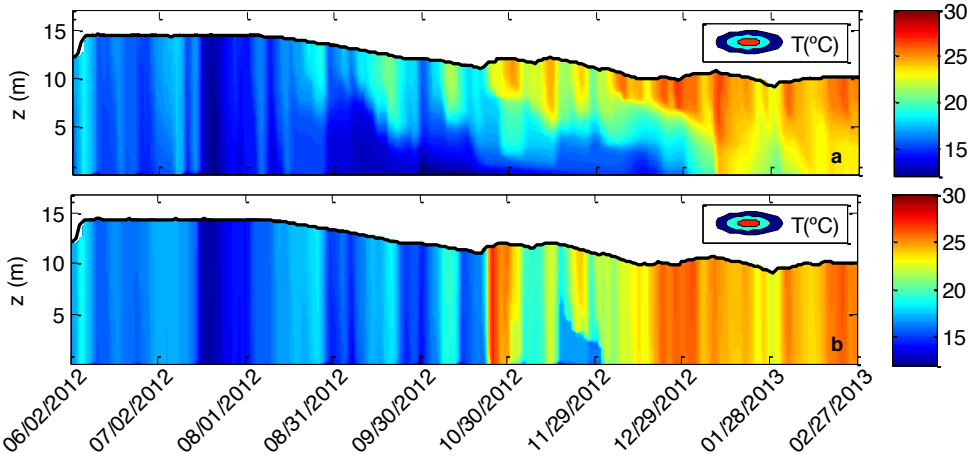

Figure 2. Water temperature modelling in Vossoroca Lake. a) Meterological data measured at the lake margin. b) Meteorological data estimated based on Capivari results (from the floating platform)

REFERENCES

Polli, B. A., Bleninger, T. (2015), Modelagem do transporte de calor no reservatório Vossoroca. In: XXI Simpósio Brasileiro de Recursos Hídricos, Brasília (Brazil).

Woolway, R.I., Jones, I.D., Hamilton, D.P., Maberly, S.C., Muraoka, K., Read, J.S., Smyth, R.L., Winslow, L.A.. (2015), Automated calculation of surface energy fluxes with high-frequency lake buoy data. Environmental Modelling and Software 70, 191-198.

Understanding forcing mechanisms and hydrodynamics in Loch Linnhe, Scotland, as a basis for sustainable growth

B. Rabe[1]* and J. Hindson[1]

[1] *Marine Scotland Science, Marine Laboratory, Aberdeen, UK*

**Corresponding author, e-mail b.rabe@marlab.ac.uk*

KEYWORDS
Scottish sea loch; hydrodynamics; aquaculture environment interactions; fjord; estuarine circulation.

EXTENDED ABSTRACT

Introduction

The Scottish west coast is characterized by a number of fjordic sea lochs, showing many features arising from previous glaciation. Fjords are characterized by a connection to the sea, the presence of sills, deep basins behind the sills, and complicated circulation patterns. Sea lochs, with many smaller ones separated from the main basins by shallow sills, are influenced by tides, meteorological forcing, freshwater input, and sea bed topography. A multi-disciplinary study was conducted in Loch Linnhe, one of Scotland's largest sea lochs (Fig. 1). In Loch Linnhe, a dynamically wide sea loch system, we investigated the system's dynamics and the influence on sea lice dispersal. Our understanding of the dynamics of the system is important for the sustainable environmental management of this socio-economically valuable region.

Materials and methods

The study uses observations from upper and lower Loch Linnhe (excluding side lochs) during 2011-2013 including CTD, ADCP, VMADCP, data buoy, weather stations, and river flow data (from the National River Flow Archive, NRFA). The hydrodynamic Scottish Shelf Model includes a high resolution Loch Linnhe case study which takes orographically steered winds into account.

Methods include, for example, coherence squared analysis, harmonic analysis, and an evaluation of the dimensionless Ekman and Kelvin numbers to describe the system in terms of importance of rotation. The Ekman number, E_k, is defined as $E_k=(A_z)/(f*H_0^2)$, and the Kelvin number, K_e, as $K_e = B/R_{in}$ with A_z the vertical eddy viscosity coefficient, f the Coriolis parameter at this latitude, H_0 the maximum water depth, B the breadth of the sea loch, and R_{in} the internal Rossby radius of deformation. The Ek versus Ke parameter space helps determine the variability of flow patterns according to Valle-Levinson (2010).

Results and discussion

The complex hydrographic environment of Loch Linnhe shows circulation patterns complicated by interactions between tides, meteorological forcing, sea bed topography, and freshwater inputs.

The physical processes exhibit temporal (seasonal and interannual) and spatial variability.

Meteorological forcing, channeled in the along-loch direction, influences especially the surface layer particularly during neap tides. However winds are not the only driving force, as

is the case in some smaller systems. During spring tides the main influence, even in the surface layer, is the tides, which are dominated by the semi-diurnal M_2 constituent. The large freshwater input from an extensive catchment area leads to a buoyancy-driven circulation, independent of wind stress, and leads to variability in water masses. Loch Linnhe is also wide enough for rotation to have an effect. An investigation of the Ekman and Kelvin numbers shows that the loch is both vertically and laterally sheared. Fresh outflow occurs on the north-west coast with a deepening of the halocline.

The Scottish Shelf Model Loch Linnhe case study has been validated for 2011 and can be used in the future for more detailed analysis of the dynamics in the loch system.

The fundamental physical characteristics of the Loch Linnhe system are the basis for the biology, ecology, and productivity of the area, which in turn are the foundation of the ecosystem services on which a wide range of marine activities in the area depend. An increasing interest in the extension of existing uses of the system and potential new forms of development, as one of the key objectives for Scotland is sustainable economic development, will require a good understanding of all aspects of the system. The benefits of understanding the physical processes and of links between physical and biological processes to manage the system in a sustainable manner has already been explored through the development of a sea lice dispersal model for the area.

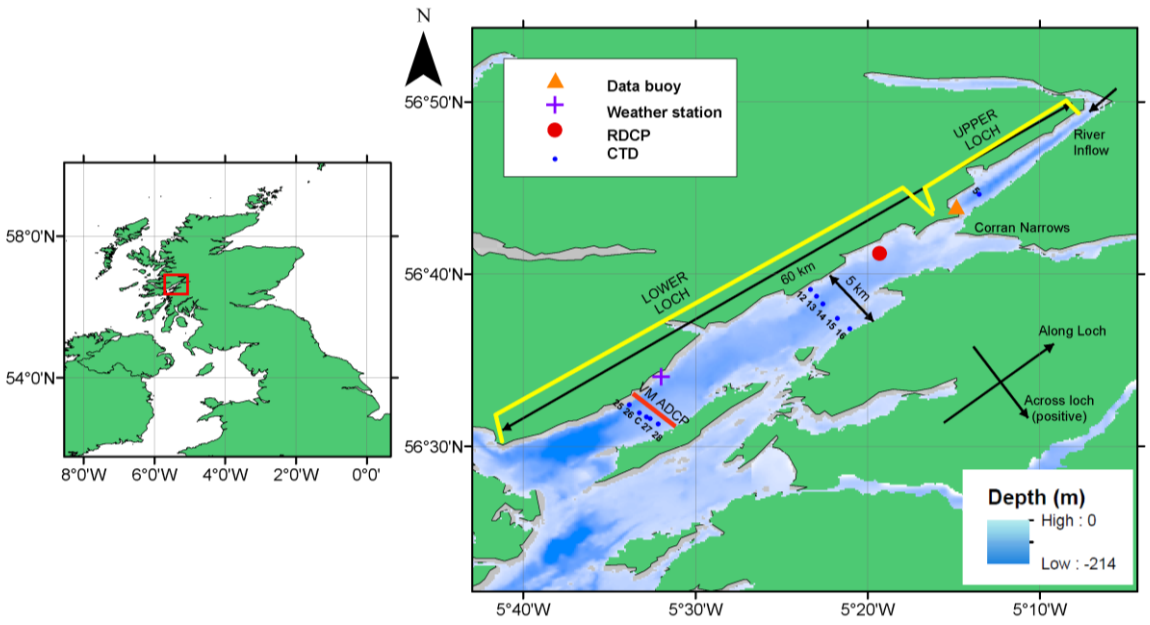

Figure 1. Maps of the study area, Loch Linnhe, on the west coast of Scotland including bathymetry, instrument deployment locations, and place names.

REFERENCES

NRFA (2016) National River Flow Archive. http://nrfa.ceh.ac.uk.

Valle-Levinson, A. (2010), Definition and classification of estuaries, in: Valle-Levinson, A. (Ed.), Contemporary Issues in Estuarine Physics. Cambridge University Press, pp. 1–11

Characterizing littoral impacts of wind-driven upwelling events in a large lake using high-frequency nearshore water quality data

D. Roberts[1,3]*, S.G. Schladow[1,3], B. Hargreaves[2]

[1] *Department of Civil and Environmental Engineering, University of California, Davis, CA, USA*
[2] *Formerly Department of Earth and Environmental Sciences, Lehigh University, Bethlehem, PA, USA*
[3] *Tahoe Environmental Research Center, University of California, Incline Village, NV, USA*

**Corresponding author, e-mail:* Derek Roberts, dcroberts@ucdavis.edu

KEYWORDS
lakes; water quality; upwelling; littoral.

EXTENDED ABSTRACT

Introduction

We have characterized the physical motion and corresponding water quality fluctuations in the nearshore of a large lake during a wind-driven deep-water upwelling event. We report on the relative water quality impact of this upwelling event in comparison to a regular pattern of wave-driven benthic resuspension events.

Methods

A long-term deployment of seven nearshore CTD-fluorometer stations anchored to the lake bed around the perimeter of Lake Tahoe, at 2 meter depth, continues to record temperature, conductivity, depth, wave height, chl-*a* fluorescence, CDOM fluorescence, turbidity, and dissolved oxygen data at thirty-second intervals. A thermistor chain records temperature at a thirty-second interval along sixteen vertical nodes in 120 m of water on the west side of Lake Tahoe. The latter has been used to characterize the magnitude of Fall 2015 upwelling events hinted at by rapid temperature decreases recorded at the nearshore stations. Water quality data from the nearshore stations is used to characterize the impacts of these upwellings. Profiling data collected days before upwelling events is used to reference nearshore water quality signals to lake profile characteristics.

Long-term nearshore station data is used to quantify the contribution of wave events to littoral water quality fluctuations. Upwelling impacts are then compared to this characterization for an analysis of the relative influence of upwelling events on nearshore water quality.

Results and Discussion

Thermistor chain data show a partial upwelling event November 24-25, 2015 in response to a wind-driven surface seiche (Figure 1). A comparison of windward lake level data (Meeks Bay nearshore station) to leeward lake level data (Glenbrook nearshore station), along with corresponding wind data, confirm the presence of a wind-driven surface seiche. Nearshore station data from this time period show temperatures corresponding to water upwelled from 70 m depth. Chlorophyll-a fluorescence data show increased algae concentrations in the

nearshore with the presence of upwelled water of depth-origin corresponding to a deep-chlorophyll maximum (DCM) measured using a SeaBird profiler on November 20th. Elevated CDOM fluorescence during the event may be due to decay associated with biological processes in the DCM. No marked increase in turbidity is recorded during the upwelling event. This result is expected given SeaBird profile data indicating little variation in epilimnetic turbidity and decreased turbidity at depth.

Post-upwelling nearshore data show a return to baseline levels of chlorophyll-a and CDOM but a notable decrease in temperature. We hypothesize that downwelling following the release of the wind-driven surface seiche advected algae and other organics back to depth, but that mixing during the upwelled period caused lasting cooling of the surface-layer.

Data from the same nearshore station during a wave event on November 26th show elevated levels of turbidity but no significant response in chlorophyll-a or CDOM. Relaxation of waves is followed by a return to baseline turbidity levels. These observations are in line with rapid sediment settling post-wave resuspension in Lake Tahoe observed by Reardon et al. (2015).

Steissberg et al. (2005) used thermal satellite data to characterize upwelling and associated surface mixing in Lake Tahoe. We extend upon this work by offering in-situ characterization of water quality change during one of these events. Our data show that upwellings can cause short-term water quality change via advective transport of deep water. We note that the temporal nature of upwelling events is comparable to that of wind-wave events; wind-direction determines the presence of upwelling or waves on opposing lake shores. However, the nature of the water quality change is different for upwellings versus wind-wave sediment resuspension events. The dominant southwesterly weather pattern causes regular upwelling events on the west side of Lake Tahoe, with corresponding wind-wave events on the east side. Differences in the impacts of these events might partially explain spatial variability in water quality around the margins of Lake Tahoe. We plan to generalize nearshore response to upwelling versus wind-waves by investigating more of these events at study sites around the lake. We will then be able to use our long-term nearshore water quality data set to discuss how prevailing wind patterns may drive variability around the perimeter of Lake Tahoe.

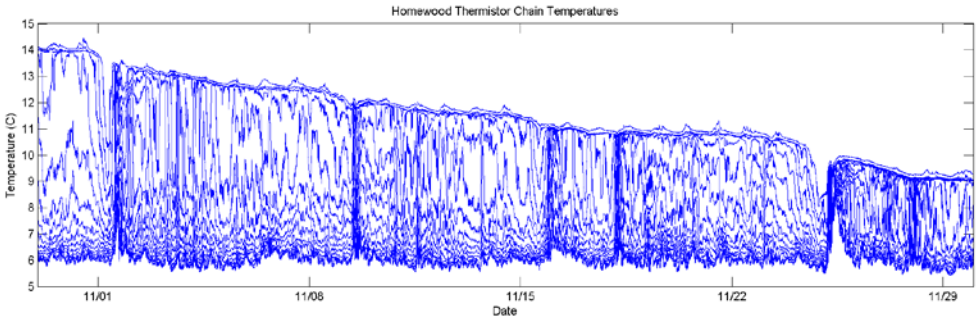

Figure 1 – November 2015 thermistor chain data, Homewood, Lake Tahoe.

REFERENCES

Steissberg, T.E., Hook, S.J., Schladow, S.G. (2005), Characterizing partial upwellings and surface circulation at Lake Tahoe, California-Nevada, USA with thermal infrared images, *J. Remote Sensing of Environment*, **99**, 2-15, doi: 10.1016/j.rse.2005.06.011

Reardon, K.E., Bombardelli, F.A., Moreno-Casas, P.A., Rueda, F.J., Schladow, S.G. (2014), Wind-driven nearshore sediment resuspension in a deep lake during winter, *Water Resources Research*, **50**, 8826-8844, doi:10.1002/2014WR015396

Barotropic Seiches in Quesnel Lake, BC

J. A. Shore[1]*, J. Morrison[2], S. Vagle[2], M.G.G. Foreman[2]

[1] *Department of Physics,*
Royal Military College of Canada, Kingston
[2] *Institute of Ocean Sciences*
Fisheries and Oceans Canada , Sidney

**Corresponding author, e-mail jennifer.shore@rmc.ca*

KEYWORDS
Oligotrophic lake; surface seiche; modelling.

EXTENDED ABSTRACT

Introduction

Quesnel Lake in British Columbia is a central habit for a diverse number of land and fish species including sockeye salmon which spawn in the tributaries to the lake. On 4 August 2014, a nearby mine tailings pond failed and released about 25 million m^3 of tailings water into the lake directly into the path of salmon just beginning their annual return to the local spawning grounds. As a result of the spill, observations in the western basin of the lake showed an increase in temperatures, salinity and turbidity in the surface water above the thermocline and a deposit of mine tailings onto the bottom sediment (Petticrew et al., 2015). Seiching is responsible for the transport of a significant amount of material out of this basin but the natural periods are largely unknown.

Materials and methods

To quantify the barotropic seiche properties of the lake, we compared the results from three methods which estimate the free-oscillation modes for the lake. Firstly, we applied Merian's formula (e.g. Dean and Dalrymple, 2002) for the lake and various basins to derive the primary seiche periods:

$$T = \frac{2L}{n\sqrt{gH}} \tag{1}$$

where, L is the length of the basin, g is gravity, H is the basin depth, and T is the period of the n-th mode seiche

Secondly, we solved the linear, inviscid, barotropic shallow water equations on a simple finite element mesh of the Lake Quesnel domain to determine the primary spatial oscillation modes and their associated frequencies.

Thirdly, we initiated a 3-d prognostic finite volume numerical model of Lake Quesnel with constant density and an unlevel surface to induce barotropic seiching. We identified seiche frequencies by applying FFTs to the resulting surface elevation signal and followed on with a harmonic analysis to derive the spatial structure of the standing wave oscillations.

Results and discussion

The estimated seiche period for the whole lake using Merian's formula is about 80.7 minutes (Table 1). The smallest seiche period is estimated to be about 7 minutes for the East Reach because, despite its short length, it is very deep.

	Whole Lake	East Only	East Reach	West Basin	North Arm
Depth (m)	157	200	250	41.9	81
Length (km)	95	55	10	15	36
Period (min)	80.7	41.4	6.7	24.6	42.6

Table 1: Estimates of 1st mode seiche periods (in minutes) using Merian's Formula. Basin lengths represent distance along the thalweg and depths are averages for the basin.

Solving the the linear, inviscid, barotropic shallow water equations for the lake with a constant depth of 157 m gives the primary seiche period to be 74.4 minutes. This period is slightly less than the 80.7 minutes estimated for a simple rectangular basin of the same depth, indicating that the complex lake geometry results in a slight speed up of the free oscillation.

The harmonic analysis method estimated the primary seiche period to be 64.8 minutes. Again, similar to, but less than predicted by the other two methods. This third method provides spatial amplitude maps for each period with each successive map having more node lines. The spatial map for the predicted 34 minute seiche is shown in Figure 1. It shows node lines consistent with observations of isotherm displacements after a 2-day storm in September 2003 (Laval et al., 2008).

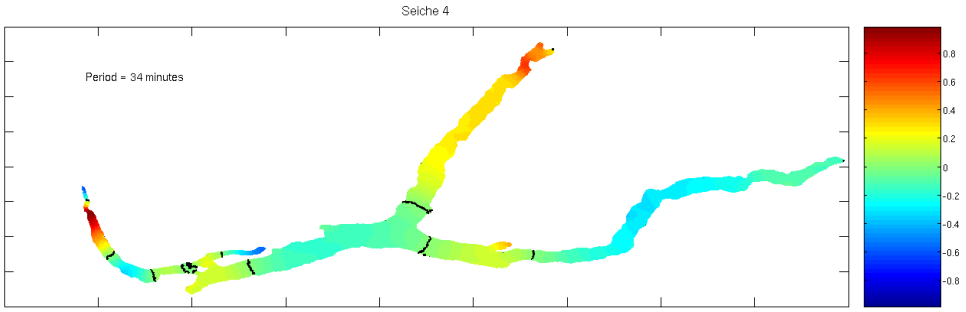

Figure 1: Spatial maps of the normalized amplitudes of the fourth free oscillation modes of the 34 min seiche (produced using harmonic analysis) . Node lines are shown in black.

We used three methods to estimate the primary periods for the free-oscillation modes in Lake Quesnel, B.C. These seiches contribute to the transport of water and material into local tributaries that support salmon spawning.

REFERENCES

Dean, R. G. and R. A. Dalrymple Coastal Processes with Engineering Applications. Cambridge University Press. (2002). Cambridge, U.K., pp 481.

Laval, B., J. Morrison, D. J. Potts, E. C. Carmack, S. Vagle, C. James, F. A. McLaughlin, and M. Foreman 2008. Wind-driven summertime upwelling in a fjord-type lake and its impact on downstream river condition: Quesnel Lake and River, BC, Canada. *J. Great Lakes Res*., 34, 189–203.

Petticrew, E. L., S. J. Albers, S. A. Baldwin, E. C. Carmack, S. J. Déry, N. Gantner, K. E. Graves, B. Laval, J. Morrison, P. N. Owens, D. T. Selbie, and S. Vagle (2015). The impact of a catastrophic mine tailings impoundment spill into one of North America's largest fjord lakes: Quesnel Lake, British Columbia, Canada. *Geophys. Res. Lett*., **42**, 3347–3355.

Biogenic mixing induced by vertically migrating zooplankton in a small lake

S. Simoncelli[1]*, S. J. Thackeray[2], and D. J. Wain[1]

[1] *Department of Architecture and Civil Engineering, University of Bath, Bath, United Kingdom*
[2] *Centre for Ecology and Hydrology, Lancaster Environment Centre Lancaster, United Kingdom*

**Corresponding author, e-mail s.simoncelli@bath.ac.uk*

KEYWORDS
Lakes; mixing; turbulence; zooplankton; water quality.

EXTENDED ABSTRACT

Introduction

Bio-turbulence or bio-mixing refers to the contribution of living organisms towards the mixing of waters in oceans and lakes. Our project focuses the attention on the stirring generated by *Daphnia spp.* in a small lake. This very common zooplankton species is engaged in a vertical migration (DVM) at sunset, with many organisms crossing the thermocline despite the density stratification. During the ascension they may create hydrodynamic disturbances in the lake interior where the stratification usually suppresses the vertical diffusion.

Experimental measurements in an unstratified tank by Wilhelmus & Dabiri (2014) show that zooplankton can trigger fluid instabilities through collective motions and that energy is imparted to scales bigger than organism's size of few mm. Modelling through scale analysis and simulations, for low-Reynolds-number organisms in stratified water, seems to support the idea of *Daphnia* generated mixing. Length scales analysis, for low-Reynolds-number organisms in stratified water by Leshansky & Pismen (2010) and Kunze (2011), estimate eddy diffusivity between 10^{-7} and 10^{-5} m^2/s. Numerical simulations in the same regime by Wagner et al. (2014), suggest a mixing efficiency of 3.3%. Finally, Wang & Ardekani (2015) provides a diffusivity of 10^{-5} m^2/s for *Daphnia* from DNS in the intermediate Reynolds-number regime. However, Noss & Lorke (2014) experimentally measured a diffusivity as low as 10^{-7} m^2/s by *Daphnia* migration in a lab experiment. Theoretical studies as well as mixed results and conclusions motivate the study of biomixing in lakes.

Materials and methods

Measurements experiments were conducted in Vobster Quay, a small and deep (40m) quarry with small wind fetch and steep sides, located in the South West UK. Zooplankton vertical concentration was evaluated using a zooplankton 100-μm mesh net, by collecting and analysing samples in 8 layers of the lake. A bottom-mounted ADCP was also employed to track their concentration and migration with the measured backscatter strength.

Turbulence and mixing were measured before and during the DVM with the SCAMP, a microstructure temperature profiler. Dissipation rates of turbulent kinetic energy were determined by fitting the Batchelor spectrum of temperature fluctuations and removing invalid spectra with statistical criteria by Ruddick et al. (2000). Dataset was acquired on 16/07/15 when the theoretical sunset was at 21:20. During the experiment there was no wind.

Results and discussion

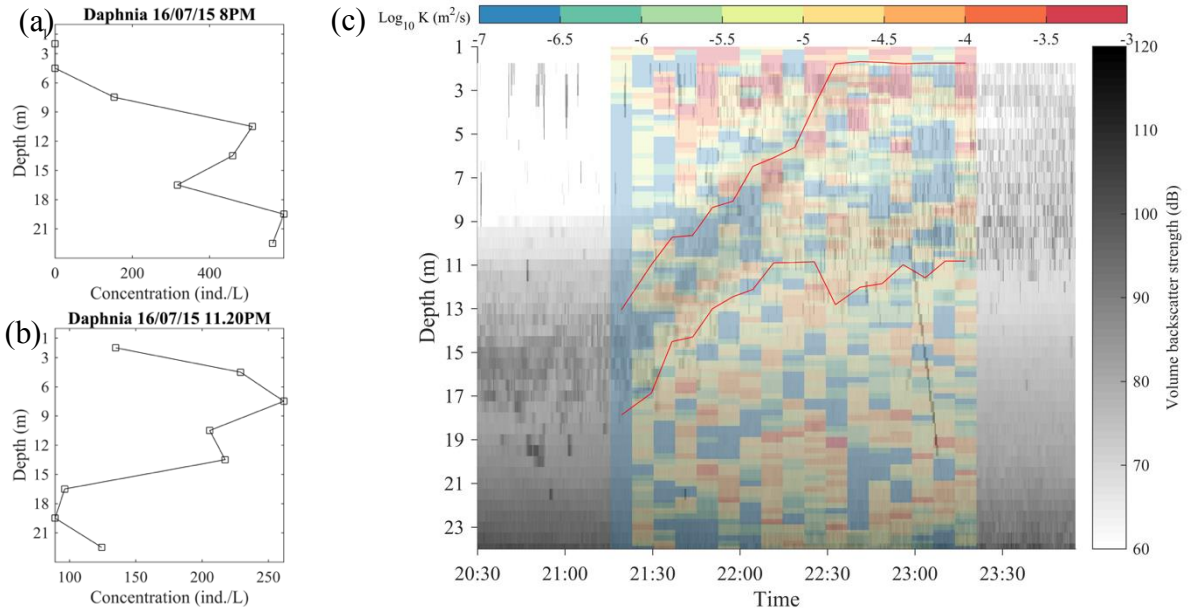

Figure 1. (a) and (b) *Daphnia* distribution before and after the DVM. (c) Eddy diffusivity map during the DVM. Red lines indicate the zooplankton layer position.

Measured dissipation rates ε during the day show low mixing level (K <= $10^{-6.5}$ m^2/s) in the thermocline and in the zooplankton layer, which floats between 15 and 17m. On 16/07/15, zooplankton at the sampling site show higher counts of *Daphnia spp* near the bottom before sunset (Figure 1.a). Samples after dusk show instead an increase on the surface layer with a minimum below 15m (Figure 1.b). The backscatter from the ADCP is consistent with these profiles and shows a clear migration of zooplankton (Figure 1.c, grey plot).

During the vertical ascension both turbulence and mixing are enhanced with respect to the profile before the migration where K=10^{-7} m^2/s (Figure 1.c, spectral colour map). Mixing is highest on the surface during the experiment, likely due to penetrative convection process. Before reaching the mixed layer, the zooplankton layer is sandwiched by low mixing and average K inside is $10^{-4.5}$ m^2/s. This is 2 orders of magnitude greater than K assessed from numerical simulations by Wang & Ardekani (2015).

However, mixing shows a great variability during the experiment as well as there are turbulent patches outside the migrating layer for which the source is not known. Before and after the time series there was no wind. Penetrative convection associated with night-time cooling did not affect our measurements as shown by the thermistor data.

A tracer experiment is also planned to experimentally measure the eddy diffusion coefficient and compare the results and its importance with the well-known mixing mechanisms in lakes due to wind and internal waves.

REFERENCES

Wilhelmus, M.M. and J.O. Dabiri (2014), Observations of large-scale fluid transport by laser-guided plankton aggregations, *Phys Fluids*, **26(10)**, 101302, doi:10.1063/1.4895655

Leshansky, A.M. & L.M. Pismen (2010), Do small swimmers mix the ocean?, *Phys Rev E*, **82(2)**, 025301, doi: 10.1103/PhysRevE.82.025301

Kunze, E. (2011), Fluid mixing by swimming organisms in the low-Reynolds-number limit, *J Mar Res*, **69(4-6)**, 591–601, doi:10.1357/002224011799849435

Wagner, G.L., W.R. Young, & E. Lauga, (2014), Mixing by microorganisms in stratified fluids. *J Mar Res*, **72(2)**, 47–72

Wang, S. & Ardekani, A.M., 2015. Biogenic mixing induced by intermediate Reynolds number swimming in stratified fluids. *Nature, Scientific Reports*, **5**, 17448. doi:10.1038/srep17448

Sediment deposition from turbidity currents in simulated aquatic vegetation canopies

M. Soler[1*], J. Colomer[1], T. Serra[1], X. Casamitjana[1] and A. Folkard[2]

[1] *Department of Physics, University of Girona, 17071, Girona, Spain*
[2] *Lancaster Environment Centre, Lancaster University, Lancaster LA1 4YQ, United Kingdom*

**Corresponding author, e-mail marianna.soler@udg.edu*

KEYWORDS
Gravity current; inertial regime; drag-dominated regime; sediment deposition; canopy

Introduction

The dynamics of gravity currents has been studied for many years using lock exchange experiments, in which two fluids of different densities within an experimental flume are initially at rest and separated by a lock gate. Gravity currents may become drag-dominated when they propagate into partially or fully vegetated channels (Tanino et al., 2005). Hatcher et al. (2000) showed that gravity currents produced by a release of a finite reservoir flowing through arrays of obstacles decrease their velocity as: $x_c \sim ((q_o \cdot g'd)/(C_D \cdot \emptyset))^{1/4} \cdot t^{1/2}$ (1)
where q_o is the total current volume per unit across-flume distance; g' is the reduced gravity; d is the individual obstacle width; $\phi = (\pi/4)ad$ is the volume fraction of the obstacles; a is the frontal area of cylinders per unit volume; and finally C_D is the array drag coefficient.
Bonnecaze et al. (1993) analysed a two dimensional particle-driven gravity current of fixed volume spreading over a rigid horizontal surface without entrainment and found the length of the particle-driven current as function of time, $x_c \sim (q_o \cdot g')^{1/3} \cdot t^{2/3}$ (2)
This study sets out to investigate characteristics of both turbidity currents and arrays of obstacles through which they flow on their hydrodynamic and sedimentary development.

Materials and methods

Experiments were carried out in a laboratory flume where a particle laden gravity current was measured as it passed through an array of rigid obstacles. The turbidity currents, of naturally-sourced poly-dispersed sediment, had 1 to 10 gL^{-1} concentration. The array of obstacle had solid plant fractions (SPF) of 1% and 2.5%; and control cases with no obstacles were carried out too. Depositional flux of sediment was measured with 13 traps positioned along the flume using LISST-100. Five turbidity sensors and two CCD cameras mounted on stationary tripods over the tank were used to measure the progression of the current's front and determine its speed.

Results and discussion

Analysis of frontal progression of salinity-driven gravity currents through arrays of obstacles in lock-release experiments shows that it in the initial inertial regime $x_{toe} \sim t$ and

Figure 1. Temporal evolution of the front position of the turbidity current

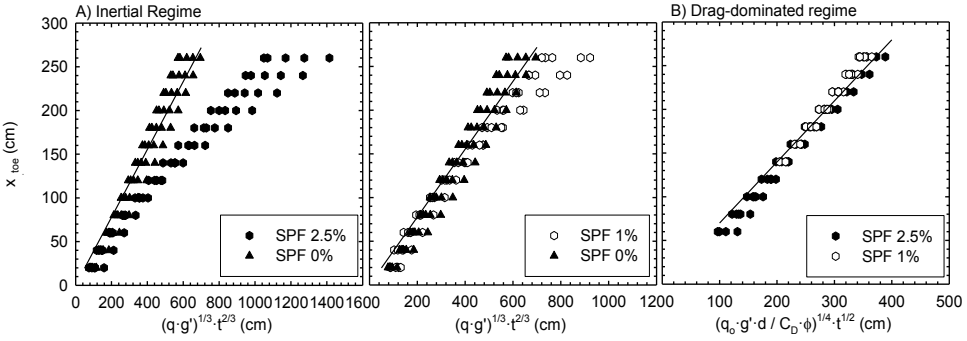

in the subsequent drag-dominated regime $x_{toe} \sim t^{2/3}$ (Tanino et al., 2005, Zhang and Nepf, 2008). In contrast, our results for a particle-driven gravity current show that, in the inertial regime, $x_{toe} \sim t^{2/3}$) in agreement with Bonnecaze et al. (1993) and in the drag-dominated regime $x_{toe} \sim t^{1/2}$ in agreement with Hatcher et al. (2000). The point at which gravity current transition from the inertial to the drag dominated regime occurred at $C_DaL = 5$.

From the results of all of our runs, the depositional flux rate was found to depend on the canopy density and the initial sediment concentration of the current, and to differ depending on whether the fine or coarse particle size fraction was being considered. (Fig. 2). The normalised flux rate decreased with C_DaL for both the fine (Fig. 2A, C) and coarse (Fig. 2B, D) fractions when the gravity current was in the inertial-dominated regime, whereas it increased in the drag-dominated regime. This was found for all runs except for the fine fraction in the cases where the initial sediment concentration was high (10 gL^{-1}) and the canopy density was low (SPF = 1%), in which the rate increased through the inertia-dominated regime.

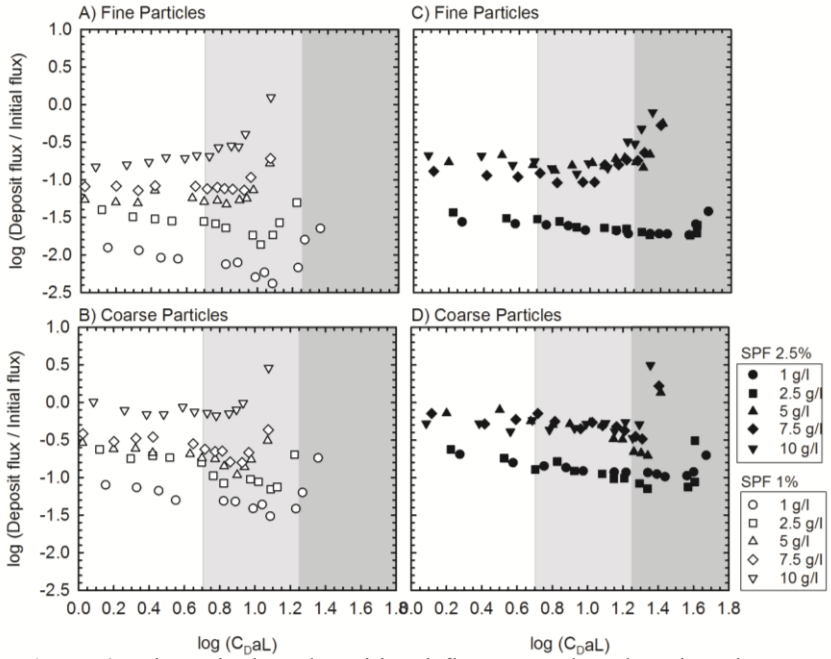

Figure 2. Dimensionless depositional flux rates plotted against the array drag, C_DaL. divided them into fine (2.2–6.2 μm) and coarse (6.2-104 μm) fractions The light grey zone corresponds to the transition regime from inertial to drag-dominated ($5 < C_DaL < 18$) and the dark grey zone to the fully drag-dominated regime ($C_DaL > 18$).

In summary, the propagation of particle-driven gravity currents, and the patterns of deposition that they create were found to be functions of canopy density, suspended sediment characteristics (concentration and grain size) and distance from the current's source. The evolution of the currents and their depositional patterns may be categorised into an early, inertia-dominated stage in which deposition rates mainly decrease from monotonically, to a transitional stage, and a late drag-dominated stage, in which deposition rates tend to peak. These stages are effectively delineated, by values of the array drag term $C_DaL < 5$ (inertia dominated) and >18 (drag dominated), which are close to those reported for salinity-driven gravity currents by Tanino et al. (2005).

REFERENCES

Bonnecaze, R.T., H.E. Huppert, and J.R. Lister, (1993), Particle-driven gravity currents. *J. Fluid Mech*., **250**, 339-369

Hatcher, L., A.J. Hogg, and A.W. Woods, (2000), The effect of drag on turbulent gravity currents. *J. Fluid Mech*., **416,** 297-314.

Tanino, Y., Nepf, H.M. and Kulis, P.S. (2005) Gravity currents in aquatic canopies. Water Resources Research, 41, W12402, doi: 10.1029/2005WR004216.

Greenhouse gas modelling in lakes: the role and parameterization of mixing processes

V. Stepanenko[1,2]*, E. Mortikov[1,3], I. Mammarella[4,5], V. Lykossov[3,1] and T. Vesala[4,5]

[1] *Research Computing Center (RCC), Lomonosov Moscow State University (MSU), Moscow, Russia*
[2] *Faculty of Geography, Lomonosov Moscow State University, Moscow, Russia*
[3] *Institute of Numerical Mathematics, Russian Academy of Sciences, Moscow, Russia*
[4] *Department of Physics, University of Helsinki, Helsinki, Finland*
[5] *Department of Forest Sciences, University of Helsinki, Helsinki, Finland*

**Corresponding author, e-mail stepanen@srcc.msu.ru*

KEYWORDS
Lakes; greenhouse gases; modelling; internal waves.

EXTENDED ABSTRACT

Introduction

It is widely accepted that lakes cause significant regional thermodynamic effects on weather and climate, motivating lake modules to be implemented in Earth system models. Concomitantly, there grows an empirical evidence on considerable CH_4 and CO_2 fluxes from freshwater bodies to the atmosphere. The need to develop realistic mathematical description of greenhouse gas dynamics in lakes leads us not only to respective biochemical processes treatment but also to specific attention to vertical mixing mechanisms, since CH_4 and CO_2 predominantly originate in bottom sediments. This contribution presents a new lake model LAKE 2.0 and its verification with focus at seiche-induced vertical mixing currently lacking in most 1D lake models.

Materials and methods

The 1D LAKE model calculates temperature, horizontal velocity components, oxygen, carbon dioxide and methane in the basin. All prognostic variables are treated in unified manner via generic 1D transport equation for horizontally averaged property. Water body interacts with underlying sediments, represented by a set of vertical columns with heat, moisture and CH_4 transport inside. The momentum equations of the model include barotropic pressure gradient term, introducing in the model the oscillation of 1-st surface seiche mode.

Lake Kuivajärvi is a small (area 0.63 km^2) boreal lake in Hyytiälä, Southern Finland. Fluxes of momentum, sensible and latent heat are measured at 1.5 m above the lake surface by eddy covariance (EC) technique. The measurement setup consisting of an ultrasonic anemometer and an enclosed-path infrared gas analyzer is mounted on a fixed platform situated in the middle of the lake. More details on the measurement platform, the EC system setup and flux calculation procedures can be found in (Mammarella et al., 2015). On the platform, a four-way net radiometer provided the full radiation budget and a thermistor string enabled the collection of data on vertical water temperature distribution. All the atmospheric

measurements were performed at the height of 1.7 m above the water. In addition, the relative humidity was directly measured at the platform at the height of 1.5 m. Manual water samplings for CO_2 and CH_4 were conducted weekly in the water column from the surface to the bottom. The O_2 content was measured every half-meter until the depths of 9 m and after that every one meter. These samples were processed using the headspace equilibrium technique. The data for the period 5-th of May to 31-st of October 2013 were used for forcing and verification of the 1D lake model.

For verification of 1D LAKE model we also use a 2D version of Navier-Stokes code based on the modified immersed boundary method and developed at RCC MSU (Mortikov, 2010).

Results and discussion

LAKE model demonstrates fair agreement with observation data in seasonal pattern of Kuivajärvi Lake stratification, methane, oxygen and carbon dioxide concentration (Stepanenko et al., 2016). It was also shown, that concentrations of CO_2 and CH_4 are sensitive to vertical diffusivity, simulated by the model, as these gases originate mostly in bottom sediments. Specifically, with surface seiche parameterization included, LAKE model could reproduce measured bottom CH_4 concentration much better, because in this case the bottom current developed in the model along with corresponding shear-driven turbulence. Note, that the existence of hypolimnetic turbulent boundary layer has been corroborated by many experimental studies. Most 1D lake models lack surface seiche parameterization, and thus should fail in simulating the vertical diffusion of dissolved gases.

Internal (baroclinic) seiches are a prominent feature of dynamic regime of many stratified lakes, and are found in temperature power spectra of Kuivajärvi Lake as well (Stepanenko et al., 2016). It is expected by some researchers that internal seiches contribute to vertical mixing via additional bottom shear, or by internal waves breaking at the sloping bottom (where these waves arise as a result of wave-energy cascade from large-scale seiche modes). The only parameterization of these effects we could find in literature is an extension of k- ε model by Goudsmit et al. (2002). We argue, however, that this model makes negligible effect on vertical diffusion, since it's stationary Richardson number is about 0.30 compared to standard value of 0.25 (whereas for lakes' thermocline it is usual that $Ri >> 1$). We propose a new parameterization of internal seiches in k - ε model, and test it vs. 2D hydrodynamic code simulations.

REFERENCES

Goudsmit, G.-H.: Application of k-_ turbulence models to enclosed basins: The role of internal seiches, *Journal of Geophysical Research*, **107**, 3230, doi:10.1029/2001JC000954, http://doi.wiley.com/10.1029/ 2001JC000954, 2002.

Mammarella, I., Nordbo, A., Rannik, U., Haapanala, S., Levula, J., Laakso, H., Ojala, A., Peltola, O., Heiskanen, J., Pumpanen, J., and Vesala, T.: Carbon dioxide and energy fluxes over a small boreal lake in Southern Finland, *Journal of Geophysical Research*: Biogeosciences, **120**, 1296–1314, doi:10.1002/2014JG002873, 2014JG002873, 2015.

Mortikov, E.V.: "Application of the immersed boundary method for solving the system of Navier–Stokes equations in domains with complex geometry", *Vychisl. Metody Programm.*, **11**:1 (2010), 32–42

Stepanenko, V., Mammarella, I., Ojala, A., Miettinen, H., Lykosov, V., and Vesala, T.: LAKE 2.0: a model for temperature, methane, carbon dioxide and oxygen dynamics in lakes, *Geosci. Model Dev. Discuss.*, doi:10.5194/gmd-2015-261, in review, 2016.

The impact of SO2 deposition from wash water on North Sea pH

A. Stips[1]*, K. Bolding[2], J. Bruggeman[2], D. Macias[1], C. Coughlan[1]

[1] *European Commission, Joint Research Centre, Institute for Environment and Sustainability, Water Resources Unit, Via E. Fermi 2749, TP270, I-21027 Ispra, Italy*
[2] *Bolding and Bruggeman ApS B&B, Strandgyden 25, 5466 Asperup, Denmark*

**Corresponding author, e-mail adolf.stips@jrc.ec.europa.eu*

KEYWORDS
North Sea; water quality; modelling; scrubber wash water; acidification.

EXTENDED ABSTRACT

Introduction

The input of acid substances (like SO2) into the sea has been recognized as an environmental issue that needs to be considered in terms of ocean acidification; acid inputs and techniques to deal with them have implications for member states' obligations under the Water Framework Directive and Marine Strategy Framework Directive. This study provides an initial spatial explicit assessment of the potential impact of on-board desulphurisation equipment (open loop scrubbers) on seawater quality with focus on SOx Emission Control Areas (SECAs). We investigate the impact of ship-borne SO2 on acidification (pH decrease) of seawater in comparison to the impact from increasing atmospheric CO2 concentrations in the North Sea.

Materials and methods

A numerical modelling system consisting of a coupled hydro-dynamical model and a bio-geochemical model able to simulate the influence of ship-borne SO2 fluxes on the water properties has been established. The model configuration consists of two independent models that are dynamically coupled at runtime. The first model is the hydro-dynamical General Estuarine Transport Model, GETM (Stips et al. 2004). The second is ERSEM (The European Regional Seas Ecosystem Model, Artioli et al. 2012). Specifically the carbonate component of ERSEM is used in this study. ERSEM is coupled to the hydro-dynamical model via FABM (Framework for Aquatic Bio-geochemical Models, Bruggeman and Bolding, 2014).
The system has been set-up for the North Sea and a reference plus several scenario simulations have been carried out. The performed physical simulations are realistic in terms of the applied external forcings – i.e. meteorology, initial and lateral boundary conditions and freshwater fluxes via rivers. The bio-geochemical simulations are realistic in the sense that they describe the carbonate system at high complexity using the ERSEM/carbonate model.
The first simulation is the reference simulation using 2006 atmospheric CO2 concentration and not imposing any SO2 flux (best case, no shipping). The second simulation uses SO2 ship emission values from 2006 and atmospheric CO2 concentrations also from 2006. The third simulation uses SO2 from 2006 and CO2 concentration corresponding to present day values.

Results and discussion

The impact on the pH decrease in the open North Sea region from discharging the acid wash water into the seawater was found to be small, but not insignificant, and regionally varying. The calculated annual mean decrease of pH due to SO2 injection for the North Sea total water column is 0.00011; when considering only the change in the surface layer (0-20m), the annual decrease is 0.00024. The total annual impact from increasing atmospheric CO2 concentrations on the acidification of the North Sea surface area is about 8 times stronger (0.001) as the impact from wash water injection. However, because of the pronounced spatial variations of

SO2 input the mean impact does not reflect the overall situation well. We find critical regions with high ship traffic intensity, for example along the shipping lanes and in the larger Rotterdam port area. Here, the contribution from SO2 injection can be double the impact from increasing CO2 concentrations and 20 times larger than the North Sea mean value. Increasing the atmospheric CO2 concentration from 383 ppm in 2006 to 400 ppm in 2015 has a bigger, but spatial uniform impact on pH decrease. However, impacts are cumulative and therefore even small additional contributions from ship born SO2 lead to a further overall decrease of pH (acidification) and a consequent worsening of the marine environmental conditions.

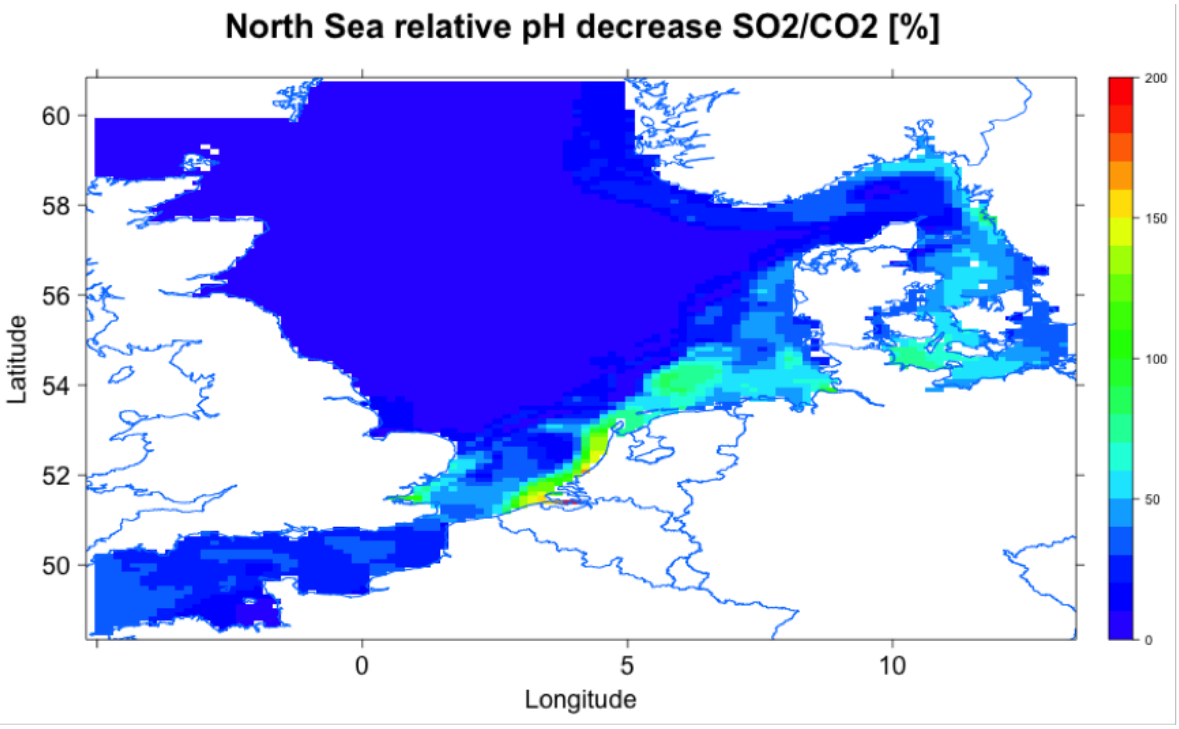

Figure 1. Relative pH decrease from ship borne SO2 compared to the decrease due to increased CO2 levels.

Critical regions indicate potential problems related to the surface water quality in ports, estuaries and coastal waters that are subject to the Water Framework Directive (WFD). The problem of decreasing pH caused by SO2 input from ship exhaust gases in regional seas is relevant to the obligation of the Member States to assess the environmental state of their marine areas and to establish a Good Environmental Status (GES) under the Marine Strategy Framework Directive (MFSD), as pH value is one of the GES criteria. Considering the complexity of the issue under investigation this scoping report is by no means fully conclusive and only touches on some of the relevant issues. A more comprehensive assessment is therefore recommended.

REFERENCES

Artioli, Y., et al. (2012). The carbonate system in the North Sea: Sensitivity and model validation. *Journal of Marine Systems*, **102-104**:1–13.

Bruggeman, J., and Bolding, K. (2014). A general framework for aquatic biogeochemical models. *Environmental Modelling and Software*, **61**:249-265.

Stips A., Bolding K., Pohlman T., Burchard H. (2004). Simulating the temporal and spatial dynamics of the North Sea using the new model GETM (general estuarine transport model). *Ocean Dynamics,* **54**:266–283.

Under ice processes in Base Mine Lake

E. Tedford[1]*, R. Pieters[1,2]*, and G. Lawrence[1]

[1] *Civil Engineering,* University of British Columbia, Vancouver, Canada
[2] *Earth, Ocean and Atmospheric Sciences, University of British Columbia, Vancouver, Canada*

**Corresponding author, e-mail ttedford@eos.ubc.ca*

KEYWORDS
Reverse stratification; ice; salt exclusion; echosoundings; internal waves.

EXTENDED ABSTRACT

Introduction

We describe the physical processes occurring under the ice in Base Mine Lake (7.9 km^2, depth ~10 m) in northern Alberta, Canada (57^{o}N). Temperature, conductivity and turbidity data were collected using instruments moored under the ice and by profiling through holes drilled in the ice. Echosoundings were collected at 10 station during two field campaigns.

Results

In addition to the reverse thermal stratification typically observed under the ice in natural lakes, Base Mine Lake exhibited a number of special features. In this presentation we will highlight four of these features:

1. There was strong evidence of upward heatflux from the underlying mud to the lower part of the water column particularly in the first two weeks immediately following ice-on. During this early under-ice period, near bottom water quickly rose in temperature from approximately 2^{o}C to the temperature of maximum density (~3.6^{o}C, see Figure 1b. late November 2014).
2. Salinity in the water increased throughout the winter at a rate that closely matches the predicted rate due to salt exclusion during ice formation. The prediction of the rate of salt exclusion required the inclusion of the insulating influence of snow (see the heavy dashed line in Figure 1c.).
3. Turbidity under the ice varied vertically from 150 NTU at the surface to greater than 500 NTU (outside the range of the sensor) near the bottom. Bottle samples collected at the same time indicate suspended solids concentrations from 20 to 200 mg/L. The associated gradients in suspended solids contributed significantly to the density stratification.
4. Methane ebullition was observed in most echosoundings and, on one occasion, by eye at the water surface in a drilled hole in the ice. The echosoundings provide a qualitative indicator of the horizontal variability of gas ebullition (Figure 2).

The dynamical roles of heating from the underlying mud, salinity exclusion from the ice, and suspended solids are quantified. The occurrence of convection at the temperature of maximum density complicates the interpretation of the observations. Internal waves also occur under the ice and will be described

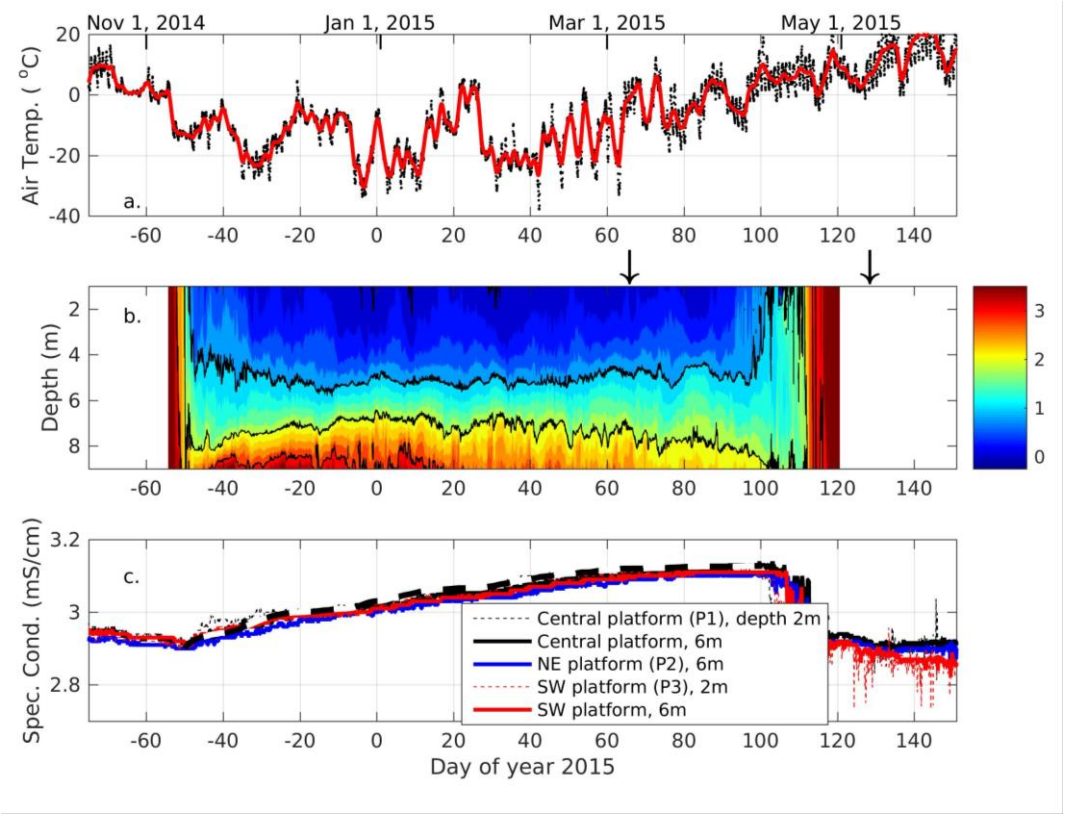

Figure 1. Measurements at Base Mine Lake during winter 2013-2014. (a) Air temperature. (b) Water temperature at various depths at the three platforms. (c) Specific conductivity (mS/cm), a salinity of 2 gL -1 corresponds to 3.2 mS/cm. The black dashed line is the predicted increase in conductivity due to the exclusion of salt based on estimated ice formation (Ice formation is estimated with the air temperature in the top panel, Eq 4.44 Lepparanta, 2015).

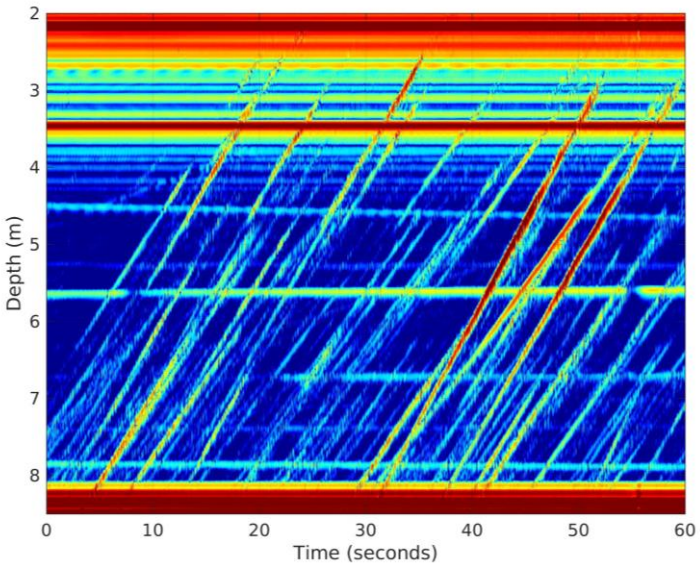

Figure 2. Echo intensity observed in Base Mine Lake under ice. The diagonal streaks indicate rising bubbles.

REFERENCES

Leppäranta, Matti. (2015), Thermodynamics of Seasonal Lake Ice. Freezing of Lakes and the Evolution of their Ice Cover. Springer, Berlin Heidelberg.

A coupled atmospheric-lake model to simulate the internal waves structure in a deep, stratified lake.

G. Valerio[1]*, M. Pilotti[1], A. Cantelli[2], P. Monti[3] and G. Leuzzi[3]

[1]*Department DICATAM, Università degli Studi di Brescia, Brescia, Italy*
[1]*Department DIMA, Università di Roma La Sapienza, Roma, Italy*
[3]*Department DICEA, Università di Roma La Sapienza, Roma, Italy.*

**Corresponding author, e-mail giulia.valerio@unibs.it*

KEYWORDS
Lakes; alpine area; wind field; modelling; internal waves.

EXTENDED ABSTRACT

Introduction

Wind distribution plays a fundamental role in lake dynamics and mixing processes can't be effectively reproduced without an adequate representation of the space and time variable wind field (e.g. Appt et al., 2004). In medium-size lakes in the alpine and pre-alpine regions, this is a challenging task due to the strong influence of the topography on the wind regime. In these geographical areas, the flow is mainly determined by the differential heating-cooling processes and is characterized by a complex interaction between up-slope winds and lake breezes (e.g. Lemmin and D'Adamo, 1997). To account for the influence of the spatial variability of the wind field on the basin-scale internal wave in a deep pre-alpine lake surrounded by a complex valley topography, we propose to simulate the wind field through an high resolution meteorological model.

Materials and methods

Lake Iseo is a 250 m deep, 60.9 km^2 large Italian lake. In this contribution we investigated the role of the wind on the internal wave activity in the period 13-18 July 2010, when a thermal stratification typical of the summer season was present and an internal wave structure was dominated by a vertical and horizontal modes 1 with a 24 hours period.
To study the sensitivity of the basin-scale internal wave structure to wind distribution, we compared the temperature measured at the northern (LDS) and southern (TC) end of the lake with the one obtained by forcing the 3D hydrodynamic model ELCOM (Hodges et al., 2000) with uniform wind fields measured at the anemometric stations in the lake area, with spatially varying wind field obtained through the bilinear interpolation of all the measured data (Valerio et al., 2012) and with the one simulated by the Weather Research and Forecasting (WRF) model (Skamarock et al., 2008).

Results and discussion

The results obtained by using the wind measured at each anemometric station as a uniform field, were not satisfactory. The on-lake station present on the lake led to an excessive energizing of the lake motions, as evident from the overestimation of the surface layer at both stations and of the isotherm oscillations (see Fig. 1). Notable improvements were obtained by forcing the model with a spatially-varying wind (Valerio et al., 2012). Eventually, the wind field obtained from the meteorological model further improved the best fit of the measured data. With regard to the thermal structure, the numerical wind field allowed to minimize the RMSE with respect to the mean temperature profile, by improving the reproduction of the

average surface layer deepening. With regard to the oscillatory pattern, it led to notable improvements especially in the southern area. Here, the numerical wind field was the only one that allowed a correct reproduction of the gradual increase of the wave amplitudes between 5 and 30 m of depth.

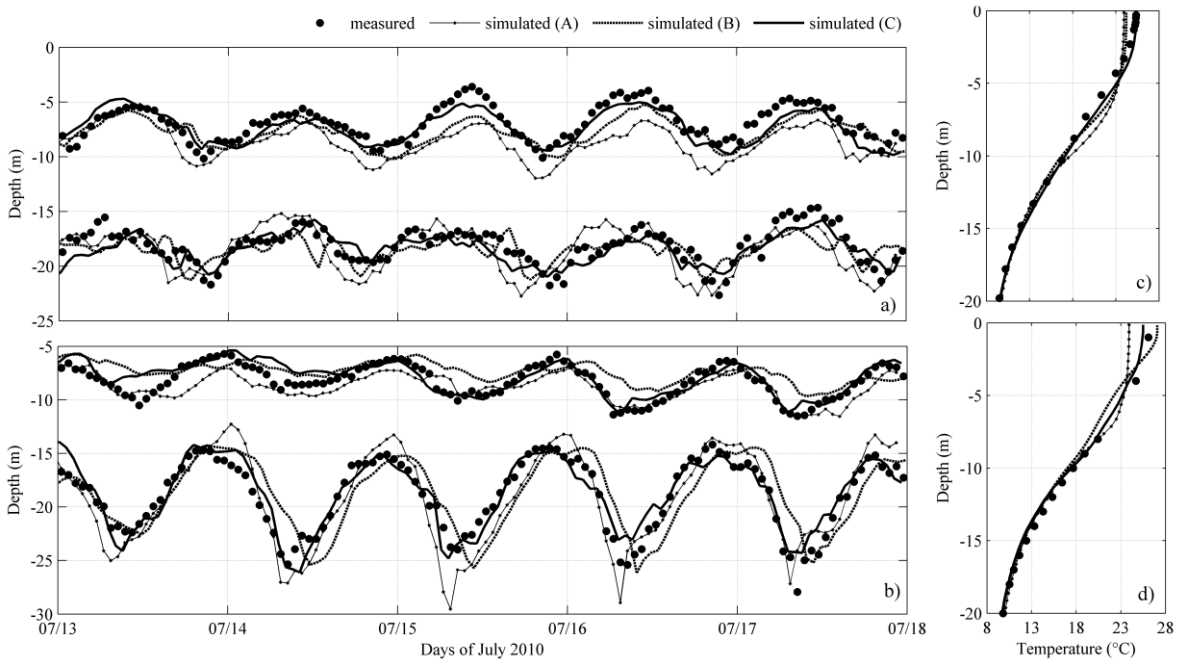

Figure 1. Time series of the vertical displacements of the 10°C and 20°C isotherms recorded at (a) the northern LDS and at (b) the southern TC thermistor chain. The black dots show the measured values, while the continuous lines indicate the results of the simulations forced by (sim A) the uniform on-lake wind measured at LDS, (sim B) the interpolated wind and (sim C) the simulated wind. (c, d) Comparison of the average temperature profile simulated and measured at (c) LDS and (d) TC.

The significant enhancement of the modeled main basin-scale internal wave motion based on the physically based distributed description of the wind stress over the lake surface confirms the importance of an accurate representation of the wind in physical limnology. Moreover, the presented coupled approach provides important insights for setting up more simplified conceptualization of the wind field.

REFERENCES

Appt, J., J. Imberger and H. Kobus (2004), Basin-scale motion in stratified Upper Lake Constance, *Limnol. Oceanogr.,* **49(4)**, 919-933.

Hodges, B.R., J. Imberger, A. Saggio and K. Winters (2000), Modeling basin-scale internal waves in a stratified lake, *Limnol. Oceanogr.*, **45(7)**, 1603–1620.

Lemmin, U. and N. D'Adamo (1997), Summertime winds and direct cyclonic circulation: observations from Lake Geneva, *Annales Geophysicae*, **14**, 1207–1220.

Skamarock, W.C. and J.B. Klemp (2008) A time-split non hydrostatic atmospheric model for weather research and forecasting applications, *J. Comp. Phys.*, **227(7)**, 3465-3485.

Valerio, G., M. Pilotti, C.L. Marti, C.L. and J. Imberger (2012), The structure of basin scale internal waves in a stratified lake in response to lake bathymetry and wind spatial and temporal distribution: Lake Iseo, Italy, *Limnol. Oceanogr.*, **57(3)**, 772-786.

Impact of nuclear produced thermal pollution on a lake with short residence time - what can models resolve?

L. Råman Vinnå[1]*, A. Wüest[1,2] and D. Bouffard[1]

[1] *Physics of Aquatic Systems Laboratory, Margaretha Kamprad Chair, École Polytechnique Fédérale de Lausanne, Institute of Environmental Engineering, Lausanne CH-1015, Switzerland*
2 Eawag, Swiss Federal Institute of Aquatic Science and Technology, Surface Waters Research and Management, Kastanienbaum, Switzerland

**Corresponding author, e-mail love.ramanvinna@epfl.ch*

KEYWORDS
Nuclear thermal pollution; hydrodynamic modeling; lakes; river intrusion.

EXTENDED ABSTRACT

Introduction

Thermal pollution can have considerable influence on water temperature in freshwater systems notably affecting stratification (Kirillin et al., 2013). Consequences can be seen across the entire aquatic food web including benthic organisms (Barnett, 1971), algae (Cairns, 1971) and fish (Sylvester, 1972). The increased usage of aquatic systems as sinks and sources of heat necessitates detailed investigations of the impact of thermal pollution on lakes and reservoirs.

Here we investigate the impact of thermal pollution on temperature and heat fluxes in the perialpine Lake Biel (7°10'E, 47°5'N, 39.3 km^2 and 74 m deep). The lake has a short hydraulic residence time of only 58 days and is under strong influence of the Aare tributary. The source of the thermal pollution, the Mühleberg Nuclear Power Plant, is located 20 km upstream. The plant emits 700 MW as cooling water into the Aare River. Consequently, as the river enters the lake, it is heated locally by up to 4.5 °C. The aim of our study is to provide guidelines regarding model selection for studies of thermal pollution in similar aquatic systems.

Materials and methods

The thermal consequences of the Mühleberg Nuclear Power Plant for Lake Biel was investigated with two hydrodynamic models. We used the one-dimensional model SIMSTRAT (Goudsmit et al., 2002) and the three-dimensional model Delft3D-Flow version 6.01.07.3574 (Deltares, 2016). The power plant is up for decommissioning scheduled for 2019. The influence of thermal pollution was therefore investigated by running the models with and without thermal emission. The temporal variability of the lake was analyzed for a cold (April to March 2010/2011) and a warm period (April to March 2013/2014).

Results and discussion

We observe a strong seasonal dependence in the response of Lake Biel to thermal pollution. By removing the thermal pollution the lake cools down by ~ -0.3 °C between October and March. The corresponding value from April to September was ~ -0.1 °C. The impact was marginally stronger for the warm period compared to the cold period.

The majority of thermal pollution (~60 %) leaves Lake Biel through the Aare outflow. This is due to the lake's short retention time and the short distance between the Aare inflow and outflow (~8 km). Surprisingly we were able to reproduce this throughflow accurately even with

the one-dimensional model. The reason being the high discharge of the Aare which quickly flushes the incoming heat out of the lake. The flushing was likewise observed in the three- dimensional model. This model could furthermore resolve the path of the river intrusion within the lake. We could identify periods where the river water travelled along the shoreline directly from the inflow to the outflow, thereby short-cutting the lake. Additionally the spatial impact of thermal pollution was, as expected, better resolved by the three-dimensional model. With observed temperature fluctuations up to –4.5 °C in Delft3D-Flow and –1.8 °C in SIMSTRAT.

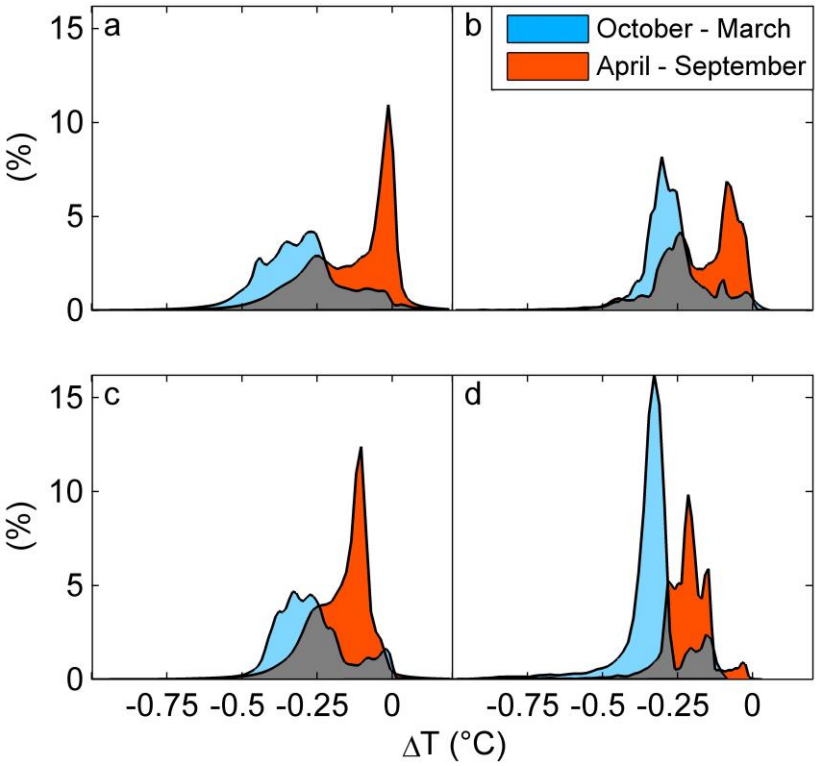

Figure 1. Temperature change in Lake Biel (ΔT) due to removal of thermal pollution. Displayed as percentage of total volume for Delft3D-Flow (a, c) and SIMSTRAT (b, d) during cold (a, b) and warm (c, d) period.

We argue that three-dimensional models should be used to assess the spatial impact of extreme levels of thermal pollution, which can have severe impact on biota. For overall system assessment one-dimensional models are sufficient. However, care is required for aquatic systems with short distance between the thermal source input and outflow.

REFERENCES

Barnett, P.R.O. (1971). Some changes in intertidal sand communities due to thermal pollution. Proc. R. Soc. Lond. B Biol. Sci. *177*, 353–364.

Cairns, J. (1971). Thermal pollution: a cause for concern. Water Pollut. Control Fed. *43*, 55–66.

Deltares (2016). accessed 1 March 2016, <https://oss.deltares.nl/web/delft3d>.

Goudsmit, G.-H., Burchard, H., Peeters, F., and Wüst, A. (2002). Application of k-ε turbulence models to enclosed basins: The role of internal seiches. J. Geophys. Res. *107*.

Kirillin, G., Shatwell, T., and Kasprzak, P. (2013). Consequences of thermal pollution from a nuclear plant on lake temperature and mixing regime. J. Hydrol. *496*, 47–56.

Sylvester, J.R. (1972). Possible effects of thermal effluents on fish: a review. Environ. Pollut. *3*, 205–215.

Surface water quality assessment using close-range imaging spectrometry

A. Wagner*, S. Hilgert

Inst. for Water and River Basin Management, Dpt. of Aquatic Environmental Engineering, Karlsruhe Institute for Technology (KIT)

*Corresponding author, e-mail adrian.wagner@kit.edu

KEYWORDS

Water quality; hyperspectral; unmanned aerial vehicle; optically active constituents; sea truthing

EXTENDED ABSTRACT

Introduction

Due to their significance for human health and well-being, surface freshwater systems require thorough protection measures interlinked with extensive water quality monitoring. Climate and land use change impact, unresolved substance emissions issues as well as increasing usage requirements and ecological standards underline the need of high spatial and temporal monitoring resolutions. Most water quality parameters change the energy spectra emitted by water bodies and can therefore be measured remotely (Ritchie et al., 2003). Suspended particulate matter (SPM) affects water quality because of its association to e.g. nutrients, hydrophobic organic pollutants and heavy metals. Eutrophication is often indicated by the abundance of chlorophyll (CHL) bearing organisms with characteristic spectral signatures. Light-absorbing coloured dissolved organic matter (CDOM) is a surrogate for biological and chemical oxygen demand and total phosphorous (Niu et al., 2014). Is is also an indicator for sources and properties of dissolved organic matter (Lambert et al., 2015). Air- and space borne multi- and hyperspectral remote sensing has been successfully used for deriving trophic states, total phosphorous loads (Koponen et al., 2002) and algae concentrations (Karaska et al., 2004) as well as for generally mapping optically active components (OACs) in lakes and rivers (Hakvoort et al., 2002; Knaeps et al., 2010; Olmanson et al., 2013).

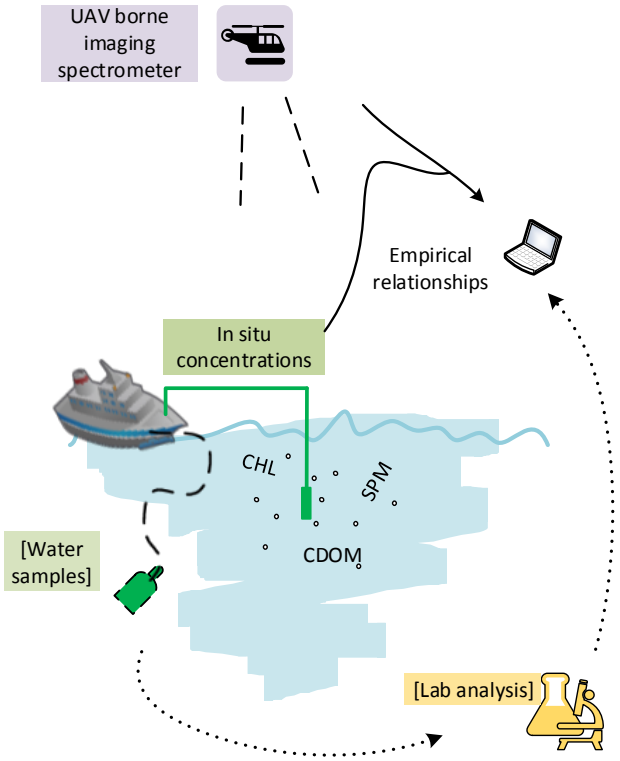

Figure 1. Schematic close-range imaging spectrometry approach which allows simultaneous sea truthing.

While this method has the advantage of covering spatial variations over large areas, sea truthing has to be accomplished within a close time span of the satellite or airplane overpass, which limits the amount of training samples (Knaeps et al., 2010). We therefore investigate the use of ground based, ship based and unmanned aerial vehicle (UAV) based hyperspectral imaging of OACs in rivers and lakes (Figure 1). Because of the possibility to retrieve large numbers of training samples, we will first focus on the application of empirical algorithms. Target applications are continuous contact-free SPM measurements in rivers for precise sediment fluxes, as well as flexible, high resolution and low-cost OAC and OAC surrogate distribution mapping in surface layers of lakes, reservoirs and rivers.

Materials and methods

In the course of summer 2016, highly controlled mesocosm experiments will be carried out using well-mixed, sunlit, black, rectangular 1.1 m³ glass-fibre reinforced plastic tanks of 0.8 m height and a ground-based AISA Airborne Hyperspectral Imaging System to examine reflectances of algae blooms and suspended matter. AISA data will be used to determine the minimum spectral resolution needed as well as key wavelengths for OAC determination. Larger particles of natural river deposits are removed from initial suspensions by allowing 5 minutes to settle and decanting the remaining suspension. Its resulting grain size distribution is determined with an EyeTech™ Particle Size Analyser. Particles are then added stepwise to clear water, resulting in an SPM range of 0–3000 mg/L. In a second experiment, algae bloom is induced by transferring bloom water from a pond to fertilized clear water to create a CHL range of about 0–200 µg/L. Lastly, sediment is added again stepwise to investigate algae-sediment interactions. SPM and CHL concentrations are determined at each step using standard laboratory techniques. Additionally, portable TriOS microFlu fluoro- and turbidimeter are used to monitor OAC concentrations throughout the experiments. The goal is

to become more independent of time-intensive laboratory analyses for further OAC determination campaigns in natural water bodies.

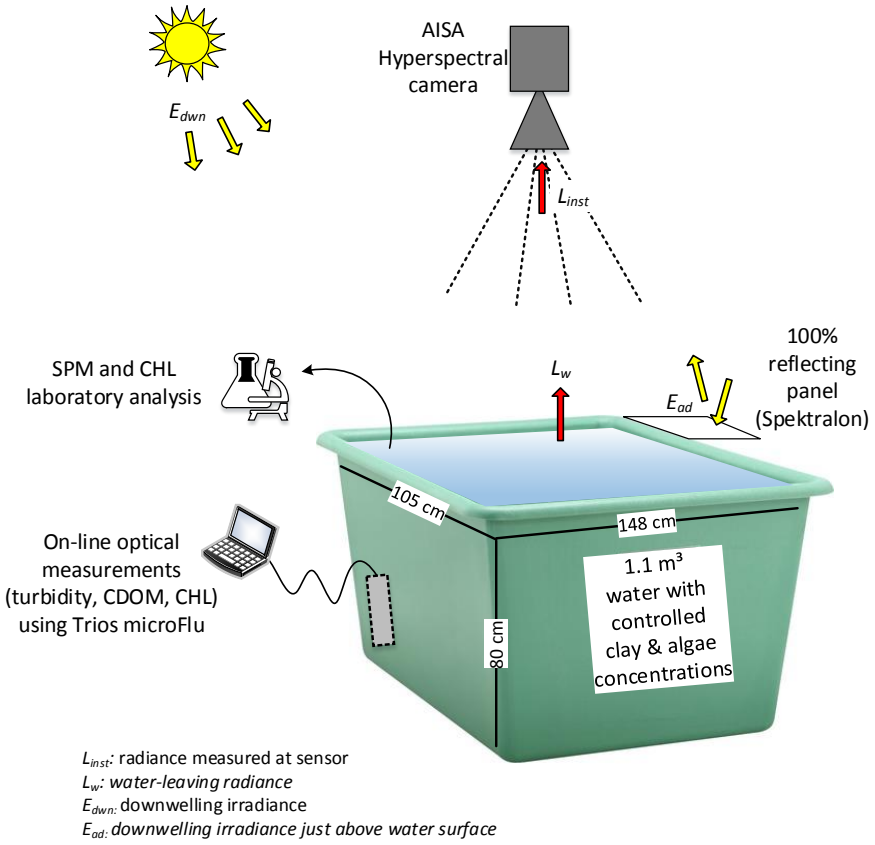

Figure 2. Experimental mesocosm setup for OAC concentration algorithm retrieval.

Results and discussion

At the time of writing, the measurement campaign was in the planning stage. Other researchers have found strong positive (negative) relationships between CHL concentrations and reflectance at around 700–710 nm (670 nm). High SPM concentrations are indicated by reflectance peaks at around 570 and 795 nm. There are numerous algorithms to derive OAC concentrations from reflectance spectra of natural waters (e.g. Olmanson et al., 2013) or mesocosms (e.g. Schalles et al., 2001). However, to our knowledge proximal imaging spectrometry has not been used for water quality applications such as continuous sediment flux monitoring and OAC mapping. Hyperspectral sensors that are able to distinguish targets with similar spectral signatures such as waters with similar OAC concentrations are becoming lighter and cheaper. Therefore, especially UAV-mounted sensors will fill a critical sampling niche for inland waters due to high flexibility and small, adjustable target distance.

References

Hakvoort, H., J. de Haan, R. Jordans, R. Vos, S. Peters, and M. Rijkeboer (2002), Towards airborne remote sensing of water quality in The Netherlands—validation and error analysis, *ISPRS Journal of Photogrammetry and Remote Sensing*, **57**(**3**), 171–183, doi:10.1016/S0924-2716(02)00120-X.

Karaska, M. A., R. L. Huguenin, J. L. Beacham, M.-H. Wang, J. R. Jensen, and R. S. Kaufmann (2004), AVIRIS Measurements of Chlorophyll, Suspended Minerals, Dissolved Organic Carbon, and Turbidity in the Neuse River, North Carolina, *photogramm eng remote sensing*, **70**(**1**), 125–133, doi:10.14358/PERS.70.1.125.

Knaeps, E., S. Sterckx, and D. Raymaekers (2010), A Seasonally Robust Empirical Algorithm to Retrieve Suspended Sediment Concentrations in the Scheldt River, *Remote Sensing*, **2**(**9**), 2040–2059, doi:10.3390/rs2092040.

Koponen, S., J. Pulliainen, K. Kallio, and M. Hallikainen (2002), Lake water quality classification with airborne hyperspectral spectrometer and simulated MERIS data., *Remote Sensing of Environment*, **79**(**1**), 51–59, doi:10.1016/S0034-4257(01)00238-3.

Lambert, T., F. Darchambeau, S. Bouillon, B. Alhou, J.-D. Mbega, C. R. Teodoru, F. C. Nyoni, P. Massicotte, and A. V. Borges (2015), Landscape Control on the Spatial and Temporal Variability of Chromophoric Dissolved Organic Matter and Dissolved Organic Carbon in Large African Rivers, *Ecosystems*, **18**(**7**), 1224–1239, doi:10.1007/s10021-015-9894-5.

Niu, C., Y. Zhang, Y. Zhou, K. Shi, X. Liu, and B. Qin (2014), The potential applications of real-time monitoring of water quality in a large shallow lake (Lake Taihu, China) using a chromophoric dissolved organic matter fluorescence sensor, *Sensors (Basel, Switzerland)*, **14**(**7**), 11580–11594, doi:10.3390/s140711580.

Olmanson, L. G., P. L. Brezonik, and M. E. Bauer (2013), Airborne hyperspectral remote sensing to assess spatial distribution of water quality characteristics in large rivers: The Mississippi River and its tributaries in Minnesota, *Remote Sensing of Environment*, **130**, 254–265, doi:10.1016/j.rse.2012.11.023.

Ritchie, J. C., P. V. Zimba, and J. H. Everitt (2003), Remote Sensing Techniques to Assess Water Quality, *photogramm eng remote sensing*, **69**(**6**), 695–704, doi:10.14358/PERS.69.6.695.

Schalles, J. F., D. Rundquist, and F. R. Schiebe (2001), The influence of suspended clays on phytoplankton reflectance signatures and the remote estimation of chlorophyll, *Verhandlungen des Internationalen Verein Limnologie*(**27**), 3619–3625.

Selective withdrawal and its effect on stratification and hypolimnetic oxygen within a drinking water reservoir – A modelling study

M. Weber[1]*, B. Boehrer[1] and K. Rinke[1]

[1] *Department of Lake Research, Helmholtz Centre for Environmental Research - UFZ, Magdeburg, Germany*

**Corresponding author, e-mail michael.weber@ufz.de*

KEYWORDS
Reservoirs; withdrawal depth; stratification; hypolimnetic oxygen; modelling.

EXTENDED ABSTRACT

Introduction

Dams and reservoirs for flood protection, drinking and irrigation water supply and electric power generation represent artificial water bodies, which affect the water flux and water quality in a downstream river. In Europe, a high number of reservoirs are run with hypolimnetic withdrawal and thus, cold bottom water is withdrawn into the downstream river throughout the year. Adjusting the existing withdrawal regime can be a modern reservoir management tool to balance economical aims against natural conservation. This study investigated the effects of a modified withdrawal regime on stratification and hypolimnetic oxygen dynamics in a large drinking water reservoir. With a 1DV reservoir model, we tested, if water of a desirable temperature can be supplied throughout the summer or whether this will lead to unacceptably low dissolved oxygen (DO) concentrations for the drinking water supply.

Materials and methods

Study site: The oligotrophic and monomictic Grosse Dhuenn Reservoir (51.066 °N, 7.190 °E) with a total volume of 81 Mio. m³ and a maximum depth of 53 m is one of the largest drinking water reservoirs in Germany. Since the first operation in 1987, water for the downstream river Dhuenn has been taken from the bottom outlet (4-6 °C). In 2014, a pivoted pipe was installed at the withdrawal tower to supply warmer water (12-18 °C) into Dhuenn River. This reconstruction of the natural temperature regime should allow a re-establishment of the natural fish-community.

Reservoir model: We applied the one-dimensional numerical model GLM/AED2 for hydrodynamics and oxygen dynamics (Hipsey et al., 2014) to simulate the effect of a selective withdrawal management. Therefore, the source code of GLM/AED2 was modified by integrating pre-defined management strategies and a new simple oxygen module. Now, the current version of GLM/AED2 autonomously determines the withdrawal height on basis of a desirable discharge temperature, the in-reservoir temperature stratification and hypolimnetic oxygen concentration. In times of low oxygen concentrations in the hypolimnion, the model automatically switches the withdrawal to the bottom outlet until the DO concentration has recovered ("oxygen check").

Withdrawal scenario: For the selective withdrawal scenario we used the upstream river temperature as the target discharge temperature and a threshold of 4 mg/L for the "oxygen check". The scenario model was run for a period of five years (1996-2000).

Results and discussion

The reservoir model was calibrated by a sensitivity analysis and showed a good agreement with observed temperature and hypolimnetic DO concentration profiles. In our scenario simulation, the model was able to select the best withdrawal height to supply a pre-defined target discharge temperature (Fig. 1). Compared to the present bottom outlet withdrawal, a selective withdrawal from the epi-/metalimnion alone has strengthened the stratification and increased the hypolimnetic (raw-) water volume on the one hand (Fig. 1a). On the other hand this was leading to conditions in the hypolimnion with remarkably decreased bottom water DO concentrations. The DO concentrations at the end of the stratification periods in 1997-2000 dropped below the threshold of 4 mg/L and the withdrawal was switched to bottom outlet until autumn turnover (Fig. 1a). As a result, this led to a sudden drop in discharge water temperature and DO concentration but should be acceptable because raw water security has a higher priority than the temperature condition in Dhuenn River. In addition, the scenario simulation showed that the withdrawal of oxygen depleted water from the bottom layers in times of critical DO concentrations ("oxygen check") requires a certain time and discharge to allow DO to recover. In conclusion, the withdrawal management is an efficient way to restore the temperature regime in the downstream river and to prevent a loss of cold hypolimnetic water. However, a selective withdrawal from epi-/metalimnion will increase the risk of partial anoxia in the hypolimnion and thus, should be considered in reservoir operations.

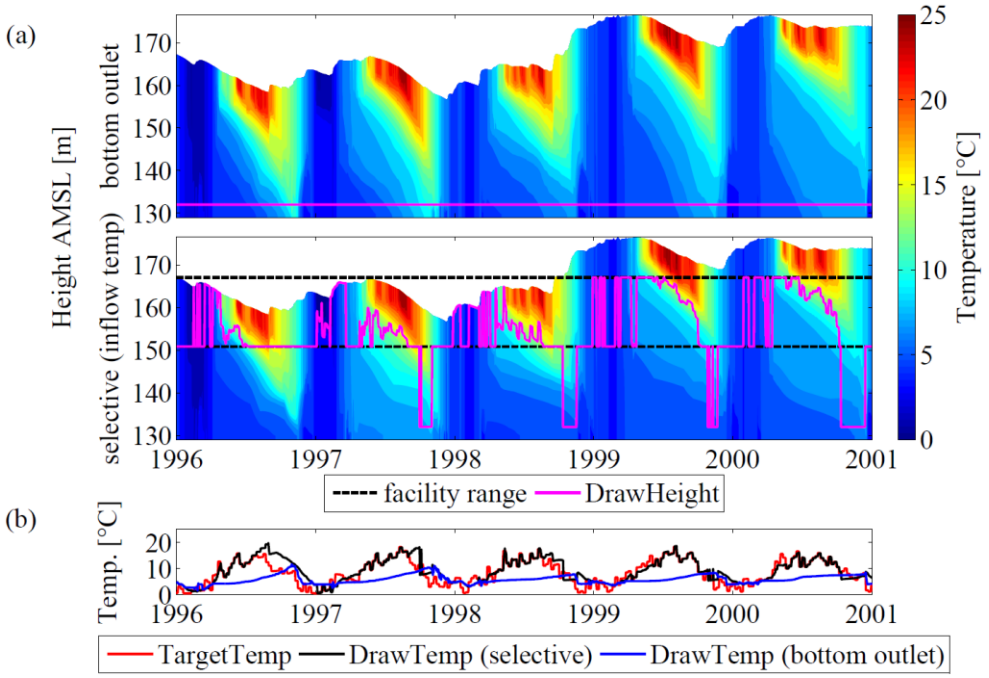

Figure 1. (a) Simulated water temperatures of the scenario model assuming bottom outlet withdrawal and selective withdrawal (upstream river temperature, "oxygen check"). The black dashed line represents the operating range of the selective withdrawal facility and the magenta solid line the modelled withdrawal height. (b) Water temperature of the reservoir outflow; the red solid line indicates the target temperature for the selective withdrawal, whereas the black/blue solid lines indicate the water temperature of the withdrawn water from the selective withdrawal, respectively, the bottom outlet withdrawal

REFERENCES

Hipsey, M.R., Bruce, L.C., Hamilton, D.P., 2014. GLM – General Lake Model, Model Overview and User Information (http://aed.see.uwa.edu.au/).

Spatial variation in benthic oxygen flux in UK shelf seas

M.E. Williams[1]*, L.O. Amoudry[1], A.J. Souza[1], H.A. Ruhl[2] and D.O.B. Jones[2]

[1] *National Oceanography Centre, Liverpool, UK*
[2] *National Oceanography Centre, Southampton, UK*

**Corresponding author, e-mail m.williams@noc.ac.uk*

KEYWORDS
Shelf seas; benthic boundary layer; oxygen flux; eddy covariance.

EXTENDED ABSTRACT

Introduction

Benthic sediments remineralize organic matter and cycle nutrients. Shelf seas make up a small portion of the ocean, but are responsible for the majority of this biogeochemical cycling by marine sediments (Jørgensen, 1983). Within these sediments, carbon and nutrient cycling and benthic habitat vary with sediment composition, for example microbial processes are accelerated in permeable sandy sediment and organic carbon is buried in cohesive muddy shelf sediments (Rocha, 2008; Muller-Karger et al., 2005).

Oxygen consumption in benthic sediments can be used to quantify carbon and nutrient cycling. An eddy covariance technique has been developed to quantify oxygen fluxes across the sediment-water interface with the advantage of a large flux footprint and little flow interference (Berg et al., 2003). Here we apply this technique in the challenging energetic environment of the UK shelf seas to explore difference in oxygen consumption and thus carbon and nutrient fluxes across a gradient of sediment composition.

Materials and methods

In the absence of sources or sinks of oxygen in the near-bed water column, the turbulent flux of oxygen can be written as a mean of the vertical velocity fluctuations (w') and oxygen fluctuations (C')

$$F = \overline{w'C'}. \quad (1)$$

Measurement requires a collocated ADV and fast oxygen sensor. As part of the UK Shelf Seas Biogeochemistry programme, these in situ measurements of velocity, oxygen, as well as nutrients and suspended sediment were made in the Celtic Sea across the sand to mud sediment gradient. Measurements were made from a tripod deployed in 100 m depth for 2.5 to 9 days in March 2014, March, May, and August 2015 to control for depth influence on benthic biogeochemistry. Large wave conditions in winter and spring deployments appear to have caused flow conditions too energetic for the oxygen sensor to produce valid results.

Results and discussion

Data from August 2015 give distinctive oxygen consumption rates at different measurement sites in the Celtic Sea (Figure 1). Measurements at the site located within a large mud patch give an order of magnitude larger oxygen flux than those at sites with higher percentage sand composition.

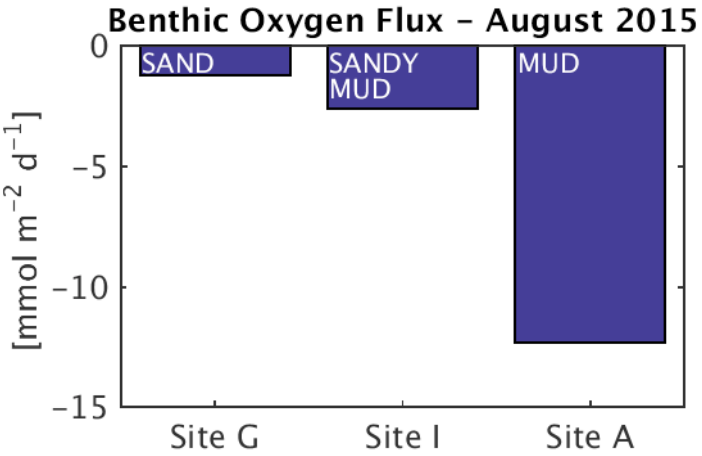

Figure 1. Benthic oxygen consumption as calculated by the eddy covariance method at three sites in the Celtic Sea. Oxygen consumption is much higher where the sediment composition is mud than where it is sand or sandy mud.

Benthic turbulence is generated by tidal flows, and velocity measurements show that these tidal flows vary between sites. Bed stress is consistently high where oxygen fluxes are large owing to circular tidal ellipses (Figure 2). Discussion of the relationship between tidal flows, turbulence, and oxygen will be presented.

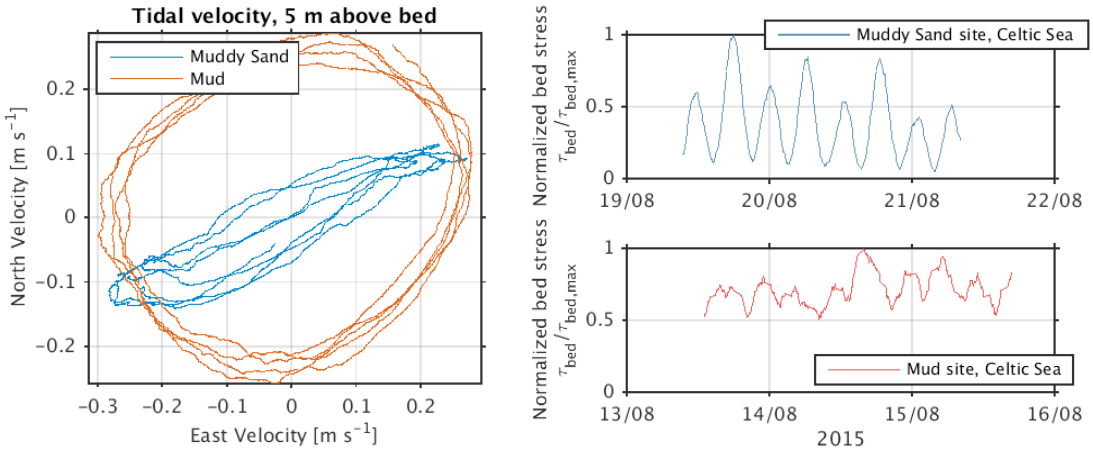

Figure 2. Velocity observations show a constantly elevated bed stress at the mud site while sandier sites experience strong tidal variability in bed stress.

REFERENCES

Berg, P., Røy, H., Janssen, F., Meyer, V., Jørgensen, B.B., Huettel, M., de Beer, D. (2003), Oxygen uptake by aquatic sediments measured with a novel non-invasive eddy-correlation technique, *Mar. Ecol. Prog. Ser.,* **261**, 75-83, doi:10.3354/meps261075

Jørgensen, B.B (1983), Processes at the sediment-water interface. *In:* B. Bolin, R.B. Cook (eds.) The Major Biogeochemical Cycles and Their Interactions, J. Wiley & Sons

Muller-Karger, F.E., Varela, R., Thunell, R., Luerssen, R., Hu, C., Walsh, J.J. (2005), The importance of continental margins in the global carbon cycle. *Geophys. Res. Lett.*, **32**, L01602, doi:10.1029/2004GL021346

Rocha, C. (2008), Sandy sediments as active biogeochemical reactors: compound cycling in the fast lane. *Aquat. Microb. Ecol.*, **53**, 119-127, doi:10.3354/ame01221

List of participants

First Name	Last Name	Affiliation
Mahan	Amani	University of Bath
Hrund	Andradottir	University of Iceland
Julio	Bernardo	Federal University of Parana
Bertram	Boehrer	Ufz-Helmholtz-Centre for Environmental Research
Andreas	Brand	Swiss Federal Institute of Aquatic Science and Technology
Lee	Bryant	University of Bath
Alberto	de la Fuente	Universidad de Chile
Daphne	Donis	University of Geneva
Gleb	Dyakonov	Institute of Oceanology of the Russian Academy of Sciences
Scott	Easter	University of Bath
Rebecca	Ellis	University of Bath
Badin	Gibbes	University of Queensland
Kelly	Graves	University of British Columbia
Alistair	Grinham	University of Queensland
Stephen	Henderson	Washington State University
Stephen	Hilgert	Karlsruhe Institute of Technology
Ben	Hodges	University of Texas at Austin
Moritz	Holtappels	Max Planck Institute for Marine Microbiology
David	Hurley	University of British Columbia
Petri	Kiuru	Finnish Environment Institute
Bernard	Laval	University of British Columbia
Bruno	Lemaire	Universite Paris-Est
Madis	Lilover	Tallinn University of Technology
Ramsay	Lind	Nortek
John	Little	Virginia Tech
Liu	Liu	University of Koblenz-Landau
Michael	Mannich	Federal University of Parana
Amaia	Marruedo	Leibruiz-Institue of Freshwater Ecology and Inland Fisheries
Frank	Peeters	University of Konstanz
Roger	Pieters	University of British Columbia
Marco	Pilotti	Università degli Studi di Brescia
Bruna	Polli	Federal University of Parana
Yves	Prairie	University of Quebec at Montreal
Berit	Rabe	Marine Scotland Science
Love	Raman Vinna	École Polytechnique Fédérale de Lausanne
Derek	Roberts	University of California
Geoff	Schladow	University of California
Jennifer	Shore	Royal Millitary College of Canada
Stefano	Simoncelli	University of Bath
John	Simpson	Bangor University School of Ocean Sciences
Emily	Slavin	University of Bath

Mariana	Soler	University of Girona
Victor	Stepanenko	Lomonosov Moscow State University
Adolf	Stips	European Commission - Joint Research Centre
Ted	Tedford	University of British Columbia
Giulia	Valerio	Università degli Studi di Brescia
Adrian	Wagner	Karlsruhe Institute for Technology
Danielle	Wain	University of Bath
Michael	Weber	Helmhotz Centre for Environmental Research
Megan	Williams	National Oceanography Centre, Liverpool
Fabian	Wolk	Rockland Scientific
Iestyn	Woolway	University of Reading
Johny	Wüest	Swiss Federal Institute of Aquatic Science and Technology
Zach	Wynne	University of Bath
Ram	Yerubandi	Canada Centre for Inland Waters
Roman	Zdorovennov	Russian Academy of Sciences

Sponsors